Titre: Title:	Effects of dispersion on rheological properties of filled polypropylene
Auteur: Author:	Min Wu
Date:	1999
Type:	Mémoire ou thèse / Dissertation or Thesis
Référence: Citation:	Wu, M. (1999). Effects of dispersion on rheological properties of filled polypropylene [Mémoire de maîtrise, École Polytechnique de Montréal]. PolyPublie. https://publications.polymtl.ca/8566/

UNIVERSITÉ DE MONTRÉAL

EFFECTS OF DISPERSION ON RHEOLOGICAL PROPERTIES OF FILLED POLYPROPYLENE

MIN WU
DÉPARTEMENT DE GÉNIE CHIMIQUE
ÉCOLE POLYTECHNIQUE DE MONTRÉAL

MÉMOIRE PRÉSENTÉ EN VUE DE L'OBTENTION
DU DIPLÔME DE MAÎTRISE ÈS SCIENCES APPLIQUÉES (M.Sc.A)
(GÉNIE CHIMIQUE)
APRIL 1999

UNIVERSITÉ DE MONTRÉAL

ÉCOLE POLYTECHNIQUE DE MONTRÉAL

Ce mémoire intitulé:

EFFECTS OF DISPERSION ON RHEOLOGICAL PROPERTIES OF FILLED POLYPROPYLENE

présenté par: WU Min

en vue de l'obtention du diplôme de : Maîtrise ès sciences appliquées

a été dûment accepté par jury d'examen constitué de:

M. BUSCHMANN Michael, Ph.D., président

M. LAFLEUR Pierre G., Ph.D., membre et directeur du recherche

M. CARREAU Pierre J., Ph.D., membre et codirecteur du recherche

M. FAVIS Basil, Ph.D., membre

ACKNOWLEDGMENTS

I am deeply indebted to my thesis director, Professor Pierre G. Lafleur and co-director, Professor Pierre J. Carreur, for their patience, encouragement and supervision in this work. Without their guidance and support, this thesis would not have been possible.

I am also very grateful to the members of my committee, Dr. Michael Buschmann and Dr. Basil Favis for their comprehensive review of this thesis.

I would like to acknowledge the assistance of Mr. Luc Parent and Mr. Sébastien Tremblay for their considerable and continuous help with all aspects of the extrusion experiments carried out. I also give my thanks to Mr. Yun-Li Fang for his kind help in doing part of my experiments. Additionally, I am grateful to all members of the Department for their kindness, helpful discussions and friendship.

I would like to express my gratitude to Ms. Min Yan for her comments and helpful discussion.

Finally, I extend my deepest appreciation to my husband, Bing Ge, for his great help, patience and support. My sincere thanks are also extended to my parents for their continuous encouragement and understanding.

RÉSUMÉ

La relation entre la rhéologie et l'état de dispersion du polypropylène chargé de carbonate de calcium a été étudiée dans le cadre de ce travail. Le niveau de dispersion de la charge dans le polymère, qui dépend des conditions de traitement, joue un rôle important sur les propriétés rhéologiques. Il est essentiel d'étudier les propriétés rhéologiques pour comprendre les phénomènes qui se produisent et leurs variations en cours de traitement.

Dans la première partie de ce travail, les facteurs qui influencent le mélange dispersif du polypropylène chargé ont été étudiés à l'aide d'une extrudeuse bi-vis. Des films ont été préparés à partir de l'extrudat (par soufflage) dans le but d'analyser la dispersion du $CaCO_3$, à la fois par microstructure et par analyse d'images. Deux types de carbonates de calcium ont été utilisés comme charges. Certains paramètres opératoires tels que la vitesse de la vis, le débit d'alimentation en matière première, la position de l'introduction des charges de $CaCO_3$ ainsi que la configuration de la vis affectent le degré de dispersion au sein du matériau. La dimension des particules influence la dispersion uniquement pour les composites à faibles concentrations en charge.

Dans la deuxième partie de ce travail, les propriétés viscoélastiques du polypropylène fondu et chargé de $CaCO_3$ ont été étudiées. Pour le polypropylène fondu fortement chargé, le comportement rhéologique change avec le temps sous l'influence des réactions entre les particules et la construction d'un réseau. La température, le taux de déformation ainsi que l'amplitude de la déformation sont les facteurs principaux affectant les forces agissant entre les particules et modifiant la structure du réseau. La déformation habituelle sous cisaillement casse les agglomérats et en même temps le réseau se brise. Imposer une faible-amplitude en cisaillement oscillant s'est avéré être une méthode optimum pour détruire le réseau de particules et pour modifier la dispersion des charges. Les propriétés rhéologiques du polymère dépendent de la contrainte et de l'amplitude

appliquée. Pour le composite contenant 50% de $CaCO_3$, aucun domaine de viscoélasticité linéaire n'a été obtenu.

Les effets de la concentration de la charge, du degré de dispersion et de la taille des particules agglomérées sur les propriétés viscoélastiques ont été déterminés. La viscosité augmente avec la concentration de la charge, particulièrement aux basses fréquences. On observe un seuil de contrainte pour les composites à une concentration de solides de 50 % en poids. À une concentration fixe, une meilleure dispersion aboutit à une réduction de la viscosité. Pour les fortes concentrations, l'augmentation de la valeur de l'indice de dispersion mène à des matériaux plus visqueux et ayant une contrainte plus élevée. L'influence de la dimension des particules sur la viscosité a été observée seulement pour les systèmes ayant de faibles concentrations. Les modèles de Maron-Pierce et Mooney ne peuvent pas décrire le comportement rhéologique des systèmes utilisés dans le cadre de notre étude. La viscosité relative du système non traité de PP chargé de $CaCO_3$ est beaucoup plus haute que celle prévue par les modèles donnés par les équations. La corrélation entre la viscosité et l'indice de dispersion est obtenue par superposition des courbes de viscosité avec différents indices de dispersion.

Dans la dernière partie de l'étude, l'influence du niveau de cisaillement et de l'élongation sur le composite a été examinée en utilisant respectivement des filières plate et convergente. La viscosité élongationnelle a été calculée à partir de la chute de pression à l'entrée, en utilisant deux techniques, celles de Cogswell et Binding. Les deux méthodes mènent à des valeurs de viscosité élongationnelle du même ordre de grandeur. Les viscosités élongationelles du PP pur et du $CaCO_3$/PP montrent un comportement rhéofluidifiant. Les valeurs du rapport de Trouton sont plus grandes que 3. Les états de dispersion avant et après cisaillement et élongation ont été analysés. Les deux champs d'écoulement changent le degré de dispersion. Les valeurs du paramètre λ qui caractérisent les deux champs d'écoulement confirment que l'écoulement élongationnel est plus efficace que le simple cisaillement pour disperser des particules solides.

ABSTRACT

The relationship between rheology and dispersion state for calcium carbonate-filled polypropylene has been studied in this work. The degree of filler dispersion in the polymer, which is closely correlated to the processing conditions, plays an important role in determining the rheological properties. It is essential to investigate the rheological properties for understanding the phenomena encountered and changes occurring during processing.

In the first part of this work, the factors influencing dispersive mixing of filled polypropylene have been studied using twin-screw extruder. Blown films have been prepared from extrudate for analyzing the filler dispersion through microstructural and images analysis procedures. Two well-characterized calcium carbonates have been used as fillers. The processing parameters such as screw speed, flow rates, filler feeding position, and screw configuration are found to affect the degree of dispersion in the compounds. The differences of particle size change the dispersion only for the low concentrated compounds.

In the second part, the viscoelastic properties of molten polypropylene filled with $CaCO_3$ powders have been investigated. For high concentrated polypropylene melts, the rheological behavior changes with time due to the interparticle reaction, particle network buildup, as well as particle-alignment under a given deformation. Temperature, deformation rate, and strain-amplitude are the key factors affecting the attractive forces acting between particles and modifying the network structure of the compounds. Steady shear deformation break up the agglomerate during the time the network is broken up. Imposing a small-amplitude pre-oscillatory shear has been found to be the optimum method to destroy the particle network and alter the filler dispersion state to the lowest limit. The rheological data of filled polymer melts depend on the applied strain amplitude. For 50% $CaCO_3$/PP compound, no linear viscoelastic domain is obtained.

The effects of filler concentration, degree of dispersion, and particle/agglomerate size on the viscoelastic properties have been determined. The complex viscosity increases with filler concentration, especially at low frequencies. An apparent yield stress is observed at a solid concentration of 50 wt%. At a fixed concentration, the better dispersion results in the reduction of viscosity. For high concentrated polymer melts, the increase of dispersion index value leads to more viscous, higher yield stress materials. The influences of particle size on the complex viscosity are observed for low concentrated systems. The Maron-Pierce and Mooney models, which are applied to non-interaction sphere suspensions in a Newtonian medium, can not describe the rheological behavior of the systems used in our study. The relative viscosity of untreated $CaCO_3$ filled PP system is much higher than that expected by the model equations. A correlation between complex viscosity and dispersion index is derived by superposition of viscosity curve at different dispersion index into a single curve.

In the last part, the influence of shear and extensional flow on the dispersive mixing has been reported using the slit and the convergent die respectively. The extensional viscosity has been calculated from entrance pressure drop, utilizing two techniques – the Cogswell and Binding analysis. The two methods lead to the elongation viscosity values in the same order of magnitude. The elongational viscosity of pure PP and $CaCO_3$/PP shows tension-thinning behavior. The Trouton ratio values are greater than 3. The dispersion states before and after elongational/shear flow have been analyzed. Both flow fields change the degree of dispersion. The values of flow field characterization parameter λ confirm that the elongational flow is more efficient than simple shear flow in efficient dispersive mixing.

CONDENSÉ EN FRANÇAIS

Il est de plus en plus répandu d'incorporer des matériaux de remplissage minéraux, tels que le $CaCO_3$, le TiO_2, le talc et autres, aux thermoplastiques. Le premier objectif pour l'utilisation de ces particules solides aux matériaux polymères est premièrement d'améliorer les propriétés mécaniques et physiques de ces matériaux composites (notamment la rigidité, l'élasticité ainsi que la température de déformation thermique) et deuxièmement de réduire les coûts de production en remplaçant des résines à coût important par des particules solides peu coûteuses. Pour optimaliser les propriétés, il est d'une importance primordiale de réaliser une dispersion adéquate des particules. Ceci s'exécute fréquemment à l'aide d'extrudeuses bi-vis co-rotatives "intermeshing", qui sont d'une grande efficacité, puisqu'elles réduisent les dommages causés par la chaleur et par le cisaillement des polymères et des additifs. Afin d'évaluer la qualité du mélange, des procédures de caractérisation microstructurale appropriées ont été appliquées. Les méthodes d'examen les plus répandues de la microstructure incluent: la microscopie optique ou électronique, la radiographie, la conductivité électrique, etc.

Les propriétés de mise en oeuvre, morphologiques et rhéologiques sont étroitement associées entre elles, mais restent mal comprises. Les données rhéologiques sont nécessaires pour comprendre les phénomènes de changements se produisant pendant le traitement. Au cours des dernières décennies, beaucoup de chercheurs ont prêté une grande attention aux propriétés rhéologiques des polymères fondus chargés de minerais. La concentration, la forme, la dimension, la distribution des particules, son état de dispersion (dispersé ou aggloméré) sont des facteurs qui influencent aussi les propriétés rhéologiques des polymères chargés. Il est bien connu dans la littérature que l'addition de matière de remplissage aux polymères augmente la viscosité. La viscosité augmente avec la charge, particulièrement à de basses vitesses de cisaillement. Le degré de dispersion est proportionnel à la concentration et inversement proportionnel à la dimension de la

particule. Le degré de dispersion est relié à la viscosité du composite. Le traitement de surface appliqué sur les charges réduit la viscosité et affecte le module dynamique.

La dispersion des particules dans le polymère joue un rôle important sur les caractéristiques viscoélastiques. Le degré de dispersion est lié à beaucoup de facteurs, tels que la taille et la forme des particules, la charge des particules, l'interaction particule-particule et/ou particule-matrice. Pendant la mesure ou le traitement, le degré de dispersion des charges peut être considérablement modifié avec le temps. Le comportement rhéologique du polymère chargé est le résultat de diverses contributions qu'il est très difficile de mesurer et de décrire exactement. Bien que ces difficultés existent, il est utile d'explorer et d'expliquer les mécanismes de ces interactions par l'intermédiaire des mesures rhéologiques.

Le premier objectif est d'établir une relation entre les propriétés rhéologiques et la dispersion des charges par la recherche d'une méthode indirecte pour évaluer la dispersion. Les échantillons utilisés pour les mesures viscoélastiques ont été préparés à partir d'extrudats obtenus par extrusion bi-vis. L'influence de la concentration des charges, du degré de dispersion, et de la taille des agglomérats sur les propriétés viscoélastiques a été determinée. Afin d'atteindre un état de pseudo-équilibre pour les systèmes fortement chargés, la stabilité rhéologique dans diverses conditions a été étudiée. Une technique expérimentale a été développée pour examiner les propriétés viscoélastiques dans des conditions pseudo-stables pour des systèmes fortement chargés. Finalement, une corrélation entre la viscosité et le degré de dispersion est développée, basée sur la méthode de l'indice de superposition temps-dispersion.

Le deuxième objectif de cette étude est de vérifier les facteurs influençant la dispersion du mélange polypropylène et carbonate de calcium par extrusion bi-vis. Deux types de particules de $CaCO_3$ ont été utilisés pour être incorporés dans une matrice de polypropylène (PP), des particules ultra fines de 0.7 microns de diamètre et des fines de

1.4 microns. On obtient des extrudats de diverses qualités en modifiant une ou plusieurs conditions telles le type de vis utilisé, la vitesse de rotation de la vis, le débit d'alimentation en matières premières et autres. Un film soufflé a été préparé à partir de l'extrudat et a été utilisé pour l'analyse de la dispersion de la charge par analyse microstructurale et par analyse d'images. La dispersion des particules est alors exprimée sur une base quantitative en terme du diamètre moyen des agrégats.

Les effets des paramètres (vitesse de la vis, le débit et la configuration de la vis) ont été étudiés en terme de l'indice de dispersion f. Le nombre de disques de mélange (kneading discs) dans l'une ou l'autre des zones de fusion et de mélange ainsi que la position de l'alimentation de la charge affectent la valeur de l'indice de dispersion. L'addition du $CaCO_3$ par l'intermédiaire d'un distributeur et l'utilisation d'une vis donnant une meilleure fusion ont donné une bonne dispersion résultant de l'absorption considérable d'énergie lors du mélange dans les disques qui agissent comme barrières partielles. Mélanger moins efficacement les matériaux dans la zone de fusion comme pour la configuration 2 cause un délai dans la fusion du polymère. Le résultat est une meilleure dispersion. La diminution du débit et l'augmentation de la vitesse de vis augmentent le degré de dispersion. La concentration croissante de la charge modifie sensiblement l'indice de dispersion sur l'intervalle des valeurs étudiées. La dimension des particules de $CaCO_3$ s'est avérée avoir une influence sur la dispersion, surtout pour les basses concentrations (25%) de la charge et avoir moins d'effets pour les hautes concentrations (50%).

Les propriétés viscoélastiques des polypropylènes contenant de la poudre de $CaCO_3$ fine et ultra-fine ont été étudiées. Les difficultés qui ont surgi lors de la mesure des propriétés rhéologiques sont dues principalement aux variations avec le temps. La formation d'un réseau de particules à concentration élevée de la charge provoque des variation des propriétés avec le temps sous une déformation donnée. La température, le taux de déformation, et l'amplitude des contraintes sont les principaux facteurs qui

affectent les forces d'attraction entre les particules et qui modifient la structure finale du composé. Un cisaillement important change le degré de dispersion dû aux bris des agglomérats. Imposer une faible amplitude en cisaillement oscillant s'est avéré être la méthode optimum pour détruire le réseau des particules et pour modifier la dispersion de la charge. Les expériences de balayage en déformation ont montré que la réponse rhéologique du polymère chargé varie avec le niveau de la déformation. Pour le composé contenant 50% de $CaCO_3$, aucun domaine de viscoélasticité linéaire n'a été obtenu. La deformation faible minimum de 1% pour un dispositif expérimental donné a été appliquée aux mesures de viscoélasticité pour tous les composés contenant 50% de $CaCO_3$ étudiés.

Les effets de la concentration de la charge, du degré de dispersion, de la taille des particules agglomérées sur la viscoélasticité ont été déterminés. La viscosité augmente avec la concentration de la charge, particulièrement à basses fréquences, comme prévu. Un évident seuil de contrainte a été observé à une concentration de 50 % en poids, causé par la concentration des particules et par la taille des agglomérats, donnant une structure solide. Les interactions particule-particule sont probablement responsables du seuil de contrainte. À une concentration fixe, une meilleure dispersion a pour conséquence une réduction de la viscosité. L'augmentation de la taille des agglomérats provoque une augmentation de l'indice de dispersion et tranforme les polymères fortement chargés en des matériaux plus visqueux et ayant des seuils de contrainte plus élevés. L'influence des différentes dimensions des particules sur la viscosité a été observée pour les faibles concentrations.

Les modèles de Maron-Pierce et de Mooney ne peuvent pas décrire le comportement rhéologique des systèmes utilisés dans notre étude, à cause des interactions significatives donnant lieu à un seuil de contrainte. La viscosité relative du système non traité de PP chargé de $CaCO_3$ est beaucoup plus élévée que prévue par les équations. La corrélation entre la viscosité et l'indice de dispersion vient de la

superposition de la courbe de viscosité avec différents indices de dispersion. Le modéle est linéaire et se décrit ainsi:

$$\eta^*(\omega, f) = a_f \eta^*(a_f \omega, f_r)$$

où η^* est la viscosité complexe, ω la fréquence, a_f le facteur de déplacement et f_r est l'indice de dispersion de référence. L'application de cette équation a été vérifiée pour les systèmes étudiés et devrait être prouvée cas par cas.

Les propriétés élongationelles ont été obtenues en utilisant une filière convergente avec une vitesse d'élongation constante, pour laquelle le champ est principalement élongationnel. La viscosité élongationnelle a été calculée à partir de la chute de pression d'entrée, utilisant deux techniques, celles de Cogswell et Binding. Les deux méthodes mènent à des valeurs de viscosité élongationnelle de même ordre de grandeur. Les valeurs de viscosité élongationnelle du PP pur et du composite $CaCO_3$/PP montrent un comportement rhéofluidifiant. Les valeurs du rapport de Trouton sont bien au-dessus de 3 et la plus petite valeur pour les trois systèmes est d'environ 7. Les niveaux de dispersion avant et après élongation et cisaillement ont été analysés en utilisant des filières convergente et plate. Les deux champs d'écoulement changent le niveau de dispersion. Les valeurs du paramètre λ caractérise les deux champs confirment que le taux d'élongation est plus efficace que le simple cisaillement pour disperser des particules.

En général, les résultats présentés dans cette étude sont très encourageants. Cependant, quelques questions non résolues laissent suggérer certains défis à relever. En particulier, nous recommandons de:

- Démontrer le rôle des interactions entre les particules sur la viscoélasticité des polymères chargés;

- Développer des modèles pour corréler les propriétés rhéologiques avec des paramètres microscopiques, structuraux et physiques;

- Développer une technique expérimentale en ligne pour déterminer la dispersion dans un écoulement donné, pour la corréler avec la réponse rhéologique.

TABLE OF CONTENTS

LIST OF TABLES

LIST OF FIGURES

LIST OF APPENDIX

LIST OF SYMBOLS AND NOTATIONS

A : Hamaker coefficient or area of observation (m^2)

a : radius of the fragment (m)

a_f : shift factor of complex viscosity

<a> : volume average radius of fragments (m)

A_s : area observed under the microscope (m^2)

B : parameter related to components and concentration of filled system

d_i : diameter of agglomerates (m)

d_n : number average diameter (m)

d_v : volume average diameter (m)

f : dispersion index

FI : dimensionless parameter ratio of viscous forces to tensile strength

f_r : reference dispersion index

k : model parameter of Mooney-Pierce equation or coefficient in equation (2.2)

k_l : rate constant

l : length of convergent die (m)

L : power-law parameter of elongational viscosity ($Pa \cdot s^t$)

m : power-law parameter of shear viscosity ($Pa \cdot s^n$)

m_c : weight of calcium carbonate (kg)

m_t : total weight of compound (kg)

n : power-law index of shear viscosity

n_i : number of agglomerates

n′ : local slop defined by equation (3.10)

ΔP_e : entry pressure drop due to elongation (Pa)

ΔP_s : entry pressure drop due to shear (Pa)

Q : total volumetric flow rate (m^3/s)

R : radius of cluster (m)

R_0 : outlet radius of nozzle die (m)

R_1 : inlet radius of nozzle die (m)

t : power-law index of elongational viscosity

t* : dimensionless erosion time

$\langle V_z \rangle$: average velocity (m/s)

W : energy dissipation (W)

W_f : weight per unit area of film (kg/m^2)

Greek Letters

β : inverse of contraction ratio in convergent die

γ : applied strain

$\dot{\gamma}$: applied shear rate (s^{-1})

$\dot{\varepsilon}$: elongational rate (s^{-1})

η : shear viscosity (Pa ·s)

η^* : complex viscosity (Pa ·s)

η_e : elongational viscosity (Pa · s)

η_m^0 : zero shear rate viscosity of the matrix polymer (Pa · s)

η_r : relative viscosity

λ : parameter to characterize flow field

λ_m : constant related to onset of shear thinning

μ : viscosity of suspending fluid (Pa ·s)

ρ_f : density of film (kg/m^3)

σ_H : shear stress at the wall (Pa)

τ : applied shear stress (Pa)

τ_y : yield stress (Pa)

ϕ_v : volume fraction of fillers in film

ϕ : volume fraction of filler

ϕ_a : area fraction of agglomerates

ϕ_m : maximum volume fraction

ω : vorticity tensor (s^{-1})

CHAPTER 1 - INTRODUCTION

1.1 Generalities

It is increasingly widespread practice to incorporate mineral fillers such as $CaCO_3$, TiO_2, Talc, etc. into thermoplastics. The primary objective for using solid particles in polymeric materials is twofold: (1) to improve the mechanical/physical properties of the composite materials, notably stiffness, elastic modulus, and heat distortion temperature, etc.; and (2) to reduce the cost of production by replacing expensive resins with inexpensive solid particles. To optimize properties, effective melt compounding is of paramount importance in order to achieve adequate dispersion of the filler particles. This operation is frequently undertaken using intermeshing co-rotating twin-screw extruders, which have great mixing efficiency and reduced tendency to cause damage of heat- or shear-sensitive polymers and additives. Furthermore, the capability of generating the necessary levels of shear stress for breakdown of particle agglomerates offers a distinct advantage. In order to assess the mixture quality in these compounds there is a need for appropriate microstructural characterization procedures. The well-established methods of microstructure examination include: optical microscopy, electron microscopy, x-radiograph, surface inspection, electrical conductivity techniques, etc.

The processing/morphology/rheological properties are closely associated to each other, but remain poorly understood. Rheological data are necessary to understand the phenomena encountered and changes occurring during processing. In the past few decades, many researchers have paid great attention to the rheological properties of mineral filled polymers in the molten state. The concentration of the particles as well as other factors, such as the shape of the particles, the particle size and its distribution, and the state of dispersion of the particles (well-dispersed state or agglomerated state), are known to influence the rheological properties of filled polymer melts. It is well known in the literature that, in general, the addition of solid particles to polymer increases the melt viscosity. The extent of viscosity enhancement increases with content of fillers,

especially at low shear rates. The existence of yield stress is related to particle size and filler concentration. The yield stress increases with decreasing particle size and increasing filler content. The appearance of yield stress has been interpreted by formation of a solid-like structure, which increase the viscosity of the compound. The surface treatment of filler particles reduces the melt viscosity and affects the dynamic modulus.

The dispersion of particles in the polymer plays an important role in determining the viscoelastic characteristics. The degree of dispersion is related to many factors, such as characteristics (size, shape, etc.) of particles, particle loading, particle-particle and/or particle-matrix interaction, etc. During measurement or processing, the degree of dispersion of the fillers may be considerably modified with time. The rheological behavior of particle-filled polymer is the results of various contributions, which are very difficult to measure and accurately describe. Though the difficulties exist, it is worth to explore and explain the mechanism for those interactions via rheological measurements, and then utilize it to control polymer-processing operations.

1.2 Scope of present work

The first objective is to establish a relation between rheological properties and the dispersion of filler in a search of an indirect method to evaluate the dispersion. The samples used for viscoelastic measurements were prepared from twin-screw extrudates. The influences of filler concentration, degree of dispersion, and particle/agglomerate size on viscoelastic properties are discussed extensively. In order to reach a pseudo-equilibrium state for high-filled systems, the stabilities of dynamic viscoelasticity under various rheological conditions were investigated. An experimental technique was developed to examine the viscoelastic properties under pseudo-stabilized conditions for high concentrated polymeric systems. Finally, a correlation between the complex viscosity and and the dispersion index was derived using the time-dispersion index superposition method.

The second objective of this study is to verify factors influencing dispersive mixing of calcium carconate filled polypropylene in the process of twin-screw extrusion. Two well-characterized $CaCO_3$ particles - ultra fine with diameter of 0.7 μm and fine with 1.4 μm were used to incorporate with PP matrix. Methods of altering processing conditions (screw speed, flow rate and downstream feeding) as well as screw geometries (mixing elements) were employed to obtain extrudates of various mixing quality. Blown film was prepared from extrudate and utilized to analyze the filler dispersion through microstructural and image analysis procedures. The filler dispersion was then expressed on a quantitative basis in terms of volume average diameter.

CHAPTER 2 - LITERATURE REVIEW

2.1 Dispersive mixing mechanisms

Mixing is a process that reduces compound nonuniformity. It is very important because the homogeneity of the additive plays a crucial role on the mechanical, physical, chemical and rheological properties of the final compound. Mixing is indeed a basic processing step encountered in every industry. Among the various mixing operations, those involving polymeric liquids and solid-polymeric liquid systems are perhaps most characteristics of polymer processing. The high viscosity of polymeric systems increases the complexity of the process. A great number of workers have paid attention to the practical and theoretical studies of mixing mechanisms.

2.1.1 Mechanism of mixing

A widely adopted approach for the assessment of polymer mixing is through the concepts of dispersive and distributive mixing. Tadmor and Gogos (1979) gave a detailed description of these concepts. Dispersive mixing process is associated with the reduction in size of agglomerates of the minor component to its ultimate particle size and depends upon the application of high shear forces to affect agglomerate breakdown.

Distributive mixing can be defined as operations employed to increase the randomness of the spatial distribution of the minor constituent within the major phase, with no change in the size of the minor particles. Dispersive and distributive mixing phenomena generally occur simultaneously or stepwise during polymer processing operations. Figure 2.1 depicts schematically these two mixing mechanisms.

Dispersive mixing is an energy intensive, and relatively difficult type of mixing carried out in batch and continuous processes. The mechanism is commonly subdivided

into four stages: (1) incorporation, (2) distribution, (3) dispersion, (4) plasticization (or stabilization of the resulting dispersion). Incorporation is the first step of mixing. During this stage, the polymer wets and encapsulates the solids, and it may penetrate into the void spaces of the agglomerate and also with the aggregates. During distribution and dispersion, the agglomerates are successively broken apart and reduced in size, and spread out by random patterns of flow. During the plasticization stage, flocculation of filler aggregates may occur. This process contributes to the formation of a filler network structure throughout the matrix.

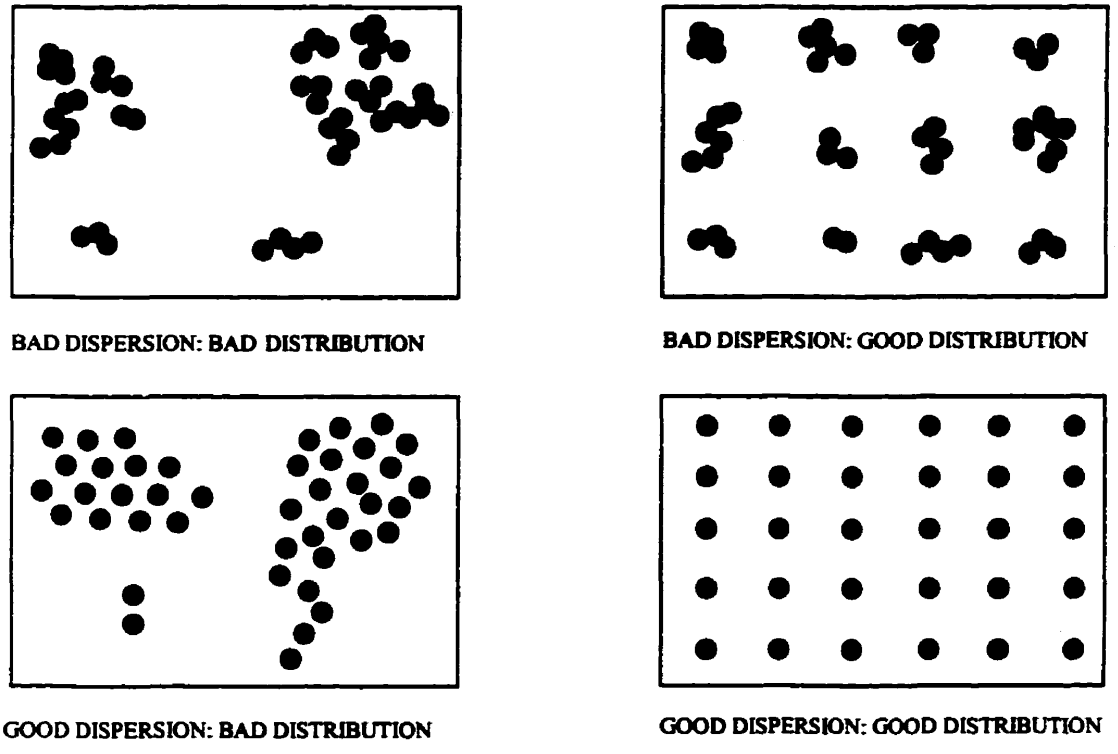

Figure 2.1: Schematic illustration of dispersive and distributive mixing mechanisms (adopted from Manas-Zloczower, 1994)

2.1.2 Models for agglomerate dispersion

Analysis of the dispersion process must consider both the forces involved in

agglomerate breakup, namely the forces of cohesion within the clusters and the hydrodynamic forces inducing their breakup. Manas-Zloczower (1994) reviewed in detail the models for agglomerate strength, as well as the different models for hydrodynamic interaction. Most existing models for agglomerate dispersion combine two of above submodels – one for the cohesiveness of the agglomerates and another for the hydrodynamics.

Most mixing models consider the rupture step to be the most important. Agglomerate rupture occurs when the hydrodynamic forces exerted on the solids exceed the cohesive forces holding the agglomerate together. Manas-Zloczower et al. (1982) developed a theoretical model for dispersive mixing in internal mixers. In their model the breakup is assumed to take place in the high shear narrow clearance between the tip of the rotor and the housing, where the effect of hydrodynamic tension would be the largest. A random distribution of orientations of the fracture surface among the agglomerates at the start of the flow or at the time of their formation was assumed. The dynamics of agglomerate size distribution was also predicted.

Another point of view expressed by Manas-Zloczower and Feke (1988) is that the dispersion process is controlled by the fragment separation. In this instance, flow kinematics is important: hence the authors suggested a model to predict the effect of flow field on the dispersion process. The model calculated the rate of separation of broken up agglomerate fragments in various flow fields. The dimensionless parameter FI scaled the magnitude of the viscous forces acting on the agglomerate relative to the tensile strength of the agglomerate, is given by:

$$FI = \frac{6\pi\mu a^3 \dot{\gamma}}{A} \tag{2.1}$$

where A is the effective Hamaker coefficient, μ is the viscosity of the suspending fluid, a

is the radius of the fragment, and $\dot{\gamma}$ is the applied shear rate.

Based on this model, the authors found that: (1) there was a critical minimum value of the parameter FI below which no separation can occur, (2) the agglomerate size did have an influence on the kinetics of the separation process, but the result was in contradiction to rupture-based mixing model prediction, (3) the pure elongation flow field is the most efficient in particle separation. The model is believed to be useful both for understanding experimental results and for making predictions about real mixing processes.

Experimental observations on dispersion phenomena for model systems in well-defined flow fields are also reported in the literature. Rwei et al. (1990 and 1991) observed two distinct mechanisms of dispersion in their experiments of carbon black agglomerate breakup in a controlled flow field. One mechanism, called "rupture", is characterized by an abrupt breakage of the agglomerate into a small number of large fragments, and tends to occur at relatively high shear stresses. The other mechanism, called "erosion", initiates at lower applied shear stresses and is characterized by the detachment of small fragments from the outer surface of the agglomerate.

For the rupture process, Rwei et al. (1990) developed an expression for the critical shear stress as follows:

$$\tau_{applied} = k\eta\dot{\gamma} \tag{2.2}$$

where η is the matrix viscosity, $\dot{\gamma}$ is the shear rate, and k is a coefficient which depends on the geometry of the agglomerates and the flow field as well. The critical shear rate for breakup of carbon black pellets was found to be inversely proportional to the viscosity of the fluid.

For the erosion process, Rwei et al. (1991) derived the rate at which particles erode from a cluster as follows:

$$\frac{dR}{dt^*} = -k_1\langle a \rangle \tag{2.3}$$

where R is the radius of the cluster, $\langle a \rangle$ is the volume average radius of the fragments, k_1 is a rate constant, and $t^* = t_1\dot{\gamma}$ is a dimensionless erosion time. Based on their observations, the size of the eroded fragments was assumed to be proportional to the size of the parent cluster.

The applicability of various dispersion models for predicting properties in mixing operations depends primarily on the information available on various system (material and processing) parameters. However, such models are important, since they provide the theoretical framework within which further investigations of the dispersion process may be conducted.

2.2 Characterization of filler dispersion

In the previous section, we reviewed the mixing mechanisms and models that describe the dispersion of the fillers or pigments. In order to assess the mixture quality in the final compound there is a need for appropriate microstructural characterization procedures, which form the subject of this section. A review was undertaken on various methods to observe particle agglomeration and then express filler dispersion on a quantitative basis.

2.2.1 Techniques

Over the past fifty years or so, many procedures have been developed for the

characterization of dispersion. Among those, which are in current use are: optical microscope procedures, transmission electron microscope procedures, scanning electron microscope procedures, x-radiography procedures, etc. Hess (1991) gave a detailed review of methods for dispersion analysis. The main emphasis of his review is on the analysis of elastomeric compounds containing carbon black.

Optical microscopy – This method is most suitable for visually comparing or measuring the level of agglomeration in elastomeric or plastic compounds. The method is applicable for analyzing almost any small piece of rubber or plastic compound, regardless of whether or not the polymer type or filler loading is known. Simple visual inspection of the cryosectioned compound under an optical microscope (40 to 400x) is sufficient to classify the dispersion from high to low quality in terms of the extent of agglomeration. If more quantitative information is desired, then the area covered by the agglomerates on the section can be measured using a graticule in the eyepiece (ASTM D2663, Method B).

X-radiography – This method is generally preferable for the analysis of inorganic pigment agglomerates or impurities in most polymeric systems. Modern commercial x-ray units are capable of x-raying relatively large samples up to 20 cm or larger in size and up to several centimeters thick depending upon composition.

Transmission electron microscopy – The TEM method offers the highest resolution of any of the microscopical procedures and is generally limited to studies on the microdispersion of primary pigment aggregates.

Scanning electron microscopy – The SEM has been applied to most of the different aspects of pigment dispersion and is probably the most versatile of all the different methods. Many of the other dispersion-analysis techniques are readily complemented by SEM analyses.

Image analysis – A major factor in the practical use of image analysis for measuring dispersion is the existence of clear boundaries and high contrast between the pigment agglomerates or fragments and the surrounding matrix. A uniform, relatively noise-free background is highly desirable, even though many currently available image analyzers have the ability to filter out unwanted noise. There is a practical limit to noise elimination, however, and it can be a very time-consuming process.

The most significant advantages of image analysis over other measurement procedures are in its ability to directly analyze the filler agglomerates or fragments for their percentage, size and spatial distribution in conjunction with microscopical methods. Disadvantages relate to difficult and/or time-consuming specimen preparation for optical analyses. At this time, image analysis has been largely restricted to measuring differences in filler agglomeration.

Optical scanning of surfaces – This is a method which measures the dispersion indirectly through surface roughness measurements. Ebell and Hemsley (1981) have utilized the technique of dark field reflected light microscopy (DFRLM) to measure surface roughness of cut rubber surfaces. The method is based on projection of a hollow cone of light incident to the cut rubber surface. The light beam does not pass through the objective lens before impinging on the sample. Therefore, there is no diffraction of light into the lens for a perfectly flat surface. Only surface irregularities act as diffracting centers, which appear as light spots on a dark background as viewed on the TV monitor. Quantification of the image is achieved by inputting the TV signal into an oscilloscope with a single line strobing facility. This produces a linear intensity trace which is analogous to the physical roughness trace of the stylus on the surface.

Surface inspection, stylus surface measurements, optical extinction coefficients, electrical conductivity, and pyrolysis gas chromatography are other techniques for analysis of dispersion states.

2.2.2 Dispersion index obtained by image analysis

The microscopy methods give only qualitative information unless subjected to extensive quantitative evaluation. Most of the studies relating the state of dispersion to the properties of compounds use a microscopy method and determine the average diameters of the agglomerates, the number of agglomerates greater than a certain size, the fraction of agglomerates, and so on. Suetsugu (1990) defined the state of dispersion based on the fraction of agglomerates for calcium carbonate filled polypropylene system. The compound was carefully microtomed for scanning electron microscopy. The dispersion index may be defined as follows:

$$\text{Dispersion index} = 1 - \Phi_a \tag{2.4}$$

$$\Phi_a = \frac{\pi}{4A\Phi}\sum_{i=1}^{N} d_i^2 n_i \tag{2.5}$$

where Φ_a is an area fraction of agglomerates, A is an area of observation, Φ the volume fraction of the filler, d_i and n_i the diameter and the number of the agglomerates. The dispersion index varies from 0 (all filler particulate remain in the form of agglomerates) to 1 (no agglomerate exists in the compound),

$$\text{(Poorest dispersion)} \quad 0 \le 1 - \Phi_a \le 1 \text{ (best dispersion)} \tag{2.6}$$

The correlation between the state of dispersion and various mechanical properties was obtained, and the author (Suetsugu, 1990) found that dispersion control is a key factor in improving the mechanical properties.

Some other types of indices are also available. Volume fraction of agglomerates, the third power of agglomerate diameter, has been found to be much affected by the small

number of large agglomerates so that the index largely scatters dependent upon the sample selected. The diameter of the agglomerate can be obtained by image analysis technique. Several kinds of average agglomerate diameter are considered in additions:

$$\bar{d} = \frac{\sum_i n_i d_i^n}{\sum_i n_i d_i^{n-1}} \qquad n = 0,1,2,3\cdots\cdots \qquad (2.7)$$

The average diameters that are mostly used are:

- Number average diameter d_n: n=1
- Volume average diameter d_v: n=4

Ess and Hornsby (1987) used volume average diameter as dispersion index to study the dispersive mixing effects in twin-screw extrusion compounding.

Bories (1998) developed a dispersion index expression based on the diameters of the agglomerates and the volume fraction of the agglomerates. The dispersion index f is defined by the following equation:

$$f = \frac{\rho_f \pi \sum_i n_i d_i^3}{6 A_s W_f \phi_v} \qquad (2.8)$$

where ρ_f is the density of the film, A_s is the area observed under the microscope, W_f weight per unit area of the film, ϕ_v volume fraction of fillers in the film. The dispersion index represents the volume fraction ratio of the agglomerates over 15 μm to the total agglomerates inside the film. The dispersion index varies from 0 (no agglomerate over 15 μm inside the film is observed) to $\frac{\rho_{mineral}}{\rho_{agglomerate}}$, which physical meaning of term is defined in detail by the author in his thesis (Bories, 1998).

$$\text{(Best dispersion)} \quad 0 < f < \frac{\rho_{mineral}}{\rho_{agglomerate}} \quad \text{(Poorest dispersion)} \qquad (2.9)$$

2.3 Mixing in co-rotating twin-screw extrusion

2.3.1 Basic concepts

Twin-screw extruders are widely used in the compounding of highly filled polymers. Of special importance are the intermeshing co-rotating twin-screw extruders. Their main advantage over conventional single-screw extruders is their unique capability of positive displacement conveying and complete melting in a very short barrel length. The mixing action in twin-screw is much more intense, reducing the tendency to cause damage to heat- or shear-sensitive polymers and additives, and resulting in homogeneous quality at stable extrusion rates. However, the flow patterns in a twin-screw extruder are complex and the fluid is subjected to a nonuniform deformation and stress field of varying vorticity (i.e., shear vs. elongation flow). Though a detailed understanding of the mixing process from both the theoretical and experimental viewpoints is still under investigation, there are some literatures on flow mechanisms in intermeshing co-rotating twin-screw extrusion.

2.3.2 Modeling of flow in various elements of intermeshing co-rotating twin-screw extrusion

Experimental techniques usually involve flow visualization of the interfaces of components as a function of time and location. Bawiskar and White (1995) studied the flow of solid pellets in a self-wiping co-rotating twin-screw extruder and compared it with single screw extruders. The mixing mechanisms were discussed based on the observations. The kneading disk blocks were found to play an important role in solid

conveying and melting. Huneault et al. (1996) reported measurements of residence time distribution in a twin-screw extruder using a calcium carbonate tracer by monitoring the ultrasonic attenuation in a specially instrumented die. They calculated the residence time distributions for individual screw functions (e.g., melting, conveying, mixing, and pumping). Narrow distributions were found for the melting and conveying stages. In the mixing and pumping sections, the distribution width was found to vary with the degree of fill and the recirculation ratio in the mixing blocks.

On the other hand, the numerical simulation approach involves solving the equations of conservation of mass, momentum, and energy with the appropriate constitutive equations and boundary condition. By integrating the Eulerian flow field obtained, fluid particles and materials interfaces can be followed for modest duration of time. In order to simplify such analysis, it is usually assumed that there is no interfacial tension between the components and that the components being mixed have similar physical and rheological properties.

The arrangement of modules on shaft is varied depending upon the mixing process required. Screw elements are used for transporting material. The primary processes of melting and dispersion are considered in the kneading disc region.

Szydlowski et al. (1987 and 1988) developed models simulating flow patterns and pressure distributions in the kneading disc region of an intermeshing co-rotating twin-screw extruder. Sastrohartono and Jaluria (1995) have reported a numerical simulation of fluid flow and heat transfer in the intermeshing co-rotating twin-screw extruders. They divided the flow domain into two regions: (1) the translation region; (2) the intermeshing region. The two regions are simulated separately and then coupled to model the overall transport. Lawal and Kalyon (1995) also solved the three-dimensional equations of conservation of mass and momentum, and utilized various dynamics to analyze the mechanisms of mixing occurring in single and co-rotating twin screw extruders.

2.3.3 Dispersion of fillers in twin-screw extrusion

The quality of filled polymers is very much related to the filler nature, particle size distribution, etc. The intermeshing co-rotating twin-screw extruders have excellent conveying capability with powder feedstocks and are capable of generating the necessary levels of shear stress for breakdown of particle agglomerates. A few studies have been carried out on the initial stages of mixing process during compounding in a twin-screw extruder. Mack (1990) made a study of split-feed compounding technique in a twin-screw compounding process. Split-feed technique stabilized the operating process and eliminated bridging in the feed zone. Ess and Hornsby (1987) utilized microstructural and image analysis techniques to study factors influencing dispersive mixing of calcium carbonate filled polypropylene during the twin-screw extrusion compounding process. The factors influencing agglomerate breakdown include material pretreatment, material characteristics and selected processing parameters, which included screw speed, temperature profile and screw geometry in the melting zone.

2.4 Rheological properties of filled polymer melts

Fillers are high-modulus particles, which are dispersed in polymer matrices to improve the mechanical/physical (or optical/thermal) properties of the final products. They could also frequently lower the material cost. Fine particle size and high surface area generally favor reinforcement. Whatever the purpose of the use of fillers might be, it has long been recognized that the incorporation of solid particulate to polymers may critically alter the flow characteristics of the system during processing. For instance, it is known that an addition of fillers increases the pressure drop across the die, due to the increase in melt viscosity, which increases with filler volume fraction, especially at low shear rates (Czarnecki and White, 1980; Ottani et al., 1988). At low shear rates or frequencies, a yield stress generally exists for flow to occur, which has been found to correlate to particle-particle interactions (Carreau et al, 1996; Ghosh et al, 1997). Other physical aspects related to the rheological behavior of filled polymers remain

unknown, such as: (1) The degree of dispersion of the solids in the matrix may change with time due to forces acting on the system. (2) Fillers in viscoelastic polymers may probably reduce the elasticity of melts (Metzner, 1985), but this effect remains to be verified and explained.

At present the processing/morphology/property relationship in highly filled polymeric systems remains poorly understood. Rheological methods are powerful tools to elucidate such relationships. The dispersion of fillers is strongly dependent on the rheological properties of the components. The rheological characterization of concentrated polymeric systems is one of the most important steps in studying the various phenomenon encountered and changes occurring during polymer processing. Rheological data are also needed to assess constitutive equations required for designing equipment and predicting changes under processing. As a result, a systematic investigation of the rheological properties of filled polymers as a function of deformation rate, volume fraction of particle, particle size, and matrix properties is of practical importance for the analysis and the control of many processing operations. In recent years, considerable research efforts (Suetsugu and White, 1983; Rong and Chaffey, 1988; Scott et al., 1988; Le and Bhattacharya, 1990; Carreau et al., 1996; Lavoie et al., 1997; Ghosh et al., 1997; Aral and Kalyon, 1997) have been directed toward a fundamental understanding of the rheological behavior of highly filled polymeric systems. Such systems may be considered as concentrated suspensions of rigid particles in viscoelastic fluids because, except for certain liquid resins (e.g. urethane or epoxy precursors), almost all thermoplastic resins exhibit non-Newtonian, viscoelastic behavior over the range of practical processing conditions.

2.4.1 Viscosity

The viscosity behavior of filled systems has been thoroughly studied. The viscosity increases with filler concentration, especially at low shear rates. At high shear

rates the flow curves of the filled materials approach the curve of the pure polymers (Czarnecki and White, 1980; Ottani et al., 1988; Poslinski et al., 1988). Ottani et al. (1988), Lavoie et al. (1996) and Carreau et al. (1996) found that particle-particle interactions in concentrated suspensions were responsible for a gel-type behavior at low shear stress and low strain, respectively. Ottani et al. (1988) discovered that the structure was disrupted at high shear stress values and the material behaves like a "dilute suspension". However, Lavoie et al. (1996) and Carreau et al. (1996) reported a strain hardening at a critical strain. Lakdawala and Salovey (1987a and 1987b) studied carbon black filled polymer/copolymer system and showed that low-shear viscosity behavior was governed more by the filler particles than by the suspending medium, whereas the opposite is expected of high-shear viscosity behavior.

The non-Newtonian behavior of polymers filled with non-interactive spheres is very similar to that of non-filled polymers, at least up to a solid fraction close to maximum packing. Poslinski et al. (1988) proposed a viscosity model to predict the suspension viscosity as a function of shear rate by taking into account the rheology of the polymer matrix and the volume fraction of suspended particulates. The expression of the model is as follows:

$$\eta_c = \tau_y(\dot{\gamma})^{-1} + \eta_c^0\left(1+(\lambda_c\dot{\gamma})^2\right)^{(n-1)/2} \tag{2.10}$$

$$\eta_c^0 = \eta_m^0(1-\phi/\phi_m)^{-2} \tag{2.11}$$

$$\lambda_c = \lambda_m(1-\phi/\phi_m)^{-2} \tag{2.12}$$

where η_m^0 is the zero shear rate viscosity of the matrix polymer, λ_m is a constant related to the onset of shear thinning, τ_y the yield stress, n the power law index, ϕ the volume fraction of filler, and ϕ_m the maximum volume fraction.

Efforts have been made to correlate relative viscosity with concentration of filler and to test the applicability of equation (2.13) & (2.14) to particle filled polymers (Kataoka et al., 1978 and 1979). The two empirical equations are:

Maron-Pierce (1956) $$\eta_r = (1 - \phi / \phi_m)^{-2} \tag{2.13}$$

Mooney (1951) $$\eta_r = \exp\left(\frac{2.5\phi}{1 - k\phi}\right) \tag{2.14}$$

Where η_r is the relative viscosity (which is the ratio of the viscosity of the filled polymer to that of the unfilled polymer at the same shear stress), k a model parameter. The two equations proved to be successful for predicting the relative viscosity-concentration relationship of suspensions of non-interactive particles in a Newtonian liquid. The same relationships were obtained in particle filled non-Newtonian polymeric systems for the volume fraction below a certain value and an asymptotic η_r was determined (Poslinski et al., 1988).

Mixing is a vital step in polymer processing because mechanical, physical and chemical properties, as well as "appearance", are strongly dependent on compound uniformity. The methods of mixing and the mixing conditions (e.g. mixing time) have a profound influence on compounds rheological properties in the molten state. Attempts have been made to study the effect of mixing methods on viscous properties by Kitano and Kataoka (1980). Three different methods, namely dry blending, extrusion, and elastic melt extrusion, were used to mix a polyethylene with glass fibers and carbon fibers respectively. The dispersion of fibers varied with the mixing methods used. The different dispersion methods result in variations of the viscous properties.

Another important variable that may affect the rheological properties of concentrated suspensions is the particle size. As the size of the filler particles decreases,

the ability to form a network and the strength of that network increases. The greater strength of the network formed by smaller particles results in a higher yield stress than the one measured for larger particles at the same volume concentration (Minagawa and White, 1976).

Bomal and Godard (1996) also studied the melt viscosity in terms of filler particle packing and maximum particle packing volume. They reported that the behavior of the particles in the matrix depended on matrix-filler interactions (polymer spreading and wetting) and particle-particle interactions (the particles tend to agglomerate due to attractive forces and form a gel-like structure). Such behavior could explain the ϕ_m values. If particle-particle interactions are prevalent over matrix-filler interactions, open agglomerates are formed and important polymer quantities are immobilized around the filler solid surface giving rise to loose packing and low ϕ_m. Such behavior is observed for untreated particles. In the case of particle-particle interactions weaker than the matrix-filler interactions, numerous connections between particles are needed to achieve immobilization. Particles then slide over each other to form compact agglomerates with very little blocked polymer. In this case, the more compact the packing is, the higher the ϕ_m value. They found that the surface treatment of particles reduced the particle-particle or matrix-filler interactions and immobilized polymer, thus decreased the melt viscosity and increased the maximum particle packing volume.

The particle-particle interactions are one of the non-hydrodynamic forces which may considerably modify the degree of dispersion of the solids or the structure with time during measurement or processing (Carreau et al., 1996). Another force – hydrodynamic force, which results from the relative motion of the suspending medium with respect to the particles, may affect the rheological behavior of concentrated suspensions as well. The hydrodynamic forces are responsible for migration of particles and structure breakdown in the cases of flocs and aggregates. Recently, there are extensive theoretical and experimental works reported on shear/strain-induced particle structures in various

concentrated suspensions that are subjected to inhomogeneous shear (Gadala-Maria and Acrivos, 1980; Leighton and Acrivos, 1987; Philips et al., (1992); Carreau et al., 1996; and Lavoie et al., 1996).

2.4.2 Primary normal stress difference

Observation of normal stresses in polymer melt rheology is a classical demonstration of melt elasticity. The first normal stress difference is a parameter characterizing the melt elasticity. Problems are encountered in normal stress measurements for highly filled systems due to the difficulty to measure normal stresses accurately, especially at low shear rates. Lobe and White (1979) found that yield stresses existed and interfered with normal stress measurements. They indicated the abnormal effects at low shear rates are due to interactions between the instrument and the yield stress property. As a result, a proper zero point for measurement could not be obtained. Tanaka and White (1980) found that there were residual stresses in the sample at the beginning, which were minimized by applying shear forces. Fillers in viscoelastic polymers are believed to reduce the elasticity of polymers (Metzner, 1985), but this effect remains to be verified and explained. Some experimental approaches have been reported to illustrate this phenomenon. Rong and Chaffey (1988) and Carreau et al. (1996) observed that the primary normal stress difference increased with increasing particle concentration.

2.4.3 Viscoelasticity

Dynamic melt rheology is an extremely powerful rheological technique offering several unique advantages. Li and Masuda (1990) investigated the viscoelasticity of calcium carbonate filled polypropylene melts in terms of particle dispersion. They observed that the filled melts possessed higher complex viscosities, which increased with particle concentration, especially at low frequencies. The high filled melts did not exhibit

the Newtonian flow region at low frequencies. A yield stress existed for highly filled melts in the low frequency region. The particle size had a markedly effect on the dynamic viscoelastic properties. The smaller particles with large surface area had a tendency to easily form agglomerated structure. The enhancement of particle-particle interactions increased the dynamic viscoelastic properties. The rheological history dependence of agglomerate formation showed that the viscoelastic behavior at high frequencies was dominated mainly by the polymer matrix. At low frequency, smaller particles form an agglomerated or network structure gradually building up with time. This could be seen from the viscoelastic property enhancement. On the other hand, the agglomerated structure of particles could be broken up under a shear stress produced by a steady shear flow.

Poslinski et al. (1988) presented an experimental result of dynamic viscosity and storage modulus for glass sphere filled polymers. They observed an increase of dynamic viscosity with filler content, especially at low frequencies, which is in agreement with the results of Li and Masuda (1990). Carreau et al. (1996) reported that the rheological properties were highly sensitive to the degree of the solids dispersion for rutile (TiO_2) filled polybutene system.

2.4.4 Cox-Merz rule

The Cox-Merz rule, equation (2.15), has been experimentally determined to be valid for a number of pure polymer melts (Kitano et al., 1980), but not for filled polymer melts (Rong & Chaffey, 1988; Wang & Wang, 1999). Shear viscosity of filled polymeric systems is always smaller than complex viscosity, the discrepancy becoming larger as shear rate (or angular frequency) and filler concentration increase. Cox-Merz's empirical rule is expressed by:

$$\eta^*(\omega) = \eta(\dot{\gamma}) \qquad \text{at} \qquad \omega = \dot{\gamma} \tag{2.15}$$

2.4.5 Yield stress

For the highly filled polymeric systems, viscosity at low shear rates or frequencies appears to be unbounded due to particle-particle interactions. This is referred to as a yield stress. Typical yield stress behavior exhibited by suspensions was described in the reviews by Metzner (1985) and Kamal and Mutel (1985). Yield stresses have been observed at filler concentrations as low as 10% vol. The relationship between yield stress and filler concentration has been shown to be an exponential one, which indicates that the strength of the interparticle network is also an exponential relationship of filler concentration (Bigg, 1983). The surface treatment significantly decreases the magnitudes of viscosity and results in lower yield values (Wang and Wang, 1999). The yield stress increases with decreasing particle size (Kataoka et al., 1978; Tanaka and White, 1980; and Suetsugu and White, 1983). Carreau et al. (1996) discovered a yield stress for non-colloidal (PVC) particle suspension in Newtonian matrix.

Yield values were found not only in shear flow but also in uniaxial extension (Lobe and White, 1979; Tanake and White 1980). These studies have indicated that the yield stress exists in both extension and shear. The most interesting effect discovered in these works is a critical dependence of yield behavior on volume concentration of the filler. Leonov (1990) made a theoretical attempt to describe the complicated rheological behavior of filled polymer. Without using mathematical yield criteria, his approach described all the basic features of the yield-like behavior of the filled polymer compounds, including the appearance of yield values in steady state flow, stress overshoots in start up flows, etc.

2.4.6 Strain-dependence

Bigg (1983) studied the rheological behavior of low-density polyethylene filled with a spherical stainless-steel powder. The system showed a strong effect of strain on

the dynamic rheological response, even though the particles are nonagglomerating. Poslinski and co-workers (1988) observed the same phenomenon for glass fiber filled polybutene system. The dynamic viscosity is indeed found to decrease with an increase of the imposed strain. Rong and Chaffey (1988) and Wang and Wang (1999) reported the strain-dependence of highly filled polystyrene and polypropylene melts (e.g., the one with 60% by mass) even at strain amplitudes as low as 0.3%. The onset of the non-linear viscoelastic region occurs at lower strain amplitude for filled systems than for unfilled systems. Carreau et al. (1996) showed an absence of linear viscoelastic domain for concentrated PVC/PB suspension. The dynamic moduli dropped drastically with increasing strain amplitude. They characterized it to a gel-type structure with very weak particle-particle interactions, which is destroyed rapidly with increasing strain.

2.4.7 Effect of surface treatment on the rheological properties

The state of polymer-particle interface will affect the interparticle morphology. Certain polymers form weak bonds with selected fillers. These bonds may be due to van der Waals, polar, or hydrogen bonding forces. Polymers can be covalently bonded to fillers through a coupling agent. Each of these situations influences the interparticle network and the rheological behavior of the system. The greater the adhesion between the polymer and the filler, the lower the tendency for the particle to agglomerate and the better the resulting dispersion.

The adhesion between polymers and fillers can often be improved by surface treatment of the filler, modifying the mechanical strength and the chemical resistance of compounds. This is particularly true for nonpolar polymers filled with polar fillers. The exact mechanism by which surface treatment, wetting agents and coupling agents work has been the subject of many articles, not all of which show agreement (Boaira and Chaffey, 1977; Han et al., 1981; Bigg, 1983; and Suetsugu and White, 1983). Most have shown that the surface modifier coats the filler particles, displacing air and water from

the particle's surface. The stability of composites appears to be related to the strength of the covalent bonds between the resin and the filler via the coupling agent. Certain functional forms of the surface-modifying molecule, along with appropriate processing conditions, may provide additional bonding between the filler and the polymer.

Bigg (1983) examined the effect of surface modifiers on particle deagglomeration for aluminum oxide filled low-density polyethylene systems. Surface treatments were found to be effective in reducing the degree of agglomeration, thus decreasing the viscosity of the composite. This greatly improves the ease of processing. Suetsugu and White (1983) studied the influence of filler surface coating on the rheological behavior of calcium carbonate filled polystyrene system. They found that compounds with coated particles resulted in major viscosity reductions. The surface coating was most effective with the smallest particles. It presumably reduced interaction between particles and the extent of aggregation. Han et al. (1981) investigated the effects of coupling agents on the rheological properties. They reported that a coupling agent which reduced the melt viscosity of a filled polymer also increased the normal stresses and vice versa. In other words, the change in viscosity due to the presence of a coupling agent was in the direction opposite to the change in normal stresses. With the proper combinations of polymer, filler, and coupling agent, it is possible to change the rheological properties of highly filled polymeric systems drastically. They also pointed out that the possibility existed that the coupling agent might have diffused into the polymer matrix, playing the role of an internal plasticizer, which would then decrease the viscosity of the 'virgin' polypropylene phase.

2.4.8 Elongational viscosity measurements

Lobe and White (1979) have made elongational viscosity measurements under constant elongational rate for carbon black reinforced polystyrene using Ide rheometer. Tanaka and White (1980) utilized the same technique to examine the elongational

viscosity for $CaCO_3$ and TiO_2 filled systems. Some interesting results are found: (1) the elongational viscosity increases with filler content level, (2) the elongational viscosity decreases rapidly with increasing elongation rate, (3) the highly filled melts also exhibit yield value in extensional flow, (4) surface treatment for $CaCO_3$ filled PS melts significantly decreases the viscosity and gives a lower yield stress. Han and Kim (1974) obtained similar results. They used isothermal melt spinning methods to investigate the spinline elongational viscosity of polypropylene filled with calcium carbonate.

CHAPTER 3 - EXPERIMENTAL

The experiments include three major steps:

- Preparing the compound of polypropylene with calcium carbonate using co-rotating twin-screw extruder
- Determining the dispersion index
- Measuring the rheological properties

In this chapter, the different experimental methods for sample preparation and measurements will be described. Since the first and the second steps are very similar to procedures used by Bories (1998), emphasis will be put on the rheological property measurement.

3.1 Materials

The polymer used in this study was a commercial polypropylene manufactured by Montell Co., Canada. PP SM6100, a high melt flow polypropylene homopolymer resin, has a weight average molecular weights M_w of 264,000, a polydispersity M_w/M_n of 11, a density of 0.9g/ml and a melt flow index of 12g/10min.

Two types of untreated calcium carbonate powders, OMYACARB F and OMYACARB UF manufactured by OMYA, INC., were used as fillers. Their main characteristics are summarized in Table 3.1. The main difference between both is the average diameter which is 1.4μm for the first and 0.7μm for the second.

3.2 Compounding procedure

3.2.1 Twin-screw extrusion

The compounds and the "pure" component were prepared with a twin screw

Table 3.1: Characterization of Calcium Carbonate

Filler	F	UF
Type	Fine	Ultra Fine
Grade	OMYACARB F	OMYACARB UF
Specific gravity	2.7	2.7
Median diameter (μm)	1.4	0.7
Particles finer than 2 μm (%)	60	90
Particles finer than 1 μm (%)	40	65
Specific surface area (m^2/g)	7	12

extruder Leistrizt 30-34 in an intermeshing co-rotating mode. All the compounds are represented by weight percentage of $CaCO_3$. Compounds of composition of 25%, 30%, and 50% were prepared. 0.2 wt% of antioxidant (Irganox B225 from Ciba-Geigy) was added to all the compounds and "pure" component. The polymer and filler were metered independently and feed directly to the throat of the extruder, using volumetric dosing units. In order to assess the influence on filler dispersion of introducing calcium carbonate filler into previously melted polymer, some runs were undertaken in which the mineral additive was introduced via the downstream feed/vent port located midway along the machine. The melt was extruded through a two capillaries die (which has diameter of 2.5 mm and length of 5.5 mm each) into a water bath and then pelletized. The melt temperature was maintained at 200°C.

In this study, four well-defined processing conditions and two types of screw configuration that contained different numbers of kneading disk blocks were used to prepare the compounds. The process variables considered were screw speed and flow rate. They are listed in Table 3.2. The twin-screw extruder configuration is showed in Figure 3.1 and detail screw configurations are illustrated in Figure 3.2. The melting and mixing zones are composed of kneading discs staggered at +30°/-60°. The discs thickness

Table 3.2: Mixing conditions

Configuration	Screw Geometry		Sample code	Filler added	Speed (rpm)	Flow rate (kg/h)
	Melting	Mixing				
1	(+)*	(+)	dps1	entrance	350	15
			dps2	center	250	20
2	(-)*	(-)	dps3	entrance	250	20
			dps4	center	350	15

* (+) ---- More kneading discs

(-) ---- Less kneading discs

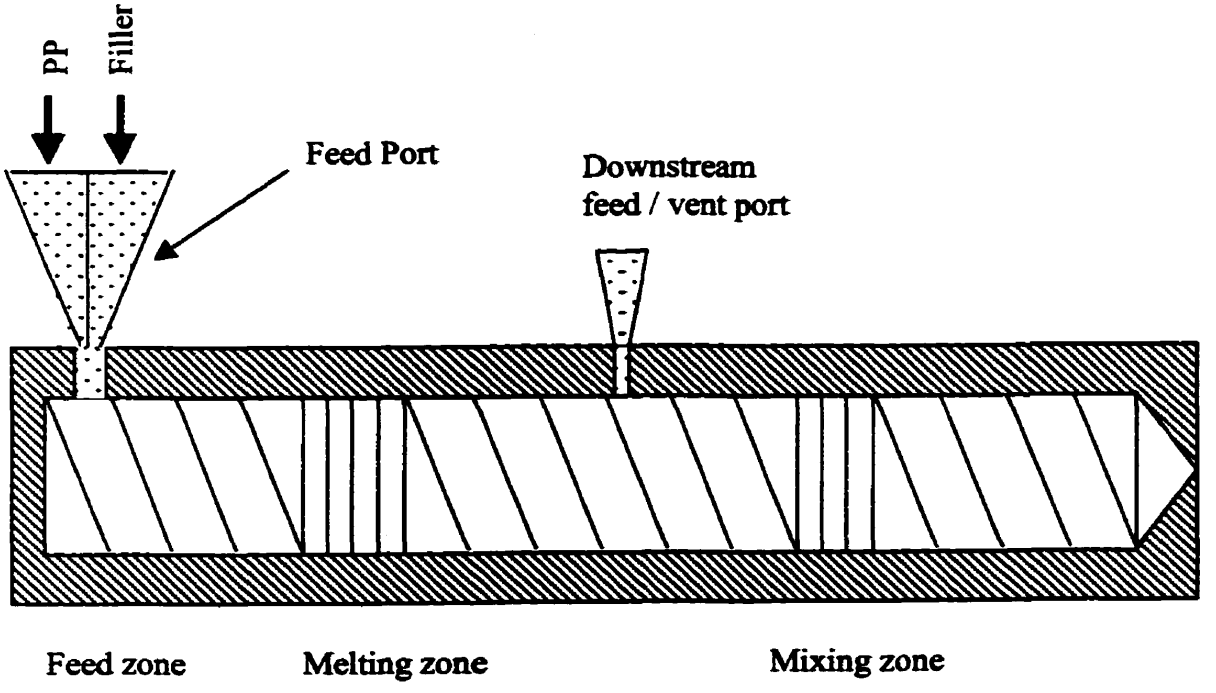

Figure 3.1: Twin-screw extruder configuration

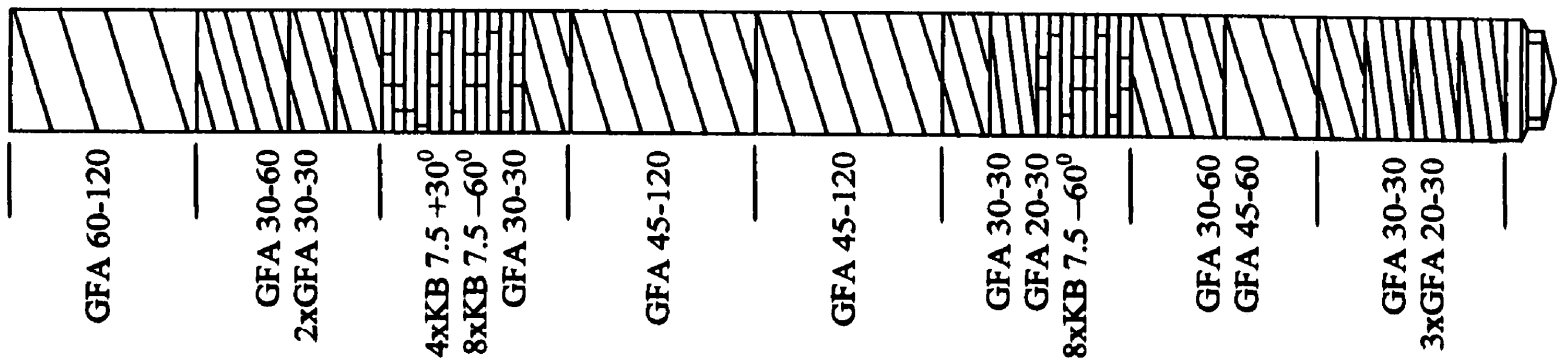

(a) Configuration 1

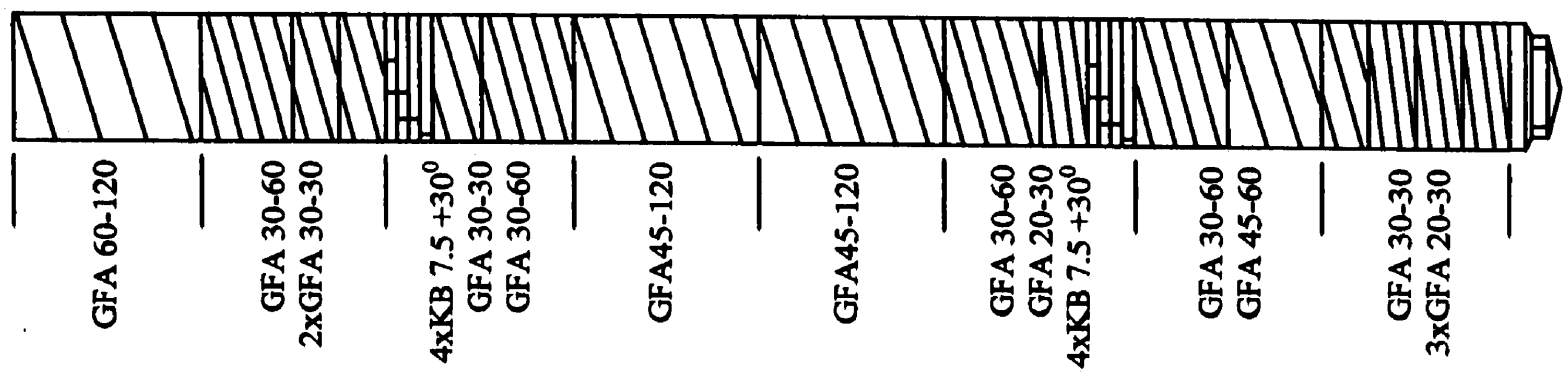

(b) Configuration 2

Figure 3.2: Screw configuration

is 7.5 mm. Configurations 1 and 2 in Figure 3.2 differ by the number of discs and the stagger angle. The kneading discs were used for dispersing the fillers.

3.2.2 Verification the concentration of compounds

The apparatus used to add fillers into twin-screw extruder was controlled by volumetry. The inconvenience of this type of apparatus is the variation of flow rate, especially for material with small particle size that tends to agglomerate and form cave during feeding. For this reason, it was necessary to verify after mixing whether the concentration of filler in the compound was close to the one expected. Pyrolysis of the polymer was used to determine the concentration of the compounds. The compound was put into a small ceramic cup, ashed in a furnace to remove the polymer matrix at 250°C for 1 h followed by 500°C for 4 h. Then, the percentage of filler was calculated using following equation:

$$filler\% = \frac{m_c}{m_t} x100 \tag{3.1}$$

where m_t is the total weight of compound and m_c is the weight of calcium carbonate. This procedure was repeated two times for each compound, and an average weight percentage was obtained.

3.3 Determination of dispersion index

Screw geometry, processing conditions and concentration of filler will affect the quality of mixing. To characterize the dispersion state in the compound, Bories (1998) gave a detailed description of the mechanism and the procedure to determine the dispersion index. It consists of two steps: (1) preparing a blown film, (2) analyzing the agglomerates within the film using microscope and image analyzer. Here, these two steps will be described briefly.

3.3.1 Blown film preparation

First, each compound prepared using the twin-screw extruder was dry blended with "pure" material to dilute it to 5 wt% $CaCO_3$. This compound was used to prepare the blown film with a 45-mm Killion single-screw extruder with a helical blown film die (outer diameter = 50.82 mm and die gap at exit = 680 μm). The extrusion was carried out at a temperature of 210°C. The flow rate was controlled by the film thickness, which should not exceed 40μm.

3.3.2 Microscope and image analyzer

From the blown film, the morphology of each sample was determined using a transmitted-light microscopy (Nikon OPTIPHOT-2). The image was captured by a Sony DXC-151A color video camera, and stored in the computer. The agglomerates of calcium carbonate, which appear as dark areas, have the required degree of contrast relative to the polymer matrix for subsequent measurements by image analysis. Later, the number and volume average diameters d_n and d_v of at least 400 particles were analyzed by an automatic particle-sizing software. The automatic particle-sizing software works as an analyzer on the principle of detecting all gray levels above an operator-determined value and expresses the detected areas in pixels. In order to obtain sufficient contrast between the polymer matrix and the filler component, the lower limiting size of agglomerates by our study was 10 pixel^2, which was a square of 10 μm in length or a circle of 15 μm in diameter. Thus, the dispersion index f can be calculated from the number average diameter using equation (2.8).

3.3.3 Dispersion index f

From the measurement of size and number of agglomerates through image analyzer, the dispersion index could be determined. The dispersion index f developed by Bories (1998) is a function of volume fraction of agglomerates, defined by equation (2.8) in

Chapter 2. The correlation of dispersion index with rheological properties could then be obtained by rheological measurements. Not only the size of agglomerates but also the numbers of agglomerates, presumably affect the rheological properties. We discuss the correlation between state of dispersion and rheology behavior in Chapter 5 using the dispersion index defined by equation (2.8).

3.4 Rheological measurements

3.4.1 Viscoelasticity

The samples for rheological measurements have been prepared by compression molding using a CARVER laboratory press at 200°C. The pressure load was increased progressively from 200 kPa to 1.1 MPa.

Rheological property tests have been carried out on a controlled stress rheometer (Bohlin CSM) equipped with concentric disk geometry. The diameter of the plates was 25 mm and the gap about 1.2 mm. The measurements were carried out under dry nitrogen atmosphere at the desired temperature. The stability was verified at two low constant frequencies (0.01 Hz and 0.1 Hz) for periods of over 1 h. The linear viscoelastic properties were measured as a function of frequency with the frequency range from 0.01 to 10 Hz. The applied stress was controlled to maintain the total deformation at around 1 %. In order to keep the measurement in a pseudo-equilibrium state, the materials were pre-oscillated for 15 min under low strain ($\gamma = 0.05$) and low frequency (0.01 Hz). Each measurement was repeated at least two times. If the results were not reproducible, a third measurement was carried out. The results represent the average values obtained from repeated experiments.

3.4.2 On-line slit rheometer

As it will be shown in the next section, shear viscosity data, and more precisely

power-law parameters of the compounds or "pure" component are needed to determine an apparent extensional viscosity. The slit rheometer has been used with the single screw extruder to measure the power-law properties. The setup of this slit rheometer is shown in Figure 3.3. A by-pass valve concept was employed in order to change the flow rate through the slit, while the total extruder flow rate remained constant thus leaving extruder-operating conditions unchanged. With this design, the morphology of the blends before die extrusion can be controlled by keeping the thermomechanical history unchanged. The slit geometry was chosen in order to use flush mounted pressure transducers located along the channel. With these, the axial pressure distribution was obtained from which the wall shear stress was calculated, the apparent shear rate was determined by measurements of the polymer flow rate. The geometry of the die was 60 mm in length, 25.4 mm in width and 1.2 mm in height. Three pressure transducers were separated in equal interval along the die with the temperature set at 200°C.

The viscosity and power-law parameters can be obtained by the following Rabinowitsch analysis (Carreau et al, 1997). Consider the flow in a thin rectangular slit as illustrated in Figure 3.4. For H<<W<<L, we neglect side wall effects and assume a fully-developed unidirectional flow situation. That is

$$V_z = V_z(y) \tag{3.2}$$

$$V_x = V_y = 0 \tag{3.3}$$

$$\eta = \eta(\dot{\gamma}_{yz}) \tag{3.4}$$

$$\begin{aligned} Q &= 2\int_0^{2W}\int_0^H V_z\,dy\,dx \\ &= -\int_0^H 4wy\frac{dV_z}{dy}dy \end{aligned} \tag{3.5}$$

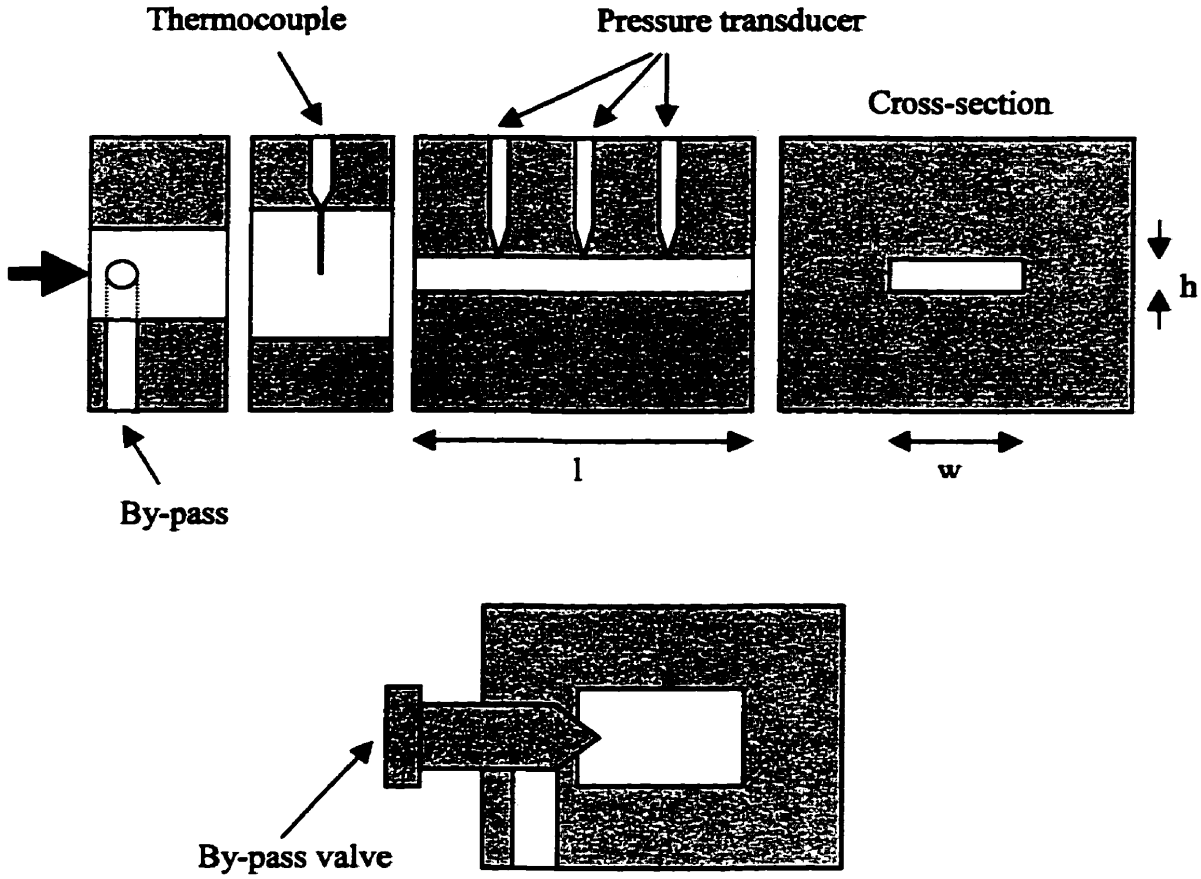

Figure 3.3: Slit die setup

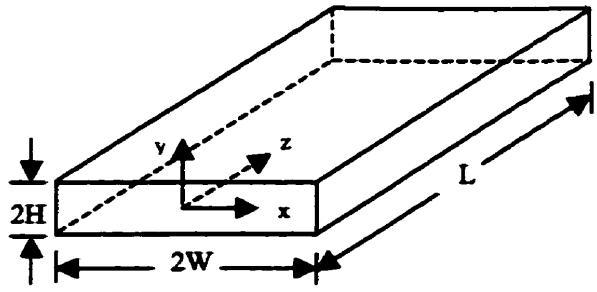

Figure 3.4: Thin slit geometry

Then a momentum balance on a differential fluid element $2WL\Delta y$ yields

$$\sigma_{yz} = \frac{\Delta P}{L} y = \frac{y}{H} \sigma_H \tag{3.6}$$

where σ_H is the shear stress at the wall at $y = \mp H$, and ΔP the total pressure drop.

Equation (3.5) becomes, after the change of variables, $y \rightarrow \sigma_{yz}$,

$$Q = \frac{4WH^2}{\sigma_H^2} \int_0^{\sigma_H} \sigma_{yz} \left(-\frac{dV_z}{dy} \right) d\sigma_{yz} \tag{3.7}$$

Taking the derivative of this expression with respect to σ_H and using Leibnitz's rule, the equation can be written as

$$\frac{d}{d\sigma_H} \left(\frac{\sigma_H^2 Q}{4WH^2} \right) = \frac{d}{d\sigma_H} \int_0^{\sigma_H} \sigma_{yz} \left(-\frac{dV_z}{dy} \right) d\sigma_{yz} \tag{3.8}$$

Hence the shear rate evaluated at the wall is expressed by

$$-\dot{\gamma}_H = \frac{1}{4WH^2 \sigma_H} \frac{d}{d\sigma_H} \left(\sigma_H^2 Q \right) \tag{3.9}$$

This result can be rewritten in the following form:

$$n' = \frac{d \ln \sigma_H}{d \ln (Q / 4WH^2)} \tag{3.10}$$

$$-\dot{\gamma}_H = \left(2 + \frac{1}{n'} \right) \frac{Q}{4WH^2} \tag{3.11}$$

The coefficient n' is the local slop of the wall shear stress versus $Q/4WH^2$ on log-log plot. For power-law fluids, the slope n' is constant and equal to power law index n. Knowing n', the shear rate at the wall can be calculated from equation (3.11), and the non-Newtonian viscosity at the wall shear rate is by definition expressed by

$$\eta(\dot{\gamma}_H) = -\frac{\sigma_H}{\dot{\gamma}_H} \tag{3.12}$$

3.4.3 Elongational viscosity

3.4.3.1 Technique

Measuring elongation flow properties is difficult for many substances, if not impossible. Many different and unique techniques have been employed to obtain a measurement of the elongation viscosity, such as fiber spinning, opposed jets, and converging flow. The most utilized technique is entry flow through a contraction where the entry pressure drop is recorded as a function of flow rate. The first to analyze this type of flow was Cogswell (1972). He divided the fluid deformation into two terms: one due to shear and the other to elongation. Binding (1988) and Mackay and Astaria (1997) re-examined and improved Cogswell's analysis (1972 and 1978) by using the technique of power consumption minimization. In our study, Cogswell (1972) and Binding (1988) analyses have been employed.

One of the critical requirements in the measurement of melt elongational viscosity is that a controlled and constant elongational strain rate should be applied. This can be achieved, however, by choosing properly the shape of the converging section. Binding and Jones (1989), Kim et al (1994) used a planar hyperbolic die to measure and explain the extensional viscosities of polymer solution. James and Chandler (1990) suggested that if the shape of a cylindrical converging die was given by $R^2(z) = \text{const}$, where R is the die

radius depending on z, a constant elongational strain rate could be reached. The elongational strain rate for an axisymmetric converging die with the shape $R = R(z)$ was defined by (Lacroix et al., 1999):

$$\dot{\varepsilon}(z) = \frac{d\langle V_z \rangle}{dz} \tag{3.13}$$

where $\langle V_z \rangle$ is the average velocity at a given z. And the velocity can be written as:

$$\langle V_z \rangle = \int \dot{\varepsilon}(z) dz \tag{3.14}$$

If Q denotes the total volumetric flow rate,

$$Q = \pi R(z)^2 \int \dot{\varepsilon}(z) dz \tag{3.15}$$

Therefore,

$$\dot{\varepsilon}(z) = \frac{Q}{\pi} \frac{d}{dz}\left(\frac{1}{R(z)^2}\right) \tag{3.16}$$

By imposing a constant elongational strain rate, the solution of the differential equation leads to:

$$R(z) = \left(\frac{\dot{\varepsilon}\pi z}{Q} + \frac{1}{R_1^2}\right)^{-1/2} \tag{3.17}$$

where R_1 is the initial radius of the nozzle die. In this study, we used two dies of different geometry to investigate the $CaCO_3$ filled polypropylene systems. One die (D1) is 10 mm

long with an exit radius of 1.995 mm whereas the other one (D2) is 20 mm long with an exit radius of 2.805 mm. Both dies have the same entry radius of 12.7 mm. The setup illustrated in Figure 3.5 was designed to measure elongational viscosity from a single screw extruder. A by-pass valve used in this design has the similar function as that in slit die. Furthermore, it allows us to extract samples before and after the converging section so that the resulting dispersion index can be analyzed in relation to the elongational effects generated by the die. The same setup has been used by Lacroix et al (1999) to investigate the morphological evolution of the PP/EVA/EMA blends. In our case, the elongational properties of the $CaCO_3$/PP composites with different dispersion index are compared to the properties of the unfilled components. The melt temperature was kept at 200°C during the experiment.

Two different approaches, the Cogswell and Binding analyses, were adopted in presenting our results of shear and extension. Lacroix et al. (1999) explained in detail the analysis using the Cogswell and Binding concepts.

3.4.3.2 Cogswell analysis

Cogswell (1972) provided a simple analytical analysis, which split the entry pressure drop into shear and elongational components:

$$\Delta P_{ent} = \Delta P_s + \Delta P_e \tag{3.18}$$

The sketch of the convergent die is presented in Figure 3.6. The shear viscosity was assumed to obey power-law, while the extensional viscosity was constant. The flow was assumed to be locally fully developed. The pressure drop due to shear is expressed as:

$$\Delta P_s = \frac{4}{3}\frac{mQ}{(n+1)\dot{\varepsilon}\pi}\left(\frac{(3n+1)Q}{n\pi}\right)^n\left[\left(\frac{1}{R_0}\right)^{3(n+1)} - \left(\frac{1}{R_1}\right)^{3(n+1)}\right] \tag{3.19}$$

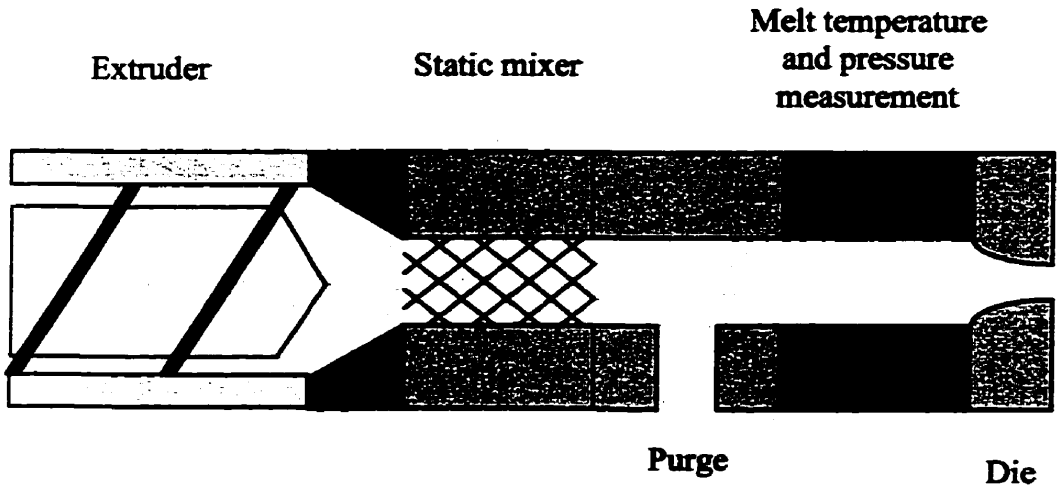

Figure 3.5: Elongational measurement setup (adopted from Lacroix et al., 1999)

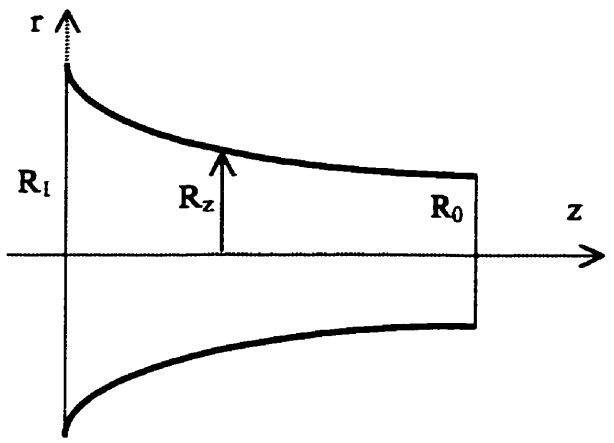

Figure 3.6: Convergent geometry

where n and m are the power-law index and parameter of the shear viscosity respectively. R_0 and R_I are the outlet and inlet radii respectively. The pressure drop due to elongational flow can be derived from energy consideration and given by:

$$\Delta P_e = \eta_e \dot{\varepsilon} \ln\left(\frac{Q/\pi R_1^2 + \dot{\varepsilon} l}{Q/\pi R_1^2}\right) \tag{3.20}$$

where η_e is the elongational viscosity and l is the length of the die. Substituting equation (3.17) in equation (3.20), we obtain:

$$\Delta P_e = 2\eta_e \frac{Q}{\pi l}\left(\frac{1}{R_0^2} - \frac{1}{R_1^2}\right)\ln\left(\frac{R_1}{R_0}\right) \tag{3.21}$$

The extensional viscosity is readily estimated from experimental entrance pressure drop/flow rate data, if the shear viscosity parameters are known.

3.4.3.3 Binding's analysis

Binding (1988) presented a more rigorous analysis by using an energy balance. In addition, he assumed that the elongational viscosity was a power-law function of the extension rate, and variational principles were employed to minimize the energy dissipation W. The power consumption W related to the entrance pressure drops by $\Delta P_{ent} Q = W$. W is divided into three contribution of shear, elongation and kinetic energy variation.

In contrast to Cogswell, Binding assumes power-law behavior for both shear and elongational flow. That is:

$$\eta_s = m|\dot{\gamma}|^{n+1} \tag{3.22}$$

$$\eta_e = L|\dot{\varepsilon}|^{t+1} \tag{3.23}$$

where t and L are power-law index and parameter of elongational viscosity respectively.

Following Binding's analysis (1988), Lacroix et al. (1999) derived the expression for a hyperbolic shaped die with constant elongational rate as:

$$W = \frac{4mQ^2}{3(n+1)\dot{\varepsilon}\pi}\left(\frac{(3n+1)Q}{n\pi}\right)^n\left[\left(\frac{1}{R_0}\right)^{3(n+1)} - \left(\frac{1}{R_1}\right)^{3(n+1)}\right] + I_{nt}QL\left(\frac{3n+1}{n+1}\right)^{t+1}\left(\frac{\dot{\varepsilon}}{2}\right)^t \ln\left(\frac{1}{\beta^2}\right) + \frac{3}{2}\rho Q^3 \frac{(3n+1)^2}{(2n+1)(5n+3)}\frac{1-\beta^4}{\pi^2 R_0^4} \tag{3.24}$$

where β is the inverse of the contraction ratio ($\beta = R_0/R_1$). I_{nt} is defined by:

$$I_{nt} = \int_0^1 \left|2 - \frac{3n+1}{n}\phi^{1+1/n}\right|^{t+1} \phi d\phi \tag{3.25}$$

The power-law parameter t of the extensional viscosity can be obtained from pressure drop/flow rate data and shear viscosity parameter. Having determined t, the constant I_{nt} is easily evaluated from equation (3.25). The value of L is then obtained from equation (3.24).

3.4.4 Flow field characterization

To assess the efficiency of elongational flow and shear flow in dispersive mixing,

the flow fields were analyzed in terms of the parameter λ defined by Cheng and Manas-Zloczower (1990):

$$\lambda = \frac{\dot{\gamma}}{\dot{\gamma} + \omega} \tag{3.26}$$

where $\dot{\gamma}$ is the magnitude of the rate-of-deformation tensor and ω is the magnitude of the vorticity tensor. The flow in slit die was simple shear flow and has the value of λ of 0.5. While the flows in converging die included the elongational and shear flow components, The converging die was divided into a number of small converging sections. The average value of the parameter λ for the entire geometry was calculated from the corresponding parameter for each section.

CHAPTER 4 - INFLUENCE OF OPERATING CONDITIONS AND SCREW GEOMETRY ON DISPERSION

Experimental work on the efficiency of screw geometry in terms of dispersive mixture quality, as well as processing conditions on the dispersion state, have been carried out. In this chapter, we first present the dispersion index results, then discuss the factors influencing dispersive mixing.

4.1 Results

Table 4.1 summarizes the results for the dispersion index f and volume average diameter d_v of the agglomerates, which relate to processing parameters, screw configuration, concentration of the mineral filler, and particle size of the filler, for all the experiments.

In our experiments, the operating conditions included screw speed, mass flow rate, the location where filler was fed, the concentration and particle size of the filler. The operating variables were selected in our study in an attempt to produce the significant variations of dispersion, so that the quality of dispersive mixing could be correlated to the rheological properties. The role of the compounding conditions on the agglomerate size was studied by Bories (1998). In the table and figures of this chapter, the codes "cfg" and "dps" have been used. They are the abbreviation of configuration and dispersion respectively. The term "cfg" represents the screw configuration while the "dps" indicates the processing parameters as specified in Table 4.1.

4.2 Discussion

As explained earlier in Chapter 3, kneading discs were placed in the melting and

Table 4.1: Dispersion Index f and volume average diameter of $CaCO_3$ in matrix PP

No	Operating Condition	Screw	Position	Speed (rpm)	Flow Rate (kg/h)	$CaCO_3$		Index f	$\frac{\rho_{mineral}}{\rho_{agglomerate}}$	d_v (μm)
						Type	wt%			
1	dps1	cfg1	entrance	350	15	F	25.4	0.82	4.63	117
2						F	48.2	1.28	7.17	200
3						UF	26.3	1.34	7.53	124
4						UF	47.0	1.42	7.82	203
5	dps2		center	250	20	F	26.5	1.63	6.44	172
6						F	47.2	3.31	12.05	261
7						UF	26.1	1.89	7.01	182
8						UF	47.0	3.25	13.85	258
9	dps3	cfg2	entrance	250	20	F	25.8	1.49	6.24	164
10						F	47.8	2.99	10.45	248
11						UF	25.0	1.68	7.25	176
12						UF	47.5	2.98	10.99	245
13	dps4		center	350	15	F	26.1	1.12	4.89	128
14						F	48.5	1.67	8.33	226
15						UF	25.3	1.44	7.58	134
16						UF	46.8	1.57	8.14	214

mixing zones of the screw. The difference between the configurations 1 and 2 is the number of kneading discs used in these two areas. Other variables considered included operating parameters (screw speed and mass flow rate), the location of filler addition to the extruder (i.e. feed to the hopper/entrance or the downstream/center entry port), and the particle size (fine or ultra fine powder). Results in Figure 4.1 and 4.2 show the effect of these variables on filler dispersion.

Using screw configuration 1, the filler powder introduced through the

downstream feed-port gave a higher value of dispersion index (Figure 4.1a). In this screw geometry, there are strong mixing elements which are located right after the feeding zone. The kneading discs act as partial barriers to flow, increasing the energy input. Therefore, melting in the twin-screw extrusion occurs over a relatively narrow region of the screw. The polymer is fully molten to wet the filler and an important break-up of agglomerates occurs. When feeding the filler via the downstream feed-port using screw configuration 1, the agglomerates may be compressed under significant force due to the strong mixing element in mixing section to form agglomerates and will be difficult to break up. Similar results were observed by Bories (1998) and Ess and Hornsby (1987).

Increasing screw speed and reducing flow rate have the equivalent effects on the final dispersion state. As the screw speed increases, the higher shear stresses are undoubtedly generated in the melt and a better dispersion is achieved. Reducing the flow rate may cause an increasing in the residence time and specific mechanical energy, which results in the decrease of the agglomerate size. Bories (1998) has also found the similar effects of screw speed and flow rate on dispersion of calcium carbonate in PP matrix during twin-screw extrusion.

The result of dispersion index using screw configuration 1 is shown in Figure 4.1. The higher screw speed and lower flow rate are incorporate to the process that the powder is fed in the hopper of the screw. Thus, a significant agglomerate breakdown is obtained compared to the process where the powder is fed in the downstream feed-port with lower screw speed and higher flow rate. This result is also observed for screw configuration 2.

Configuration 2 has less kneading discs in both the melting and mixing zones. It is interesting to note that this type of screw geometry has a distinct influence on the dispersion compared to the configuration 1 for material compositions under investigation. Observed discrepancy is shown in Figure 4.1. Size reduction only occurred during

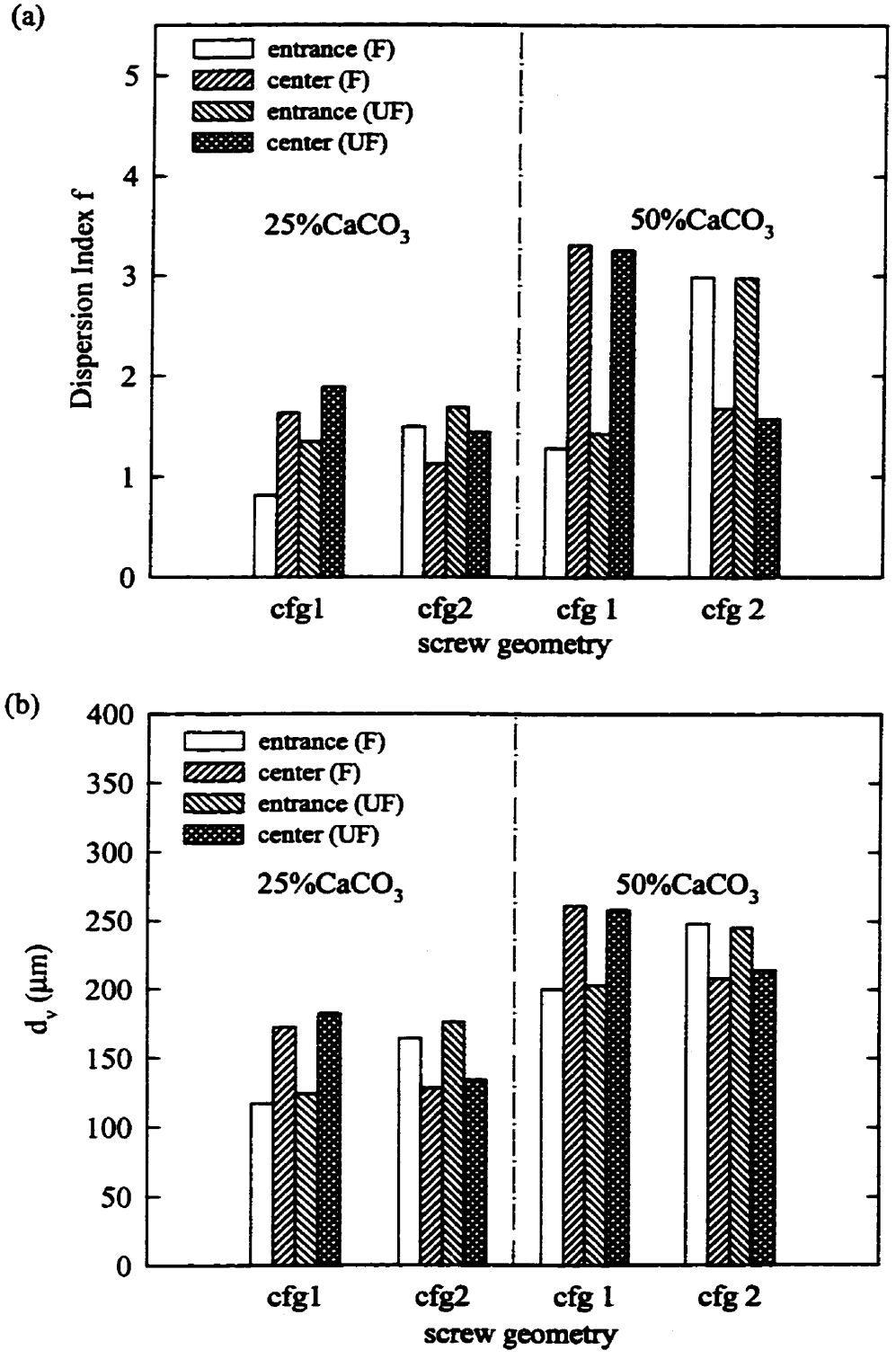

Figure 4.1: Effect of feeding position on: (a) dispersion index, (b) volume diameter

dispersive mixing operations when the filler was added in the downstream entry port. Less kneading discs in the melting zone reduce the level of shear stress. As a result, melting in the twin-screw extrusion occurs over a wider region of the screw. The polymer is probably not fully melted as it passes through the metering zone. The incorporation of the filler in solid or low-temperature molten polymer leads to a better dispersion because the hydrodynamic forces acting on the agglomerate surfaces are stronger than in configuration where the filler is incorporated to low viscosity melts (Bories, 1998). As a result, reducing the kneading discs in the melting section will result in a better dispersion when feeding the filler at the downstream feed-port. Mack (1990) observed the same phenomena in his paper.

The dispersion index is not only dependent on the maximum level of shear stresses encountered in the machine, but also on the available time during which the agglomerates are exposed to shear intensity. As we can see from Figure 4.1, the agglomerate size and the dispersion index value in the composition of dps3 is less than that in the compound of dps2. This suggests that the filler agglomerates in dps3 experience longer time through the region of shear.

The effects of the screw configuration and processing conditions on the dispersion state, in terms of dispersion index, are in the following order:

(best dispersion) dps1 > dps4 > dps3 > dps2 (worst dispersion)

Changes in filler concentration and particle size influence the dispersion for the compounds investigated. The results are shown in Figures 4.2a and 4.2b. An increase of $CaCO_3$ concentration from 25% to 50% will almost double the dispersion index. It should be noted that the influence of the filler particle size on dispersion depends on the concentration of the additive. At low concentration (25%), the smaller the particle size, the worse the dispersion is. In contrast, the particle size has less effect at high filler concentration (50%). It suggests that, the smaller the filler particle size, the smaller the

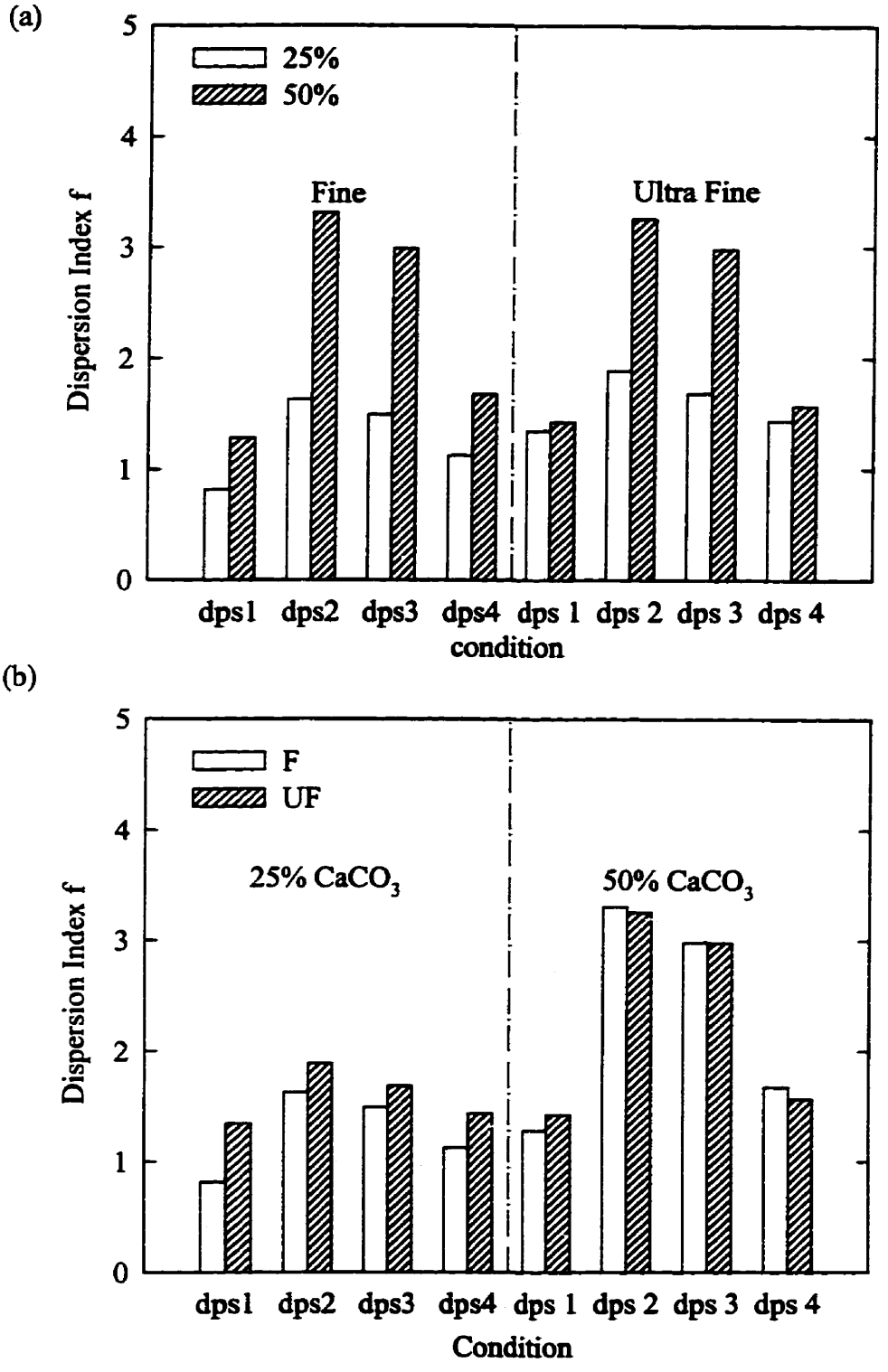

Figure 4.2: Influence of operation conditions: (a) concentration, (b) particle size

bulk density, thus increasing the amount of air supplied from the feed port. Air contained in the filler becomes compressed in the kneading disc zone and is separated as the filler is mixed and kneaded with molten polymer. Portion of air flows back toward the feed port, reducing the conveying force of the screw itself. As the content of calcium carbonate powder increases, the influence of air trapped in the powder on the dispersion become less important compared to the effects of concentration.

In this chapter, the results of dispersion index and volume average diameter of the calcium carbonate powder have been presented and discussed. In the following two chapters, these results are utilized to correlate and explain some rheological properties and phenomena encountered in the rheological experiments.

CHAPTER 5 - VISCOELASTICITY

Rheological properties are important to understand the phenomena encountered during processing. The rheological properties of the compounds are strongly dependent on filler dispersion, and the degree of dispersion is closely associated with the processing. Therefore, rheological methods can be a powerful tool to elucidate the processing/property relationships. The viscoelasticity of calcium carbonate filled polypropylene melts with various dispersions has been extensively studied. In this chapter, we present our results on the rheological behavior obtained for untreated $CaCO_3$ in PP matrix, and correlate them to the dispersion state.

5.1 Stability of filled polypropylene

Figure 5.1 reports the variation of the complex viscosity and moduli with time measured at 200°C and 0.01Hz for $CaCO_3$ filled polypropylene melts at three different concentrations. The moduli of the unfilled PP and PP with 25% $CaCO_3$ are observed to reduce by only a few percents over the time scale of the experiments. They exhibit stable behavior. However, as shown in the figure, the loss and storage moduli of 35% $CaCO_3$/PP increase significantly with time. The effect is important for the storage modulus and the behavior with time becomes more and more solid-like. While for 50% $CaCO_3$/PP, the moduli increase within the first 15 min, followed by a moderate decrease.

We believe that the phenomenon observed in compound of 35% $CaCO_3$ is due to the buildup of network caused by the interaction between calcium carbonate particles. When the concentration of the dispersed phase is higher than a certain critical value, attractive forces acting between particles in the dispersion may cause a three-dimensional structure to be built up. In the present study, the loading at around 30% - 35% is considered to be the critical concentration at which the interaction between particles dominates the rheological behavior of $CaCO_3$/PP systems. The network of particles plays

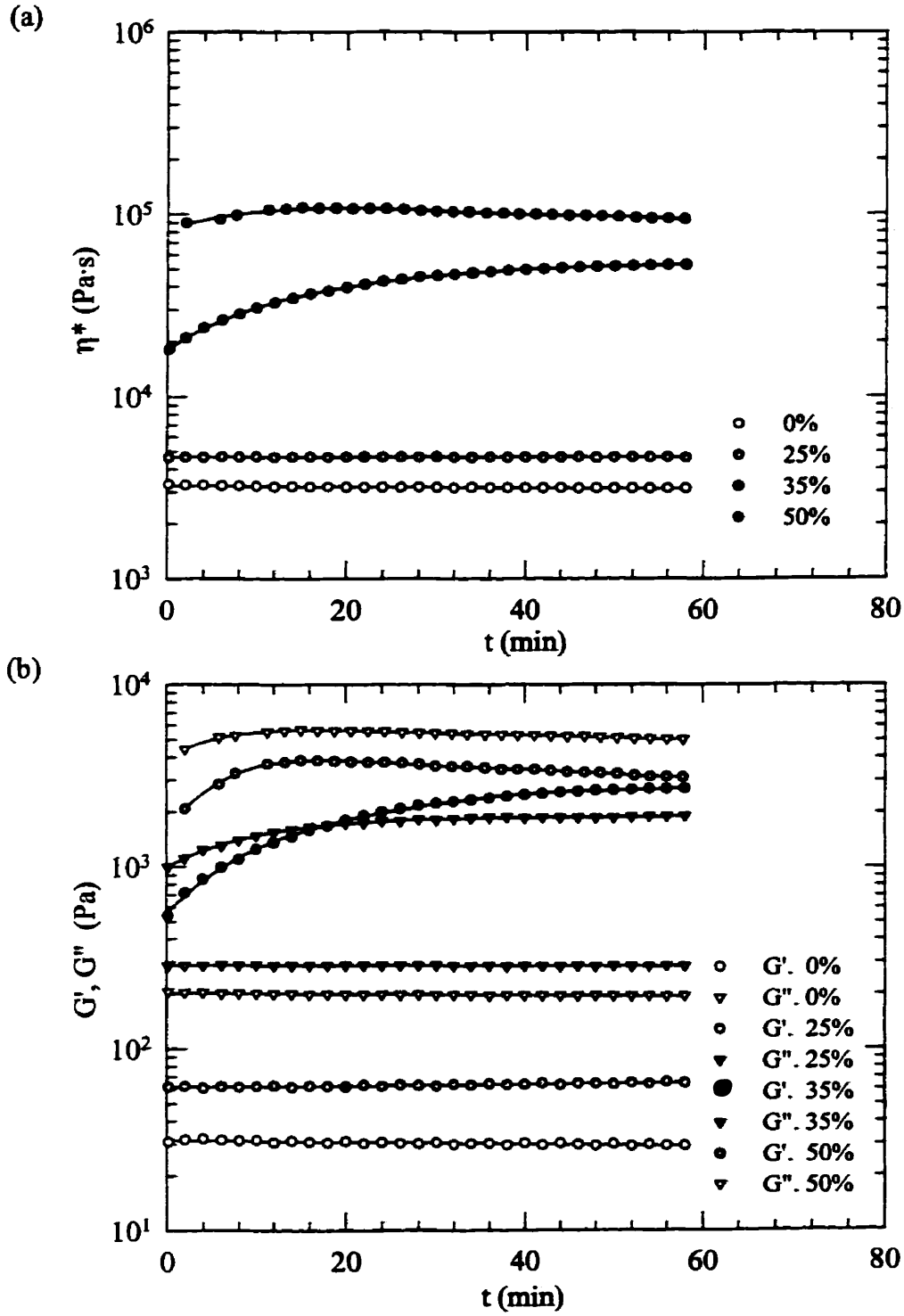

Figure 5.1: Variations of rheological properties with time measured at T=200°C and 0.01 Hz for PP with $CaCO_3$ (UF) (dps1): (a) η*, (b) G' & G"

an important role in the rheological behavior of $CaCO_3$ dispersed PP systems. Some aspects cannot be understood without taking accounts the existence of attractive forces between the particles. At a critical concentration, the moduli increase with time slowly. As we can see from Figure 5.1, the complex viscosity and moduli increase gradually during 1 h experimental period. Our results are in agreement with the findings of Li and Masuda (1990) and Wang and Wang (1999). When the concentration attains 50%, particle network created by thermal actions and by applied deformation is only observed in the first 15 min, as shown in Figure 5.1. The loss and storage moduli, as well as the complex viscosity, reduce moderately in the following 45 min. Our explanation is that the formation of particle network should be finite at a fixed temperature and a deformation rate, and a loading level. The network may break up under the applied deformation. Also, the agglomerates may probably re-alignment under flow, as indicated by Carreau et al. (1996). At the beginning of the experiment, the contribution of network built-up dominates the rheological behavior, so that the dynamic viscosity and moduli increase with the time. At the same time, the particle network starts to be broken down under oscillation. Finally, the destruction of the network controls the rheological properties of molten systems and causes the reduction of rheological data.

Figure 5.2 compares the complex viscosity and moduli data for 35% $CaCO_3$/PP measured at two temperatures 180°C and 200°C, respectively. We note a large increase of the storage modulus for the melt at high temperature. It may be presumed that increasing the temperature favored the particle motion, which result in strong particle interaction, as particle motion depends on temperature.

However, increasing the oscillatory shear frequency reduces the possibility of bond formation between particles. Figure 5.3 illustrates the variations of η^*, G' and G" with time at two different frequencies 0.01Hz and 0.1Hz, respectively. As we can see from the figure, the complex viscosity increases with time slightly rapid at low frequency than at high frequency due to the interaction between particles.

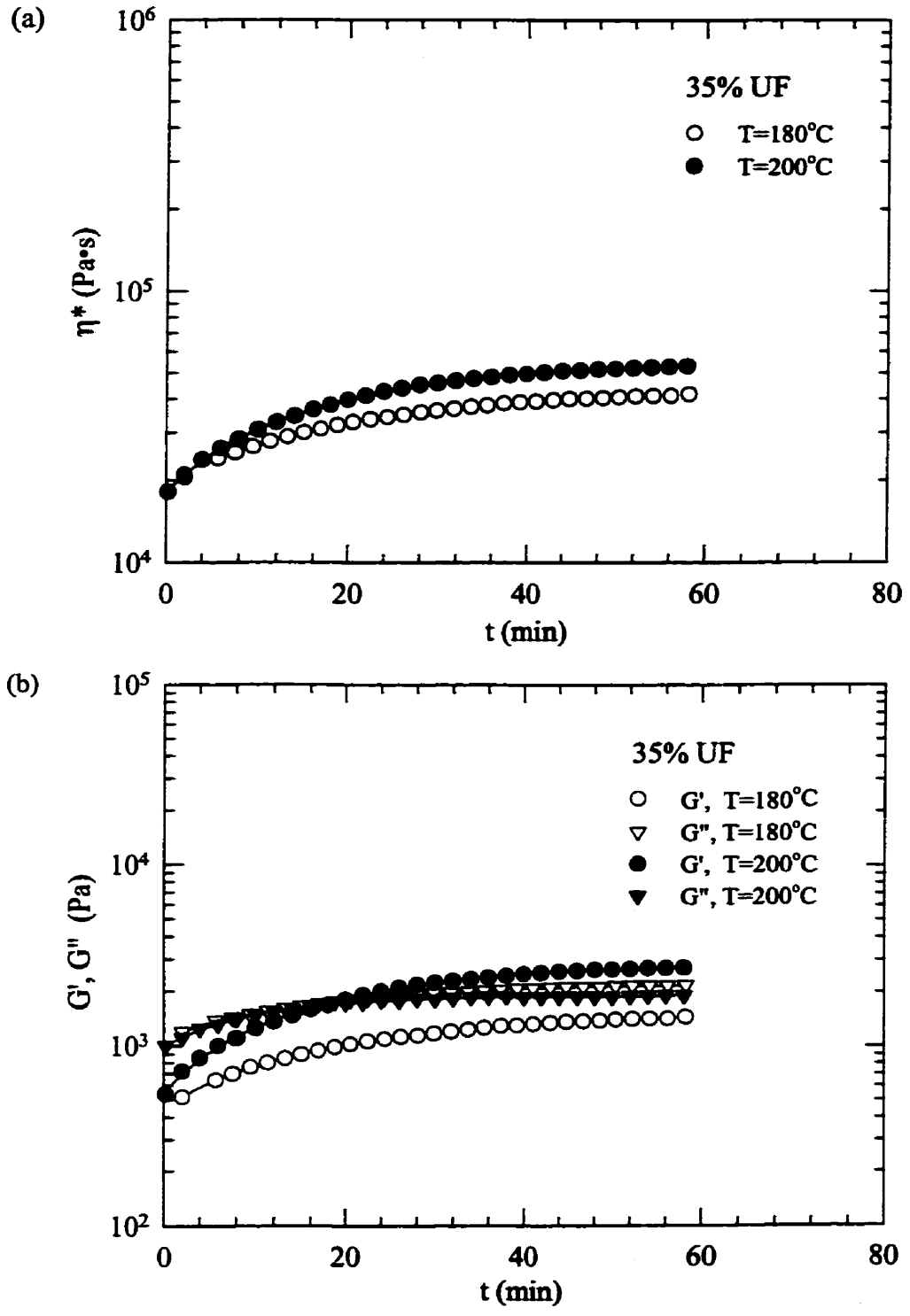

Figure 5.2: Effect of temperature on complex viscosity and moduli measured at 0.01 Hz for PP with 35% $CaCO_3$ (UF) (dps1): (a) η*, (b) G' & G"

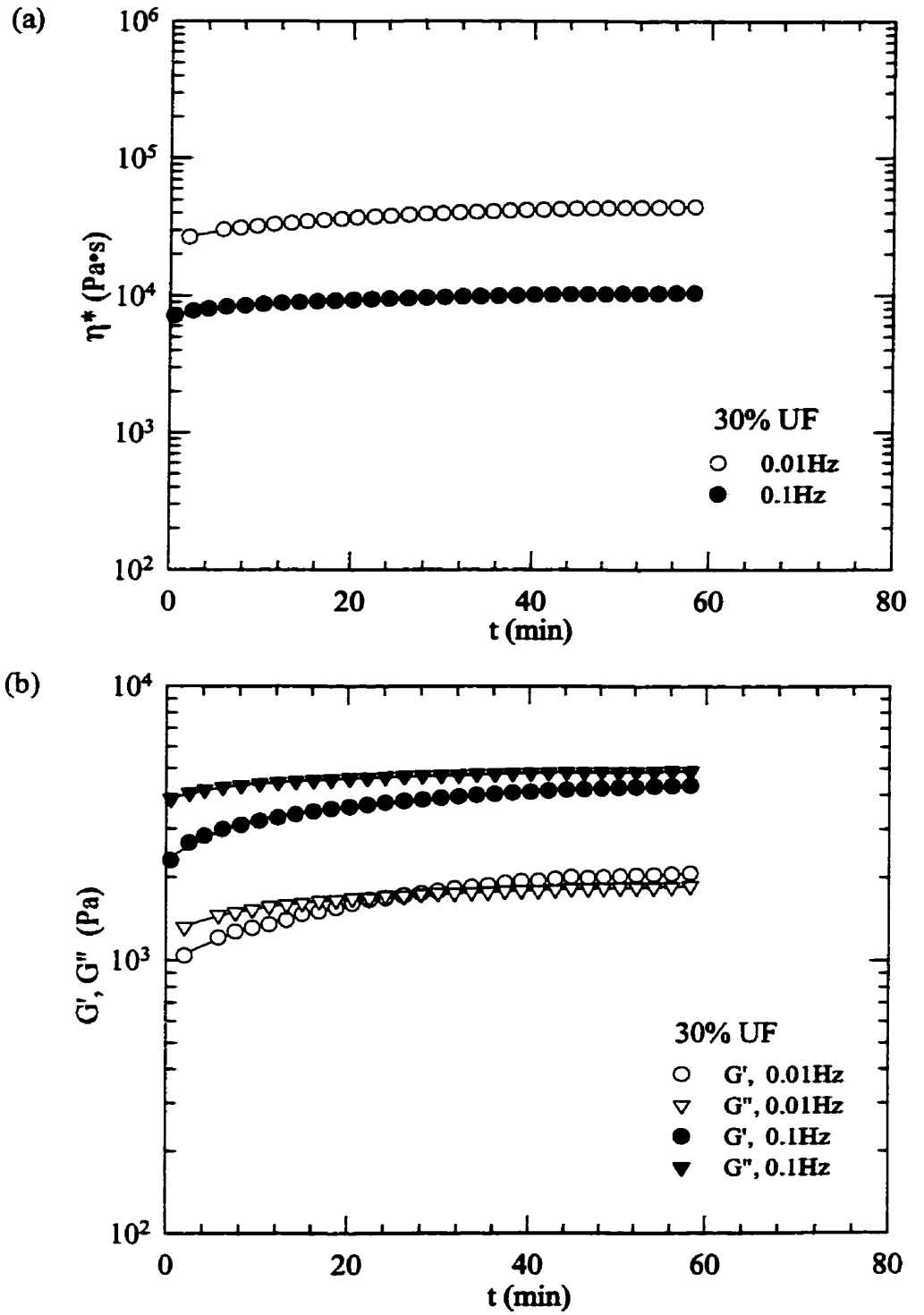

Figure 5.3: Effect of frequency on complex viscosity and moduli measured at T=200°C for PP with 30% $CaCO_3$ (UF) (dps2): (a) η*, (b) moduli

From these preliminary results it is apparent that difficulties arise in determination of the rheological behavior of filled polymer melts with network buildup and possible polymer degradation. Since the purpose of this work was not to study the role of particle interaction in the rheology, an experimental method was developed to prevent the interparticle bond buildup during the rheological measurement period. We will not include the compound of 35% $CaCO_3$/PP in the study of relationship between rheological properties and filler dispersion, due to its slow process of network buildup and breakup.

Steady shear deformation was used as a first step to break up the network structure. The samples were first under steady shear at low shear rate ($\dot{\gamma}=0.1s^{-1}$) during a given time, then stability was measured under oscillatory shear at 0.01 Hz and 5% deformation for about 1 h. Figures 5.4 and 5.5 report the effect of pre-shearing on the complex viscosity and moduli. The pre-shear time varied from 5 to 30 min. With the increase of pre-shear time at $\dot{\gamma}=0.1s^{-1}$, the dynamic rheological properties decrease rapidly. Even 5 min pre-shear causes a not negligible reduction in rheological data. This result is in agreement with those in chapter 4 and 6 on the influence of shear on dispersion state. The shear imposed on the filled polymer melts probably breakdown the agglomerates during the time in which the network is destroyed. Figure 5.5 shows the dependence of the rheological data on the shear rate used in pre-shearing. We can see that the reduction of rheological data shows no limiting value of shear for times up to 30 minutes. The polymer maintained at high temperature (200°C) for a long time may probably results in some degradation which will cause the reduction of the rheological data. The change of dispersion state in the filled systems affects our original objective which is to study the effect of dispersion on rheology properties.

Following the pre-shear experiments, the method of pre-oscillation was tested. We present in Figure 5.6 the variation of η^* and G' & G" with time after the sample experienced pre-oscillatory shear for 10 min at various oscillatory frequencies and

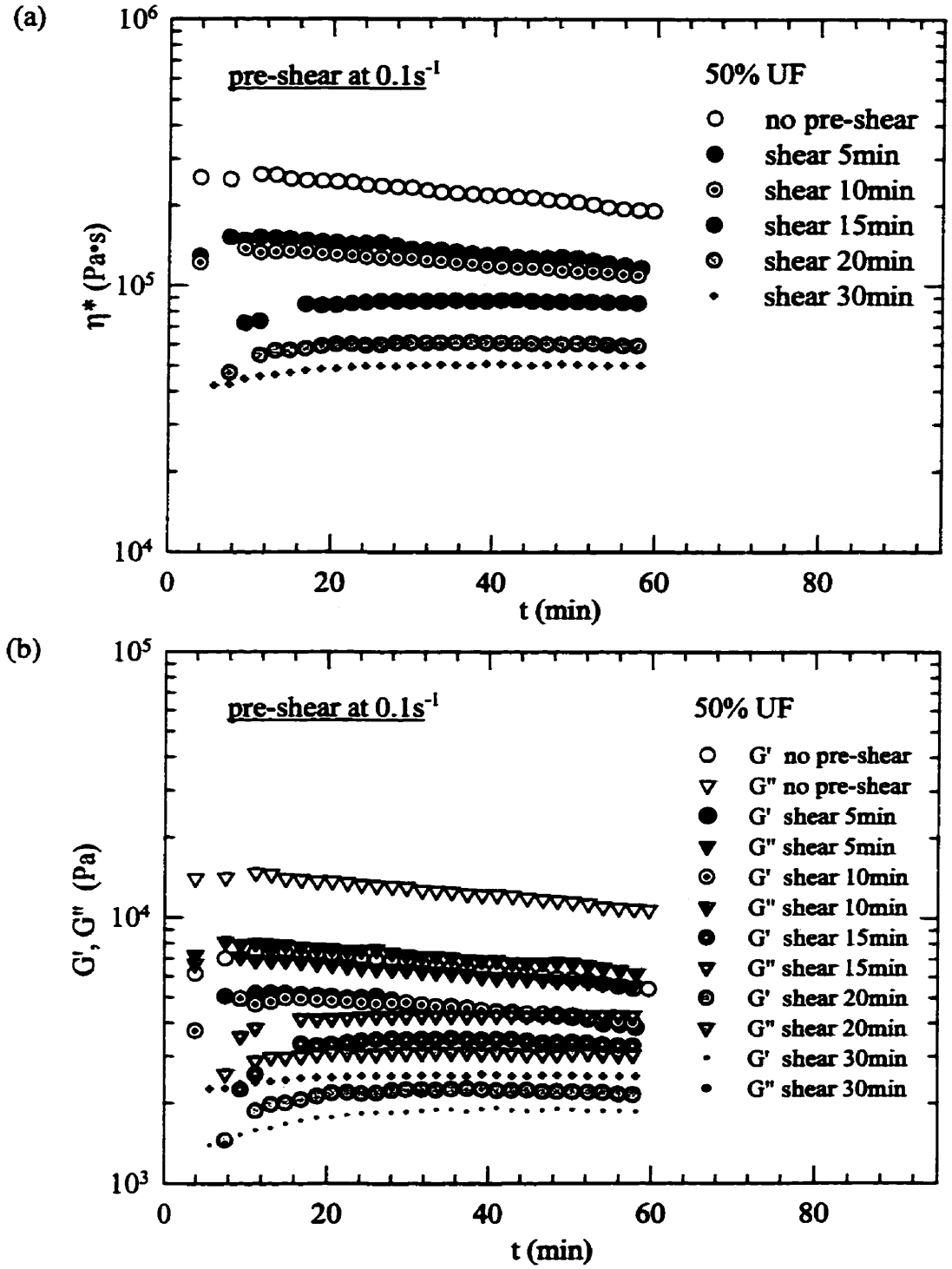

Figure 5.4: Influence of pre-shear on complex viscosity and moduli measured at T=200°C & 0.01 Hz for PP with 50% $CaCO_3$ (UF) (dps2): (a) η^*, (b) moduli

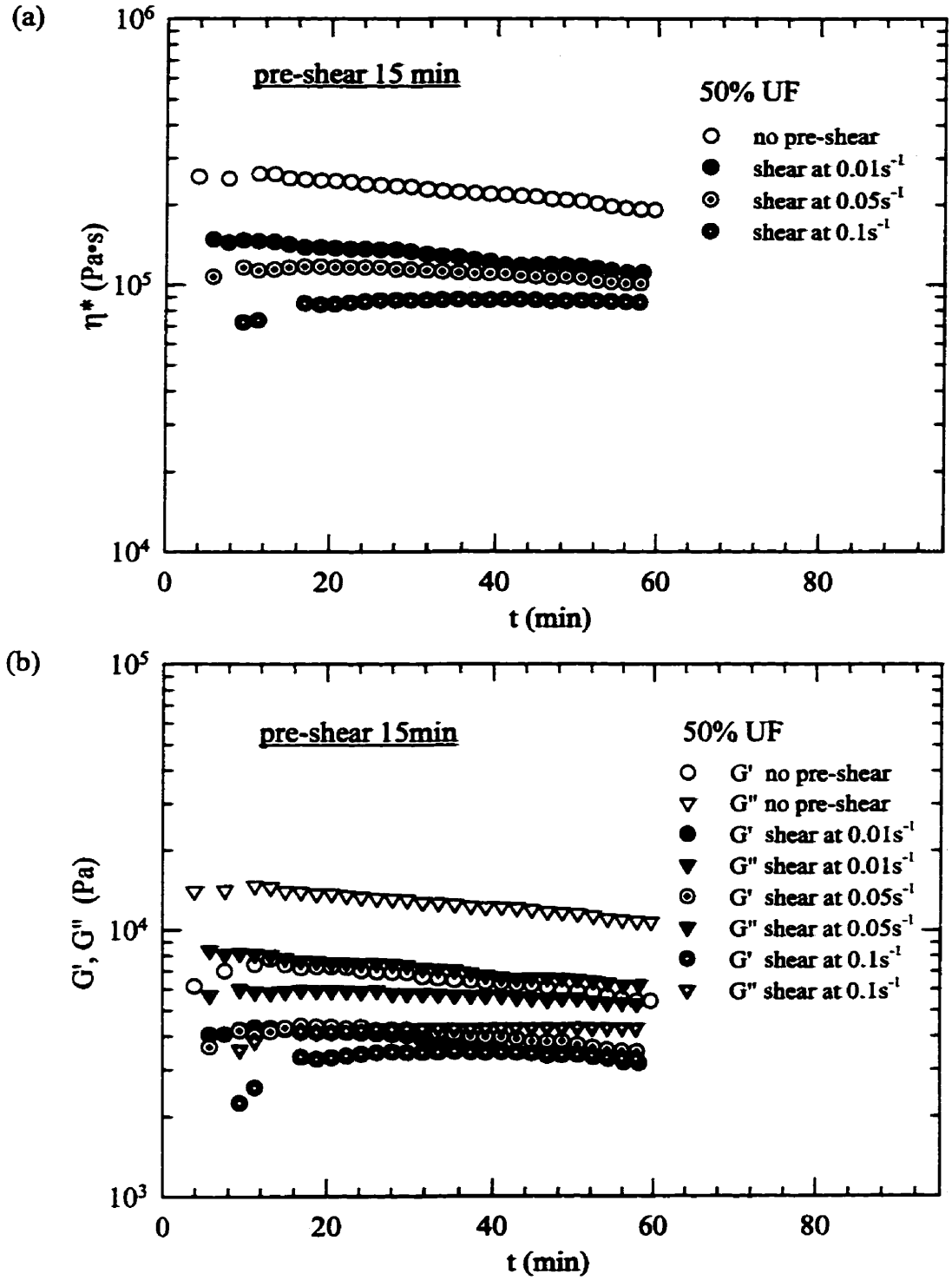

Figure 5.5: Influence of pre-shear-rate on complex viscosity and moduli measured at T=200°C & 0.01 Hz for PP with 50% $CaCO_3$ (UF) (dps2): (a) η*, (b) moduli

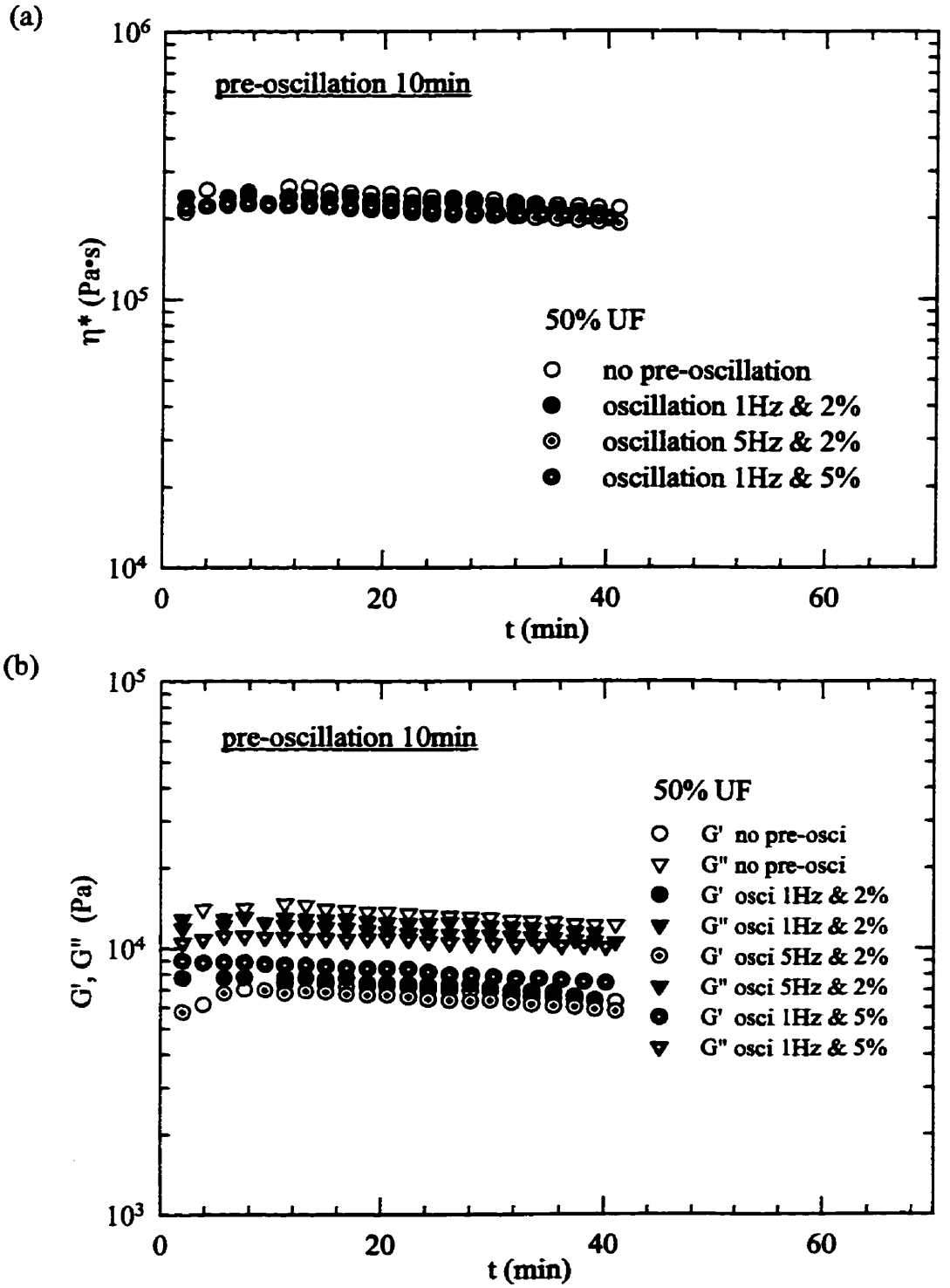

Figure 5.6: Influence of pre-oscillation frequency on complex viscosity and moduli measured at T=200°C & 0.01Hz for PP with 50% $CaCO_3$ (UF) (dps2): (a) η*, (b) moduli

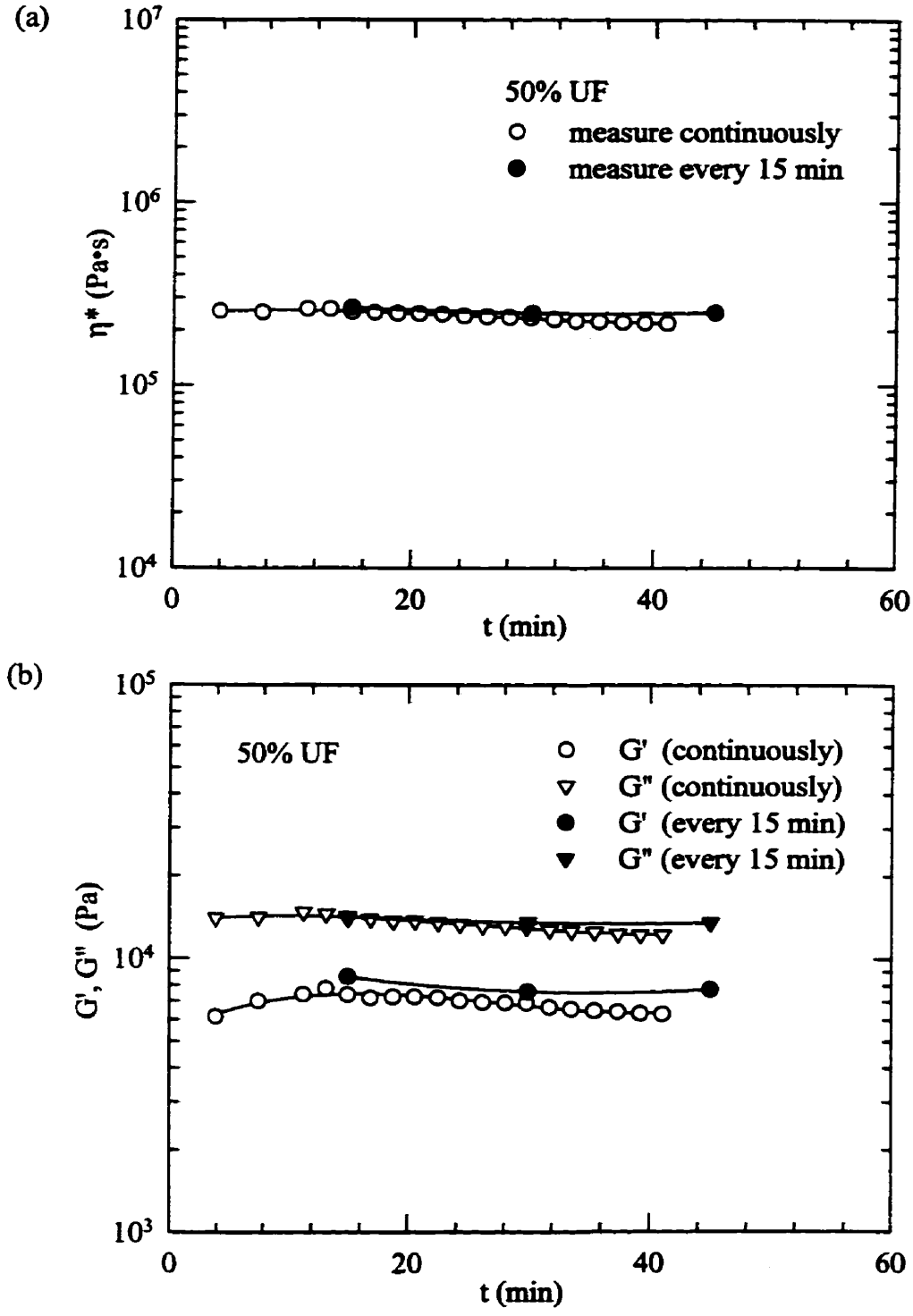

Figure 5.7: Variations of complex viscosity and moduli with measuring method measured at T=200°C & 0.01 Hz for PP with 50% $CaCO_3$ (UF) (dps2): (a) η*, (b) moduli

imposed strains. As shown in the figure, pre-oscillation could temporary breakdown the network buildup. The rheological behavior is under pseudo-equilibrium states for at least 10 to 15 min during the stability experiments. After 15 min of continuously oscillations, the destruction of particle network again reveals strong effect on the properties measured. Experiments have been performed to elucidate that the reductions in complex viscosity and dynamic moduli result from the network breakdown under applied deformation, not the degradation of polymer due to thermodynamical history over the time scale of the experiment. The results are presented in Figure 5.7. In fact, we performed two different experiments. In one experiment, the sample was oscillated continuously during measurement. In another experiment, however, the sample was pre-oscillated for 15 min. Then, the viscoelasticity was measured twice, each after 15 min without oscillation. Clearly, the experimental data obtained from discontinuously measurement changes insignificantly, indicating that the decrease of data in continuous experiments is due to the destruction of network caused by the oscillatory shear flow.

Those stability tests demonstrate the difficulties which arise in the study of the rheological properties of $CaCO_3$ filled PP. At the same time, all these experiments give us an incentive to explore a practical method to carry on the rheological study. Finally, we consider that pre-oscillation is the best way for the further viscoelasticity studies. All the dynamic viscosity and moduli data presented in this chapter are measured after samples underwent pre-oscillation at a frequency 0.01 Hz and strain amplitude $\gamma = 5\%$ for 15 min. To insure all the data obtained are examined under pseudo-equilibrium states, the measurements on each sample after pre-oscillation was not allowed to exceed 15 min. Some results of stability studies, as well as micrographic structure of compound before and after shear, which are not reported here, are presented in Appendix A and B.

5.2 Strain dependence

In order to determine the strain amplitude range over which linear viscoelasticity

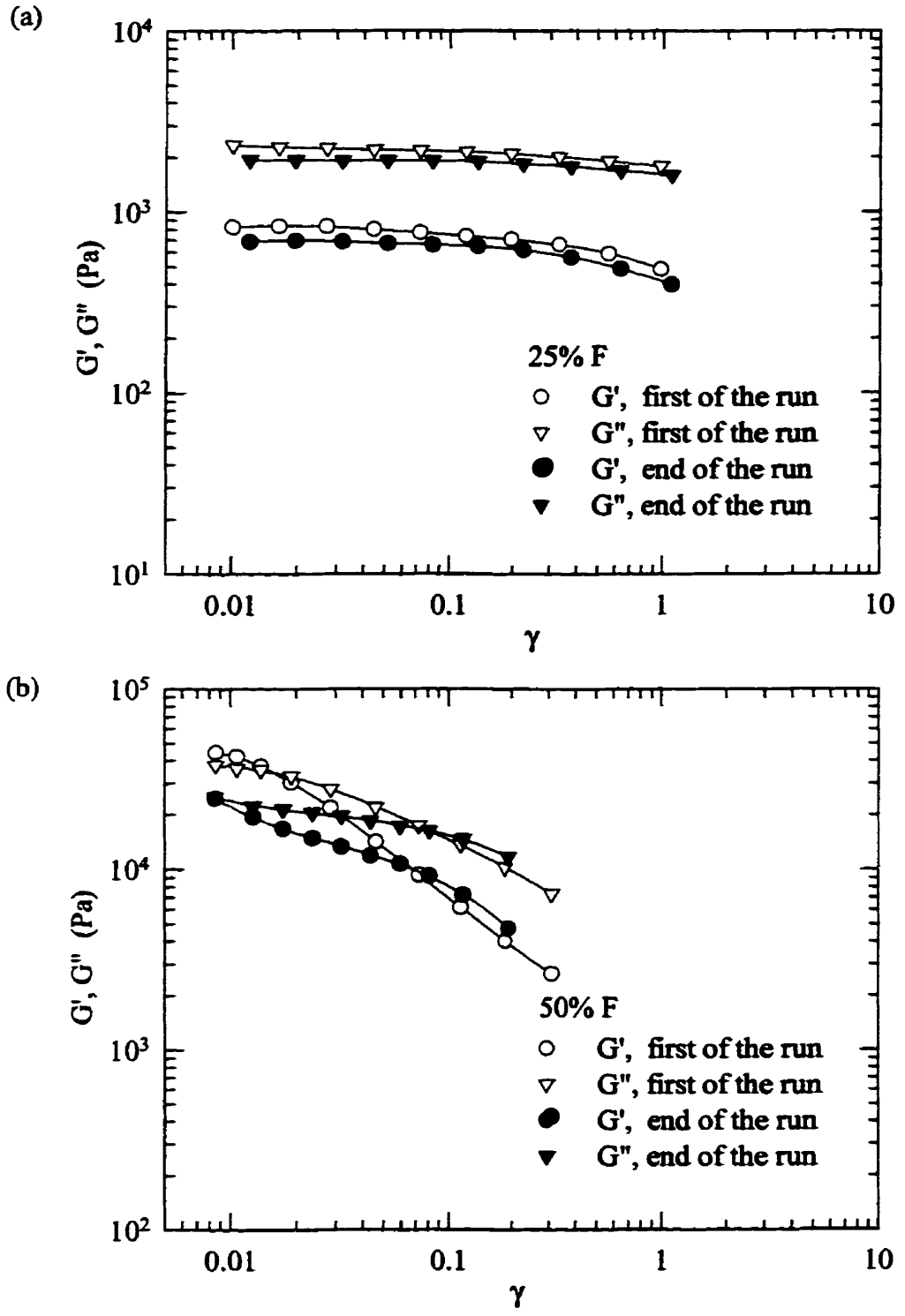

Figure 5.8: Dynamic moduli as functions of strain amplitude at 200°C and 0.1 Hz for PP with $CaCO_3$ (dps2): (a) 25% F, (b) 50% F

prevails, strain sweep experiments were carried out at a frequency of 0.1Hz and a strain amplitude range of 0.8% - 100%. Figure 5.8a shows that the dynamic moduli of the 25% $CaCO_3$ filled PP is unaffected by the amount of strain imposed during dynamic testing between 1% to 10% strain amplitude. The open symbols indicate that the data were obtained immediately after temperature equilibrium was attained. The closed symbols represent the data measured after the sample reached a pseudo-equilibrium state under low strain test (pre-oscillation 15 min under $\gamma = 5\%$ and 0.1 Hz). The data obtained from the compound of 50% $CaCO_3$ exhibit a strong dependence on the strain, as reported in Figure 5.8b. Other researchers (Bigg, 1983; Rong et al, 1988; Carreau et al., 1996; Aral and Kalyon, 1997) have also found that the onset of the non-linear viscoelastic region occurs at lower strain amplitude for filled systems than for unfilled systems. Because of the sensitivity of the rheological response of compounds to the level of strain, it would be desirable to determine viscoelasticities at strain amplitude that is low enough not to affect the material's response. For filler loading at 25%, the strain amplitude could be as high as 10 percent. As the filler loading increases, the level of strain below which the response is unaffected by strain is reduced. Figure 5.8b reveals the absence of linear viscoelastic domain for this highly concentrated suspension. It is the characteristics of a gel-type structure with particle-particle interaction, as indicated by Carreau et al. (1996). The interaction between particles dominates the rheological behavior of highly concentrated suspensions even at small-amplitude. Consider the equipment we used, 1% is the lowest strain that could be used. Strains lower than 1% did not generate a signal sufficient for the instrument's transducers to obtain a reliable response. In our experiments, for the most concentration systems (50 wt % $CaCO_3$), all the rheological data reported in the following few sections were carried out at the lowest strain of 1%. The results of strain dependence for other systems studied are reported in Appendix A.

5.3 Influence of filler concentration

We present in Figures 5.9 and 5.10 the dependence of rheological data on the

filler concentration of different dispersion systems. As expected, both complex viscosity η^* and dynamic moduli G' & G" increase with the addition of $CaCO_3$ filler, especially at low frequencies, as reported by other workers (Rong and Chaffey, 1988; Li and Masuda, 1990). The unfilled molten PP, as well as the 25% $CaCO_3$ filled polymer systems, shows a Newtonian plateau in the low frequency region. However, no Newtonian flow region is found at low frequencies for the 50% $CaCO_3$ filled polypropylene melt. The viscosity is unbounded as frequency decreases, revealing the existence of an apparent yield stress in the low frequency region, in agreement with the literature results (Bigg, 1983; Suetsugu and White, 1983; Carreau et al., 1996). The appearance of yield stress is attributed to the increase of filler concentration and agglomerate sizes that result in a solid-like structure, as can be seen from the obvious increase of the storage modulus. The formation of network due to the particle interaction still exists in the molten system and is not negligible though the rheological measurement is carried out after samples have been pre-oscillated to breakdown the inter-particle network. As discussed in section 5.1, the interaction between particles is important at high solid loading. The shear-thinning behavior may be related to particle-particle interactions and/or structure modifications or particle alignment under flow. At low filler concentration, the interactions are believed to play an insignificant role. Note that the storage modulus increase markedly at the loading of 50% $CaCO_3$, indicating the formation of solid-like structure.

5.4 Influence of dispersion

The dispersion index reflects the agglomerate size in the compound. The increase of agglomerate size gives rise to the increase of dispersion index. Figures 5.11 and 5.12 show the dependence of rheological properties on the value of dispersion index f at a filler concentration of 25% for the two types of fillers, respectively. It should not be a surprise that the viscosity increases as the value of dispersion increases, especially at low frequencies. We mention in Chapter 4 that the value of f reflects the quality of dispersion. The higher value of f represents worse dispersion, and the bad dispersions lead to more

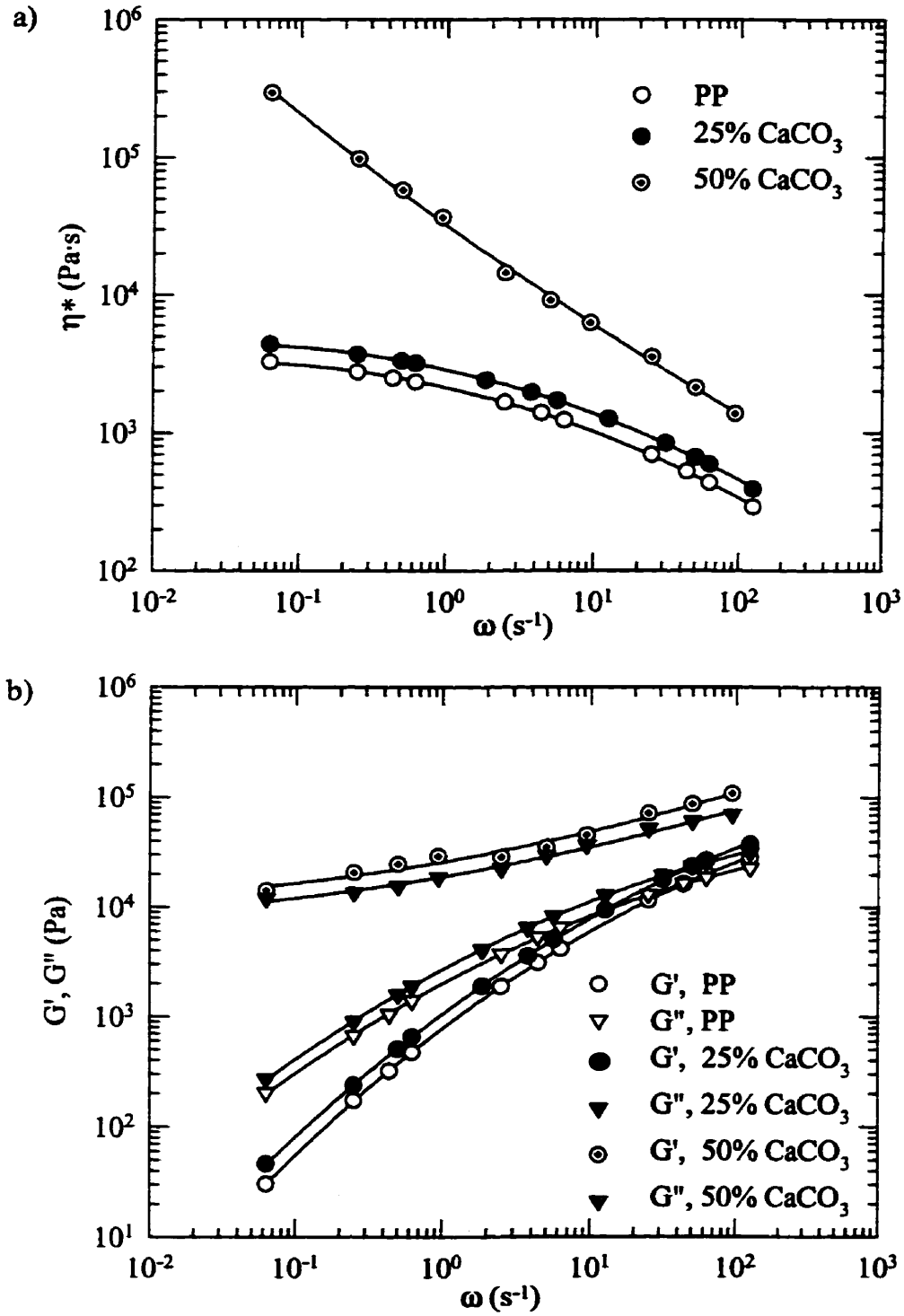

Figure 5.9: Effect of concentration on complex viscosity and moduli for PP with $CaCO_3$ (F) (dps1) at T=200°C: (a) η^*, (b) moduli

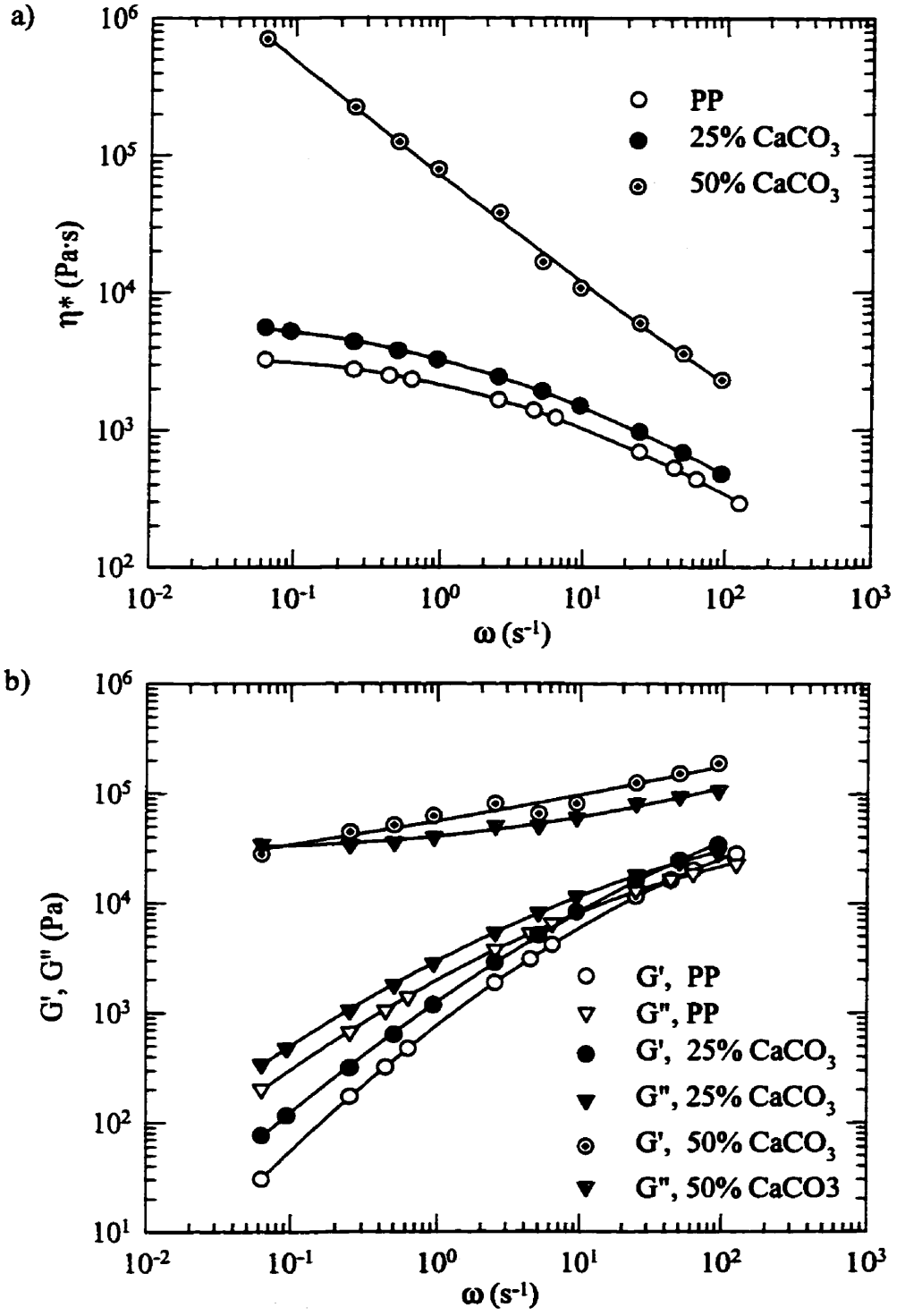

Figure 5.10: Effect of concentration on complex viscosity and moduli for PP with $CaCO_3$ (F) (dps2) at T=200°C: (a) η*, (b) moduli

viscous, more elastic materials.

Figures 5.13 & 5.14 demonstrate the influence of dispersion on the complex viscosity and dynamic moduli at the filler concentration of 50% for the two different types of fillers, respectively. The viscosity increases with the increase of dispersion index value, similar as those presented for 25% $CaCO_3$ filled polymer melts. Thus, the mixing conditions may considerably alter the viscosity of the systems by changing the dispersion state. All the eight samples, which have been investigated in our study, exhibit an apparent yield stress, regardless of the agglomerate size and the type of filler added. It is interesting to note that the viscosity curves at high concentration are almost parallel to each other. This can be explained as following: due to the strong particle-particle interactions, the behavior depicted by the high-filled melts is considerably different from that observed from the low-filled or pure polymeric system. The property/behavior of molten polymer is probably masked by the contribution of interparticle reaction in high-filled system.

5.5 Effect of particle/agglomerate size

The calcium carbonates used in our research are submicron/micron particles (0.7 μm for the ultra fine power, 1.4 μm for the fine ones). The particle size influences the agglomerate sizes of final compounds at identical condition for the low-filled systems, due to the gap of bulk density as discussed in Chapter 4. Figure 5.15 (a to d) displays the influence of the agglomerate size or dispersion index on the complex viscosity for 25% $CaCO_3$/PP systems obtained from different conditions, respectively. The viscosity of the ultra fine particle filled melt which possesses large agglomerates is higher than that of the fine particle filled one which has small agglomerates, especially at low frequency region. From the point of view of particle interaction, this can be explained by that small particles with large specific surface area have a tendency to easily form an agglomerate structure. For highly filled system, the influences of the particle size on the agglomerate

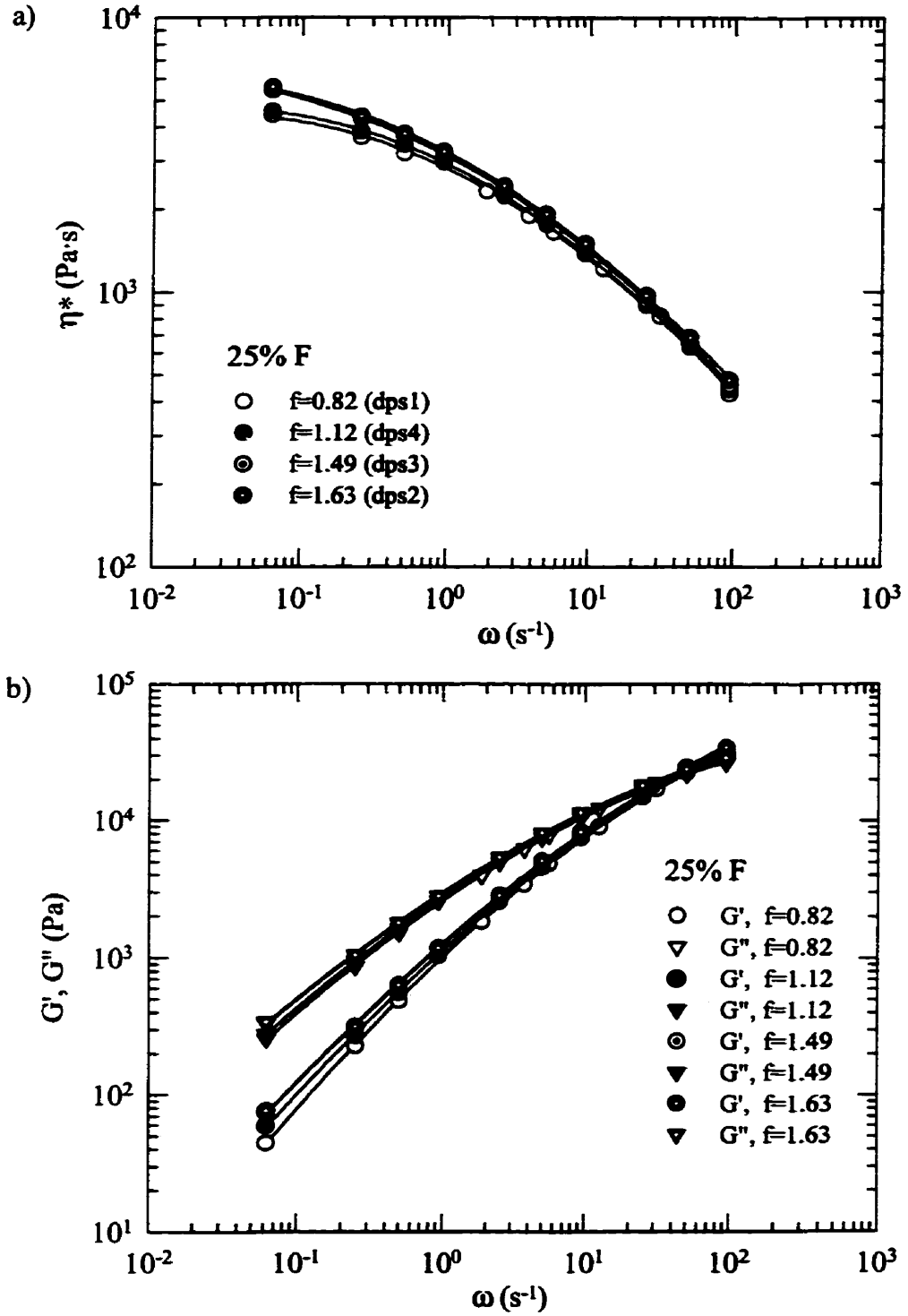

Figure 5.11: Effect of dispersion on complex viscosity and moduli for PP with 25% $CaCO_3$ (F) measured at T=200°C: (a) η*, (b) moduli

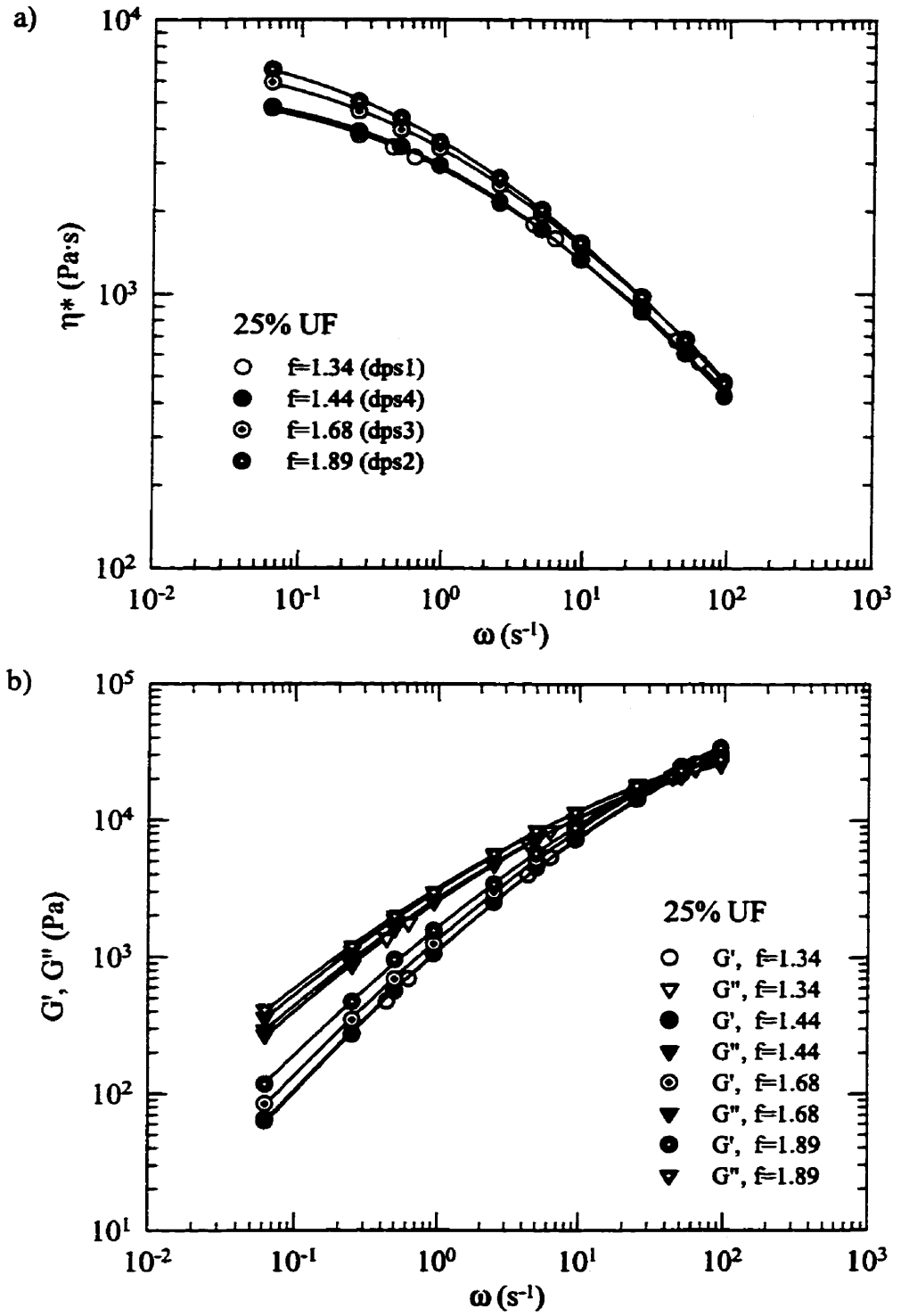

Figure 5.12: Effect of dispersion on complex viscosity and moduli for PP with 25% $CaCO_3$ (UF) measured at T=200°C

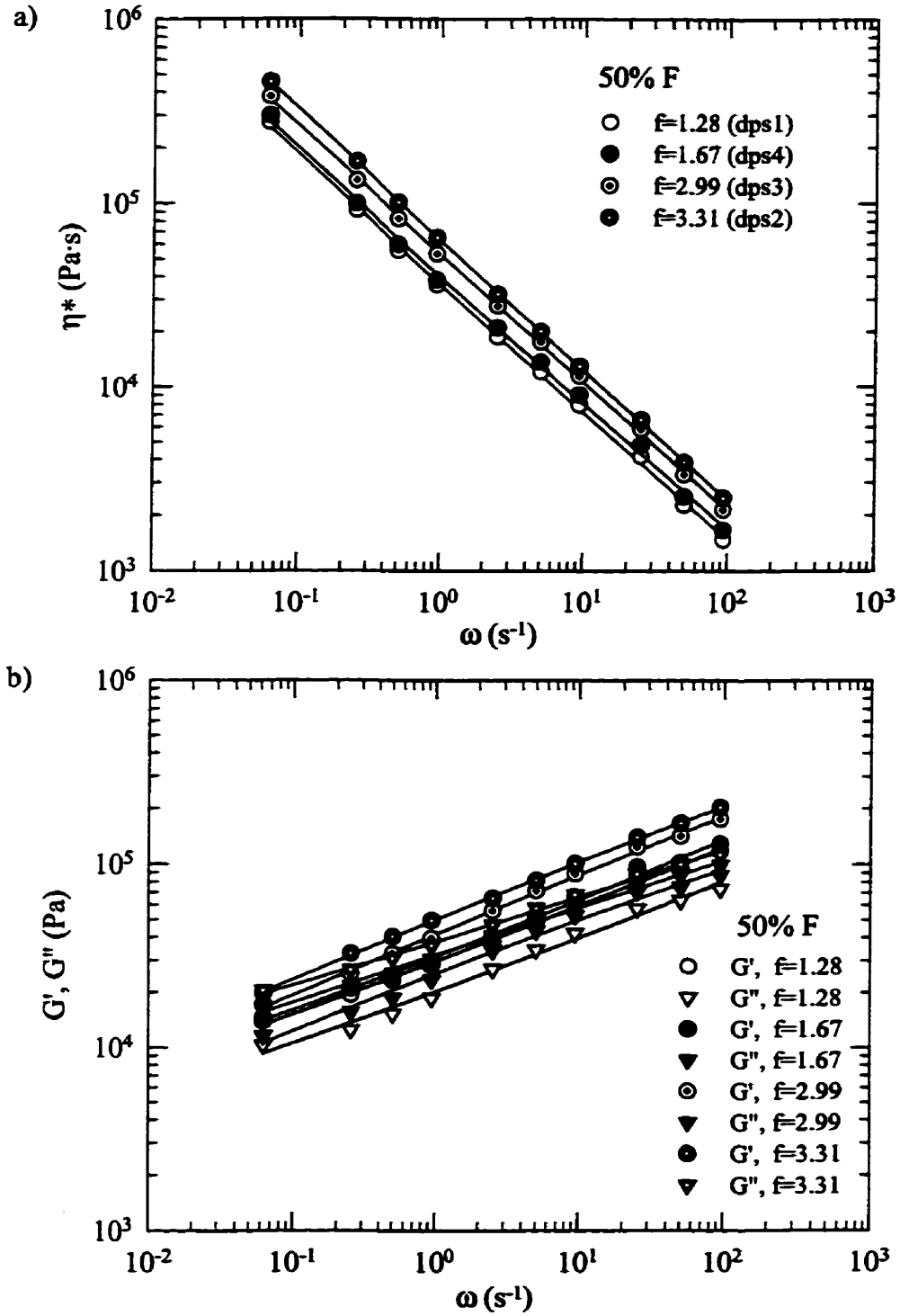

Figure 5.13: Effect of dispersion on Complex viscosity and moduli for PP with 50% $CaCO_3$ (F) measured at T=200°C & 1% strain

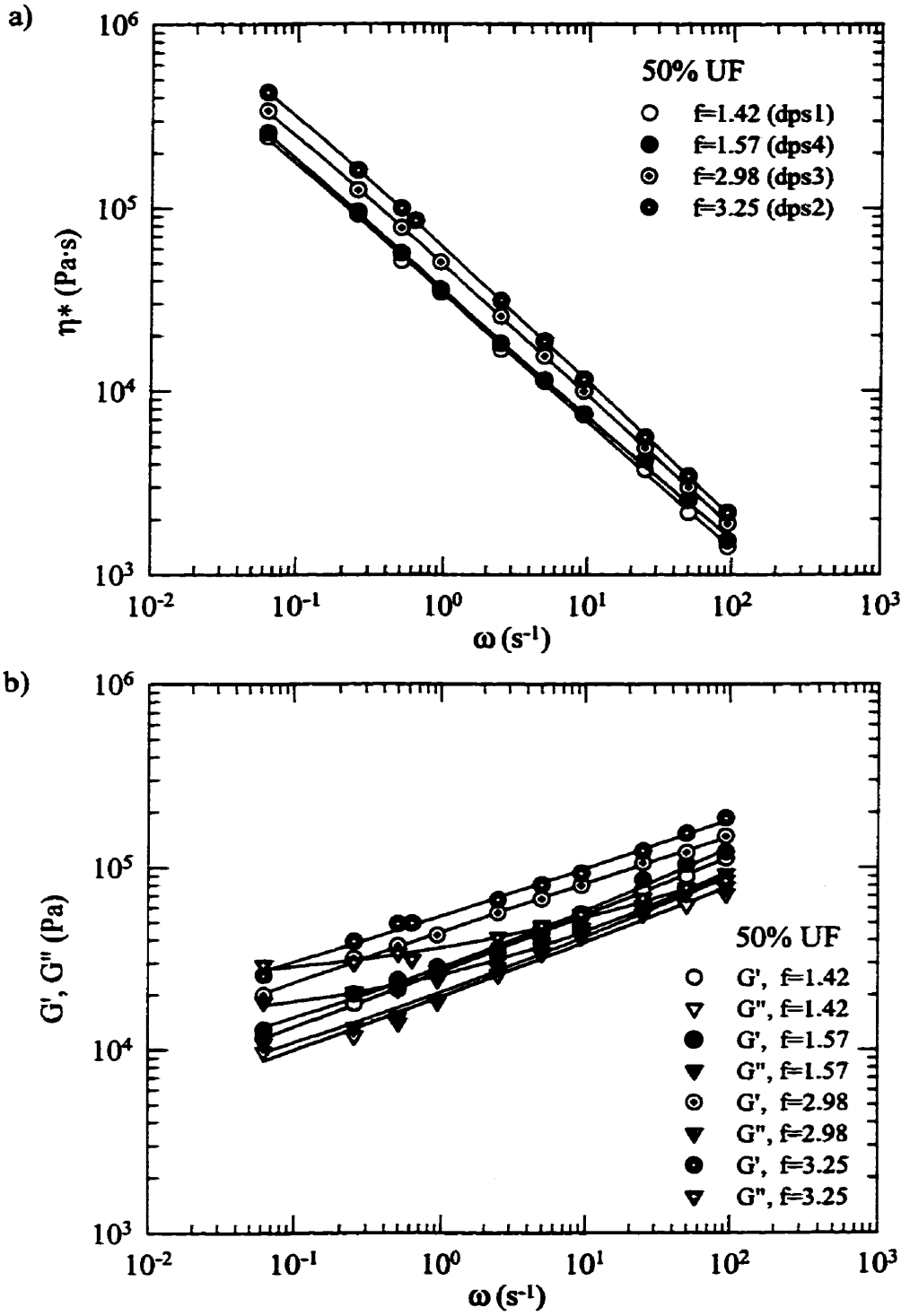

Figure 5.14: Effect of dispersion on Complex viscosity and moduli for PP with 50% $CaCO_3$ (UF) measured at T=200°C & 1% strain

size of final product are probably masked by the effects of concentration. The agglomerate sizes of the compounds obtained from different conditions do not show obvious differences. This is the case shown in Figure 5.16 for 50% $CaCO_3$/PP at various processing conditions. The viscosity of the ultra fine particle filled systems does not always hold the higher value. Actually, the dispersion state of the fine particle in polypropylene matrix does not dominate over that of the ultra fine particle, the differences of dispersion index value are quite small.

5.6 Relative viscosity

Figure 5.17 shows the relative viscosity of sample from dps2 as a function of filler concentration (vol. %). The relative viscosity η_r is taken as the ratio of viscosity of filled PP to that of unfilled PP at the same oscillating frequency (0.01Hz). The solid, broken and dotted line in Figure 5.17a are drawn according to equation (5.1) with volume fraction at maximum packing equals to 0.68, 0.52, and 0.44, respectively. The solid line in Figure 5.17b is deduced according to the equation (5.2) with $k = 1.25$.

Maron-Pierce $$\eta_r = (1 - \phi/\phi_m)^{-2} \tag{5.1}$$

Mooney $$\eta_r = \exp\left(\frac{2.5\phi}{1 - k\phi}\right) \tag{5.2}$$

The relative viscosities determined from experimental data for the systems we considered are markedly higher than that expected by the equation derived by Maron and Pierce (1956) or by Mooney (1951). Note that the equations were derived from non-interaction sphere suspensions in a Newtonian medium. For the compound of interacting particles filled in the non-Newtonian medium, the agglomeration of particle results in substantial increase of the viscosity, mainly at low frequency. This shows that η_r of high

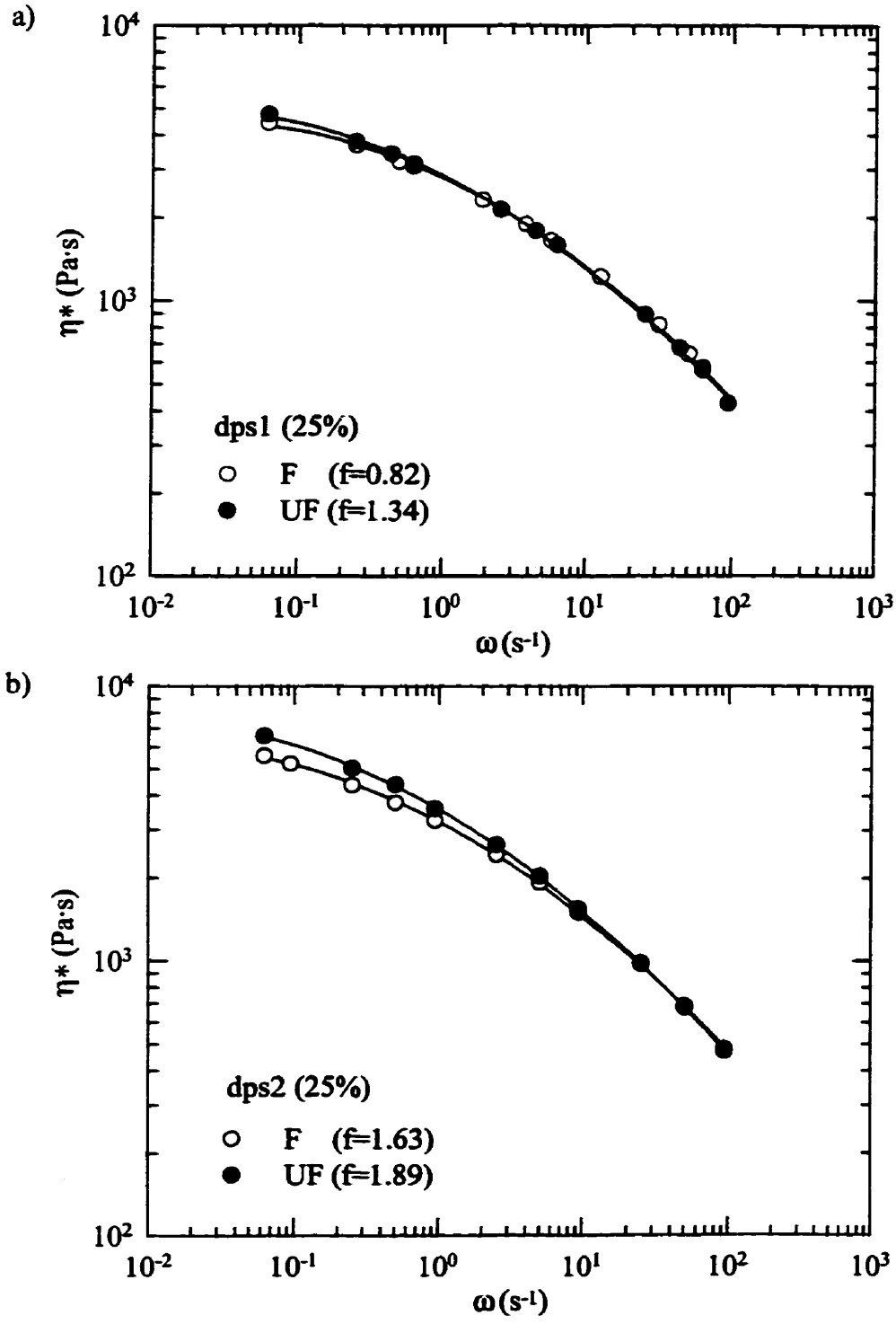

Figure 5.15: Effect of particle size on complex viscosity for PP with 25% $CaCO_3$ measured at T=200°C: (a) dps1, (b) dps2, (c) dps3, (d) dps4

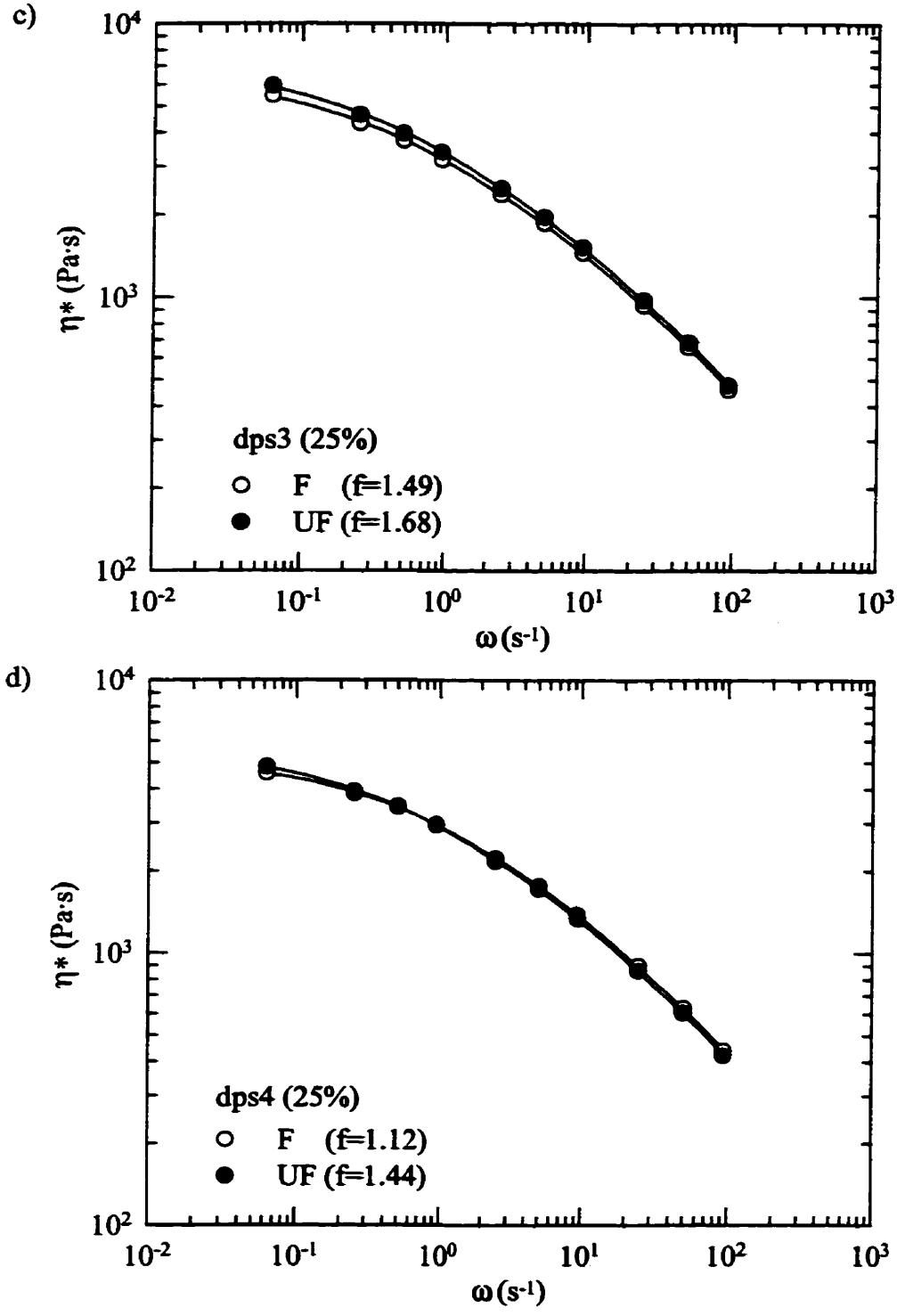

Figure 5.15 (continued)

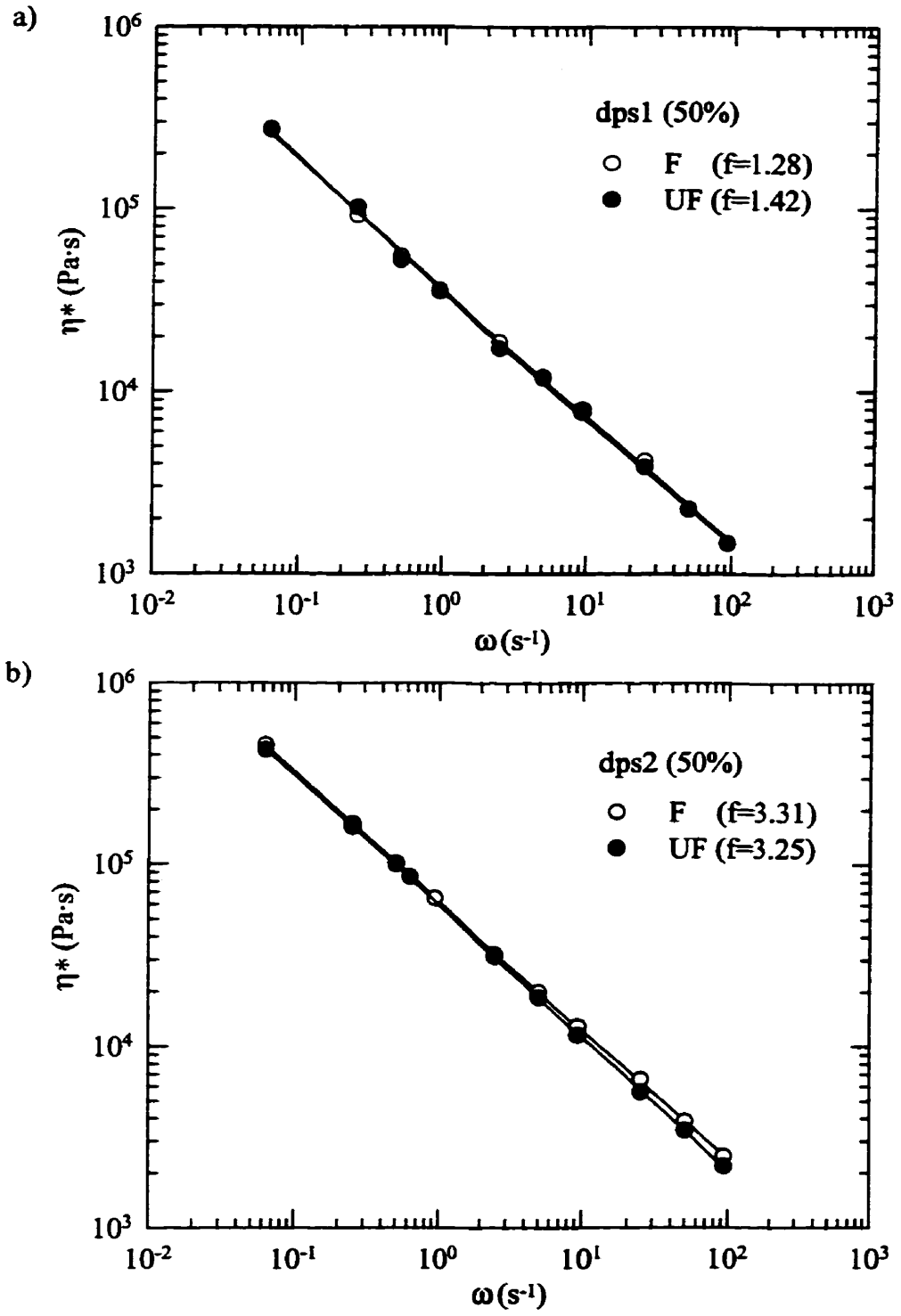

Figure 5.16: Effect of particle size on complex viscosity for PP with 50% $CaCO_3$ measured at T=200°C: (a) dps1, (b) dps2, (c) dps3, (d) dps4

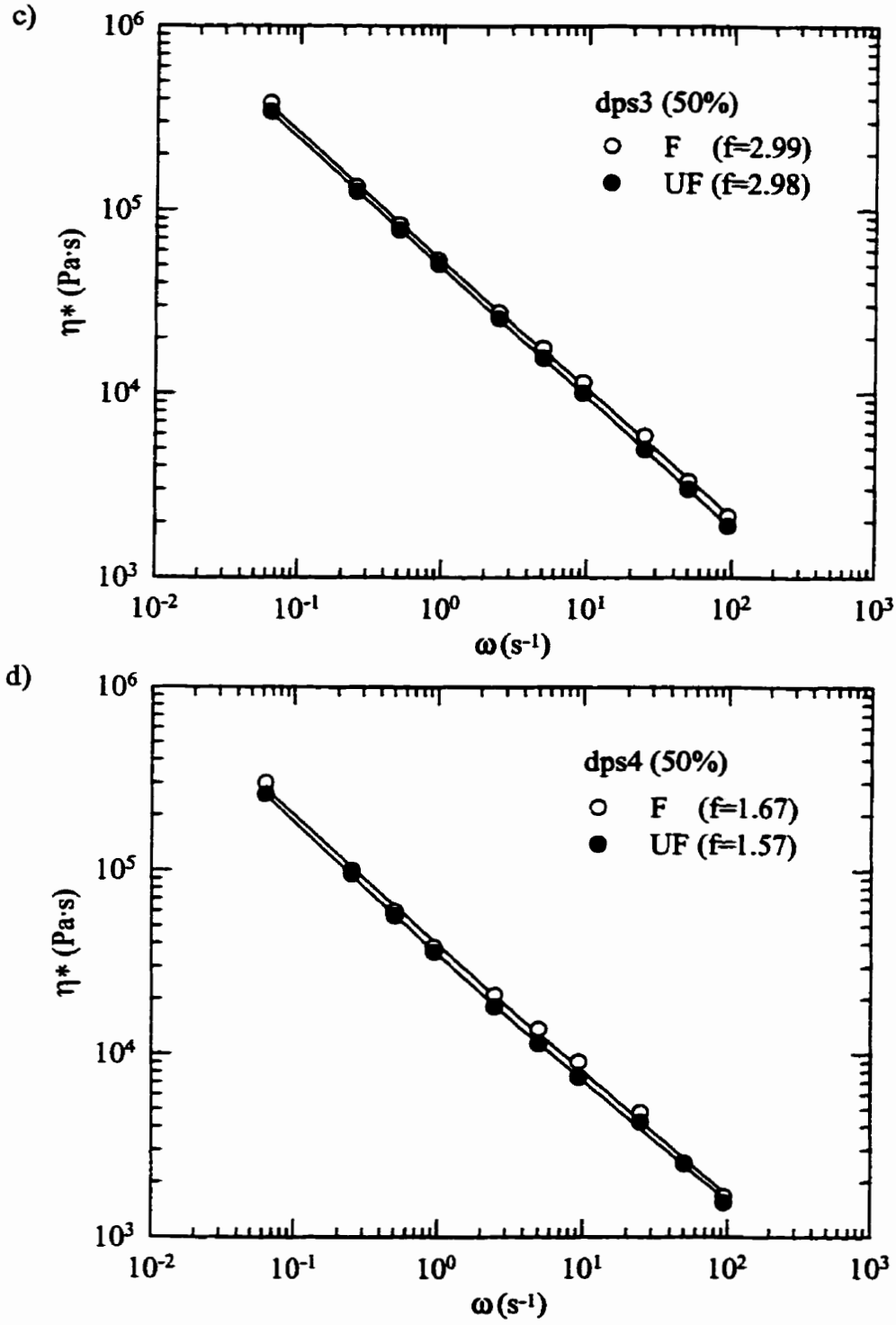

Figure 5.16 (continued)

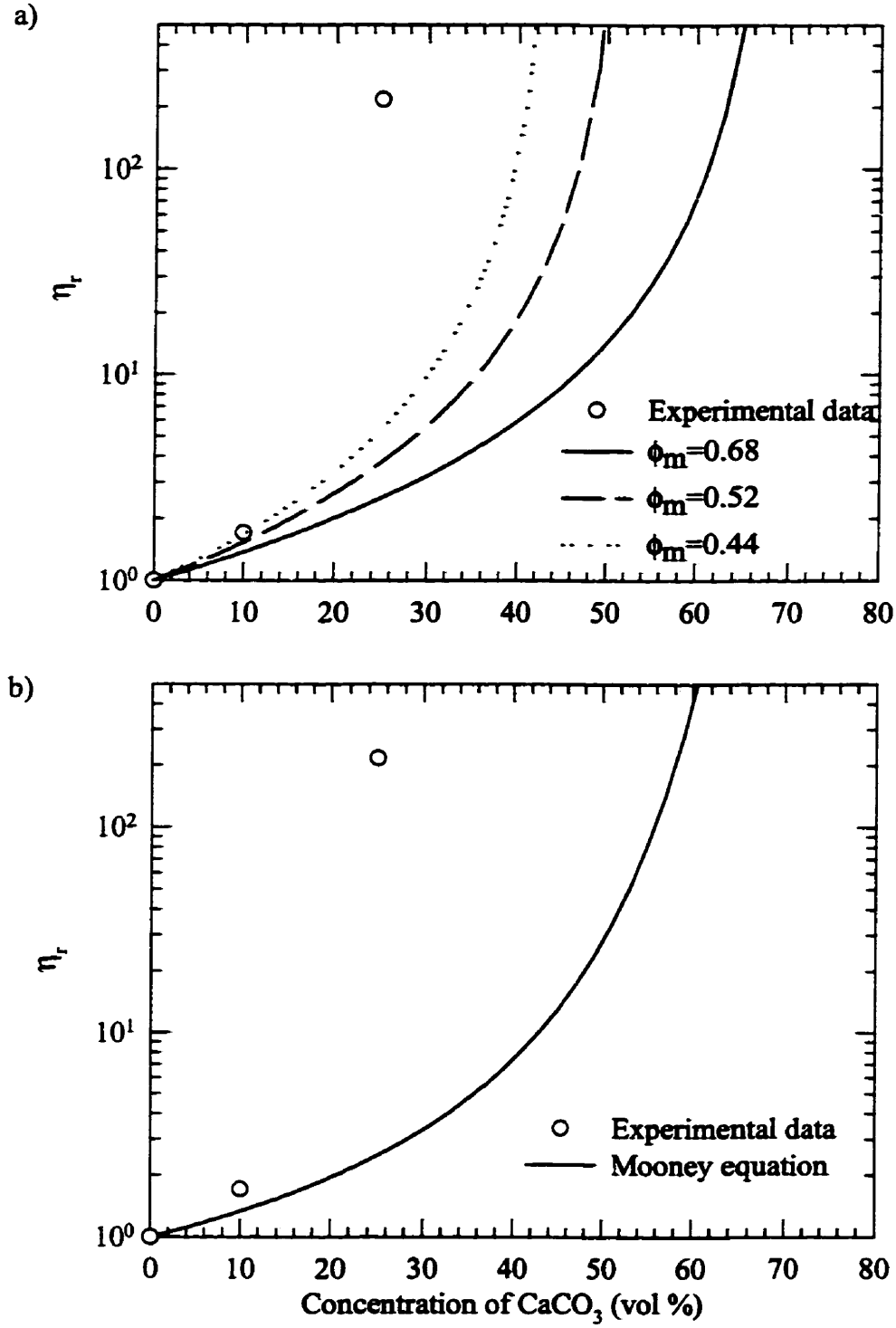

Figure 5.17: Relation between relative viscosity and concentration of CaCO3 (F) (dps2): η_r is estimated from plots as in Figure 5.10: (a) Maron -Pierce, (b) Mooney

concentrated untreated $CaCO_3$ is far from that foreseen by the empirical models.

5.7 Relation of complex viscosity to dispersion

As discussed in preceding section, the viscoelastic characteristics of $CaCO_3$ filled polypropylene are determined by the dispersion of agglomerates. In this section, we try to correlate the experimental rheological data to the dispersion index *f*. The analysis follows will, it is hoped, lead to a relatively straightforward means of estimating the rheological data from the dispersion state. However, it cannot be expected, nor is it intended to predict or explain all the other filled polymer systems that is the subject of current research.

Figures 5.11-5.14 show that the shape of viscosity-shear rate plots obtained at a fixed filler concentration is not affected by dispersion index. The similarity of curves suggests a possibility of combining data, obtained at various dispersion indices, into a single curve at an arbitrary reference dispersion index. The time-dispersion index superposition for data of 25% and 50% $CaCO_3$/PP from Figures 5.11-5.14 is shown in Figure 5.18. The reference dispersion index is the lowest dispersion index at a fixed concentration. The master curve is obtained by the following procedure:

(a) shift the curve at dispersion index *f* vertically by an amount of shift factor a_f.

(b) shift the resulting curve horizontally by an amount a_f, so that the overlapping regions of the curve at reference dispersion index f_r and the shifted curve at *f* superpose.

The relationship of shift factor a_f and dispersion index *f* is displayed in Figure 5.19 on a semi-log plot. The shift factor a_f for the system studied is found to be correlated to the dispersion index as following:

$$\ln a_f = B(f - f_r) \tag{5.3}$$

where a_f is a shift factor, f_r is a reference dispersion index, and B is a parameter related to the components and concentration of the filled system. The value of parameter B depends on the content of filler and the components that constitute the systems. For the systems we studied, the parameters are given by:

25% $CaCO_3$/PP	B = 0.14	$\ln a_f = 0.14 * (f - 0.82)$
50% $CaCO_3$/PP	B = 0.37	$\ln a_f = 0.37 * (f - 1.28)$

The viscosity of filled polymer can then be expressed as:

$$\eta^*(\omega, f) = a_f \eta^*(a_f \omega, f_r) \tag{5.4}$$

The application of equation (5.4), we believe, subjects to the filled systems studied and should be proved case by case. The influence of dispersion on the rheology has been studied for many years, but we believe the intention to predict the viscosity directly from dispersion state is new. To our knowledge, it has not been predicted in any theoretical or experimental study.

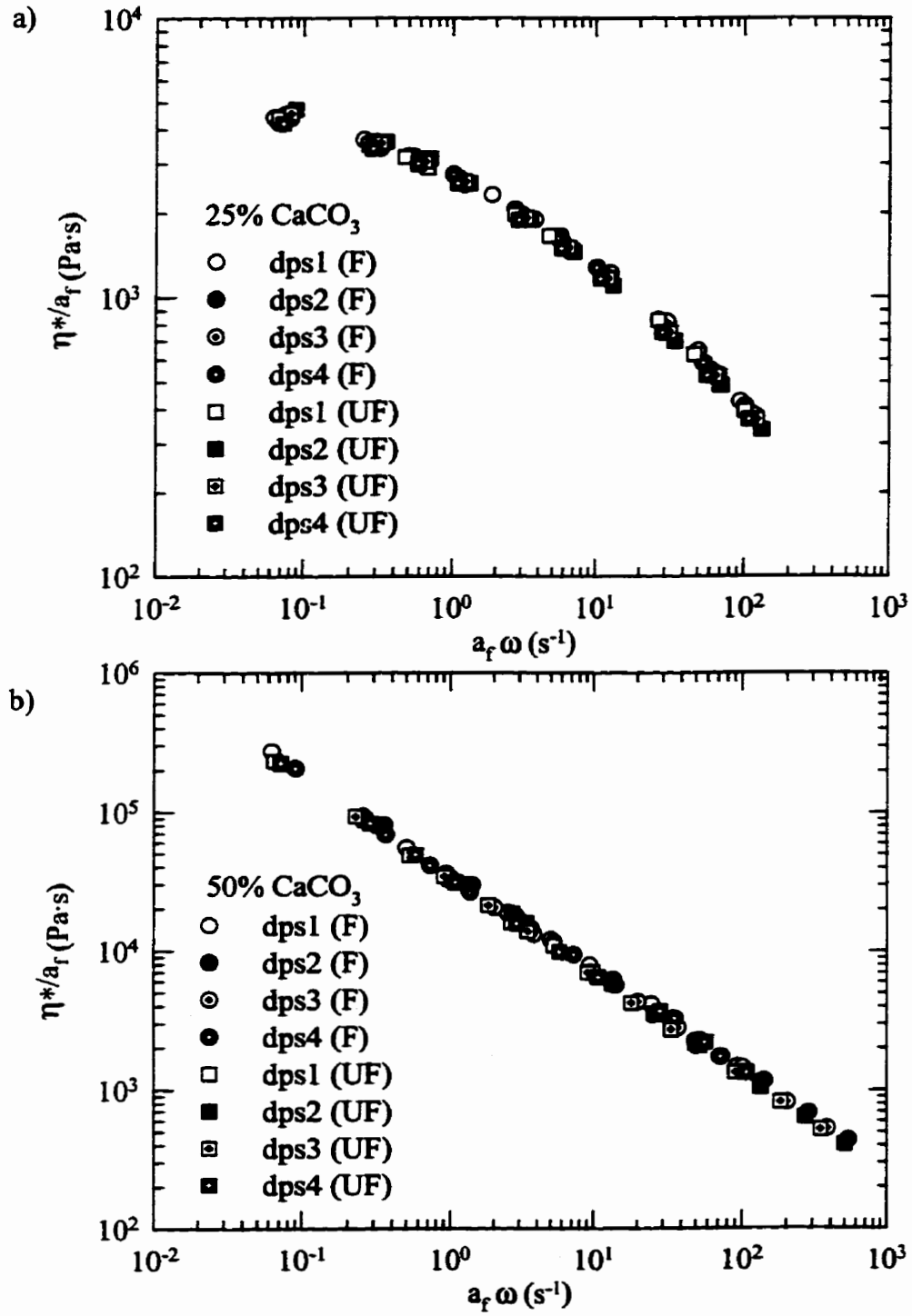

Figure 5.18: Superposition of complex viscosity for $CaCO_3$ filled PP measured at T=200°C: (a) 25%, (b) 50%

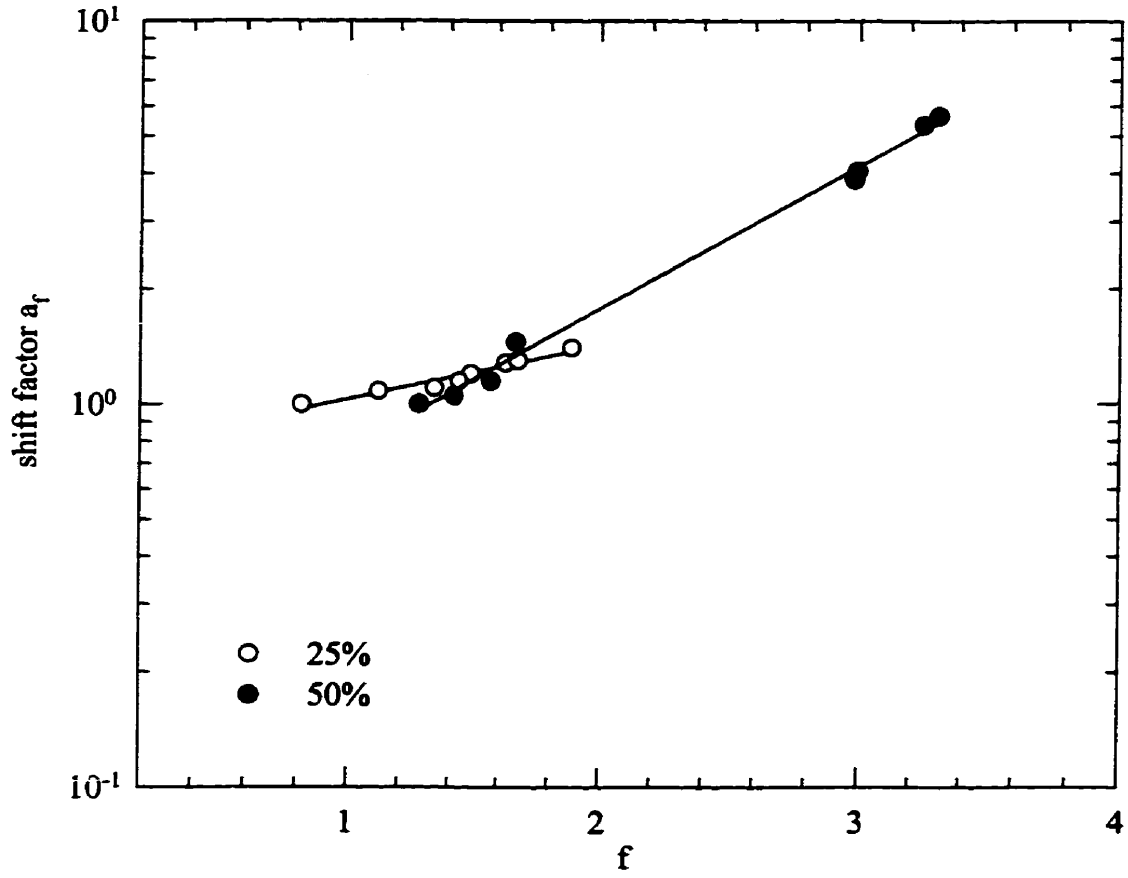

Figure 5.19: Relation of shift factor and dispersion index for $CaCO_3$ filled PP measured at T=200°C

CHAPTER 6 - RHEOLOGY IN POLYMER PROCESSING

The influence of elongational flow on the dispersion has been investigated. Two convergent dies have been used to measure the extensional viscosity of pure polypropylene as well as compounds. In order to correlate the extensional properties to the dispersion index, two compounds via different processes were prepared using screw configuration 2. One was obtained by adding the powder through the hopper, the other over the downstream entry port. Both contained 50% calcium carbonate (fine). In this chapter, the simple shear viscosity results will be presented and discussed first, followed by elongational property analysis.

6.1 Results of simple shear viscosity

The power-law parameters of the shear viscosity for pure PP and compounds (50/50 PP/$CaCO_3$) are listed in Table 6.1. With the aid of the pressure transducers that were located along the slit die channel, the axial pressure distribution was measured from which the wall shear stress was calculated. The wall shear rate was determined by measurements of the flow rate and followed by Rabinowitsch analysis. Knowing the shear stress and shear rate, the shear viscosity was then calculated. The power-law parameters were determined from a plot of log η_s vs. log $\dot{\gamma}$. Temperature variation is a very sensitive factor affecting the rheological measurements, which assume isothermal flow. In order to minimize the measurement discrepancy by variations of temperature, the melt temperature measured at the wall was kept at 200°C during experiments for all molten polymer and compounds studied. No extrudate distortion was observed with the slit die as well as the convergent dies for the polymer/compounds and flow rates investigated. The comparison of steady shear viscosity and complex viscosity is shown in Figure 6.1. The Cox-Merz empirical rule, which was established for polymer melts, seems to work well for the homogeneous PP used in our studies. However, it is

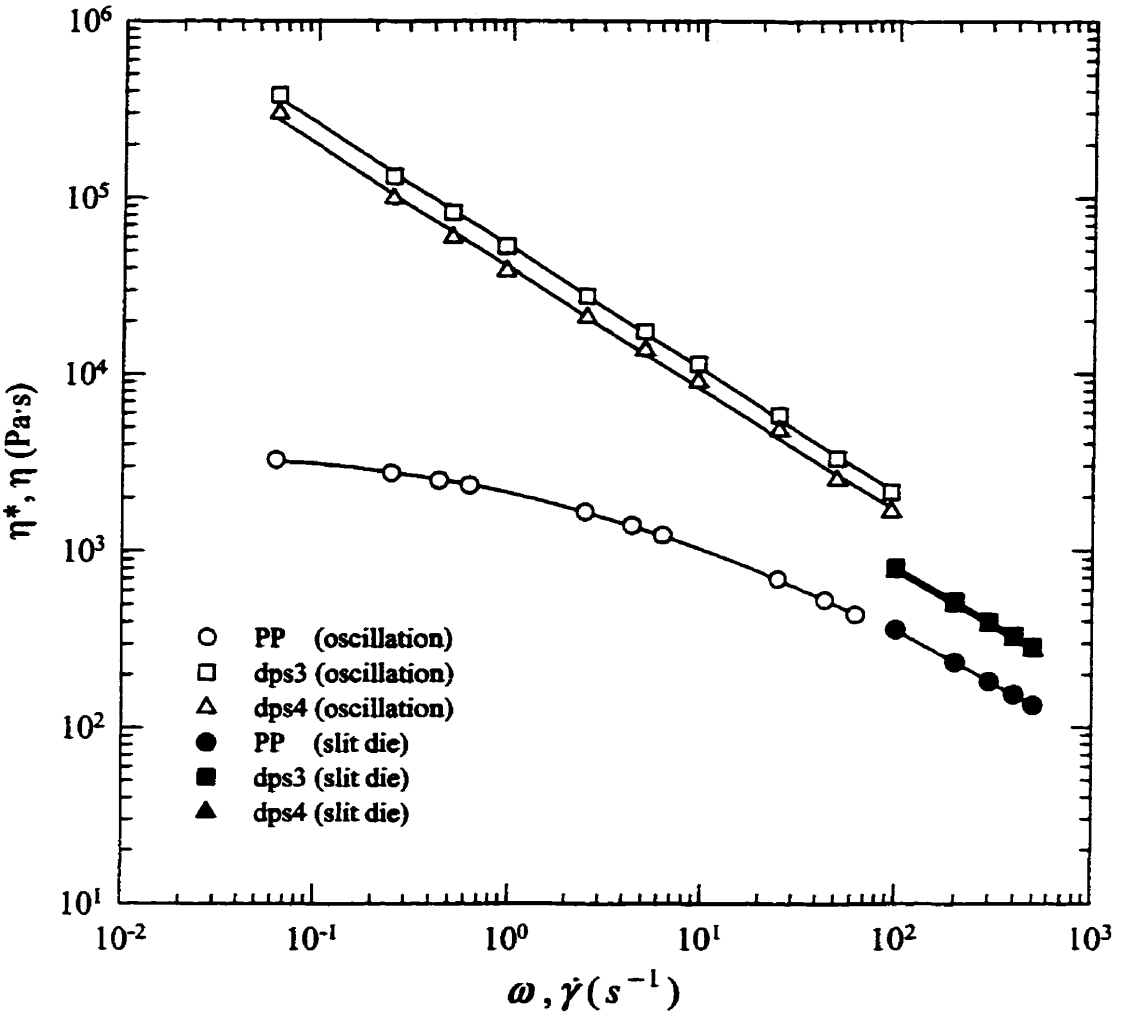

Figure 6.1: Complex and steady shear viscosity of PP and PP with 50% $CaCO_3$ at T=200°C

Table 6.1: Power-law parameters in shear of the different systems

Power-law parameter	PP	PP/$CaCO_3$ (dps3)	PP/$CaCO_3$ (dps4)
K (Pa·s^n)	6105	15371	14675
n	0.385	0.361	0.360

clearly invalid for calcium carbonate filled PP system. The steady shear viscosity is always much lower than the complex viscosity. Therefore, the Cox-Merz rule does not hold for our PP/$CaCO_3$ melts, in agreement with the literature (Rong and Chaffey, 1988; Kitano et al., 1980).

6.2 Results and discuss of elongational viscosity

Figure 6.2 gives plots of the elongational viscosity versus the elongational rate obtained using the Cogswell and Binding analysis, for the three samples examined. Some observations on these plots are worthnoting. First, the extensional viscosity decreases as the extensional rate is increased, over the range of extensional rates studied. In other words, all the systems studied exhibit tension-thinning power-law behavior. The parameters L and t of elongational power-law model from the Binding analysis are presented in Table 6.2.

Table 6.2: Power-law parameters in elongation from the Binding analysis

Parameter	PP		PP/$CaCO_3$ (dps3)		PP/$CaCO_3$ (dps4)	
	D1	D2	D1	D2	D1	D2
L (Pa·s^n)	47172	83814	139045	231876	129745	217683
t	0.34	0.14	0.20	0.012	0.20	0.012

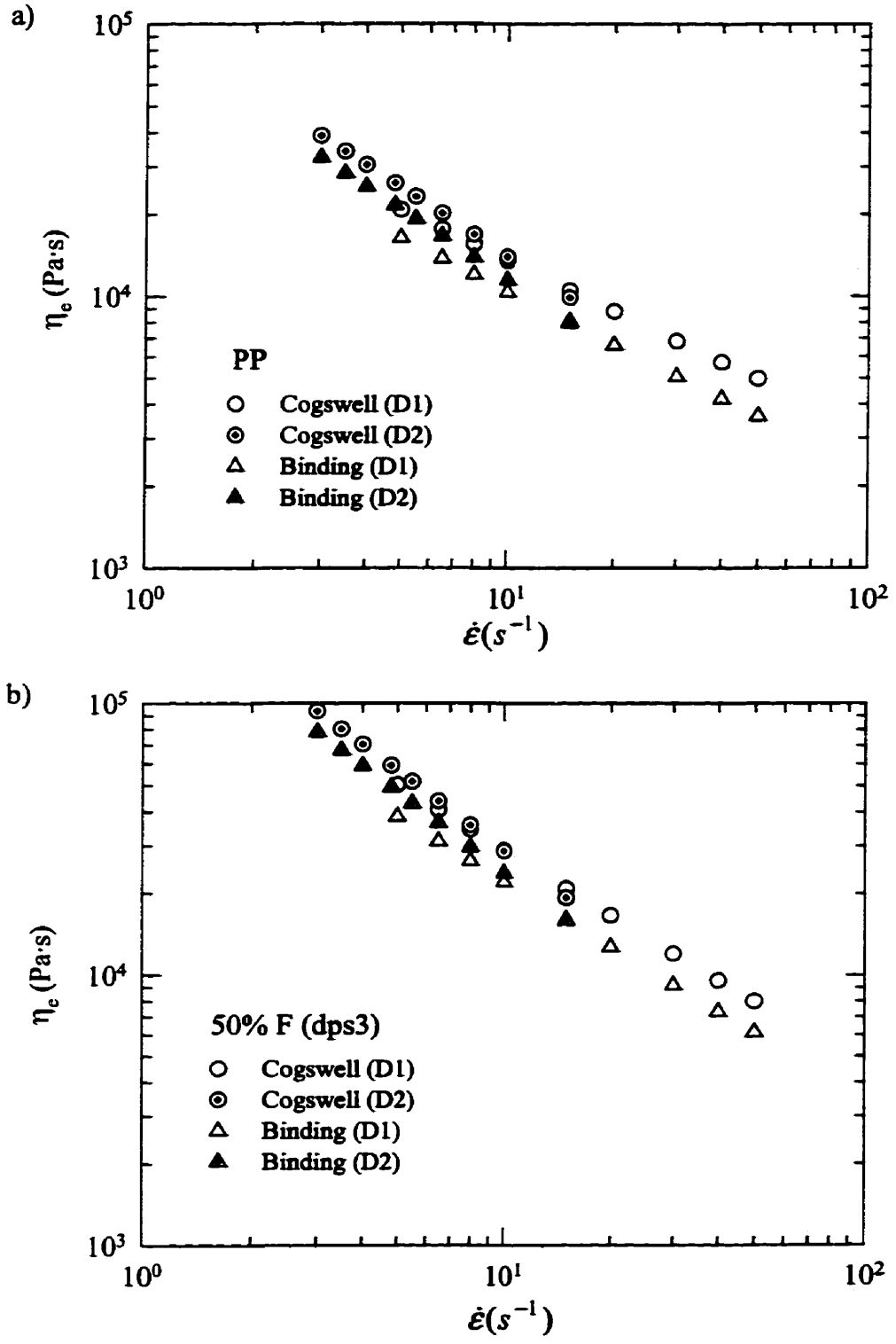

Figure 6.2: Elongational viscosity of: (a) PP, (b) PP with 50% $CaCO_3$ (F) (dps3), (c) PP with 50% $CaCO_3$ (F) (dps4) at T=200°C

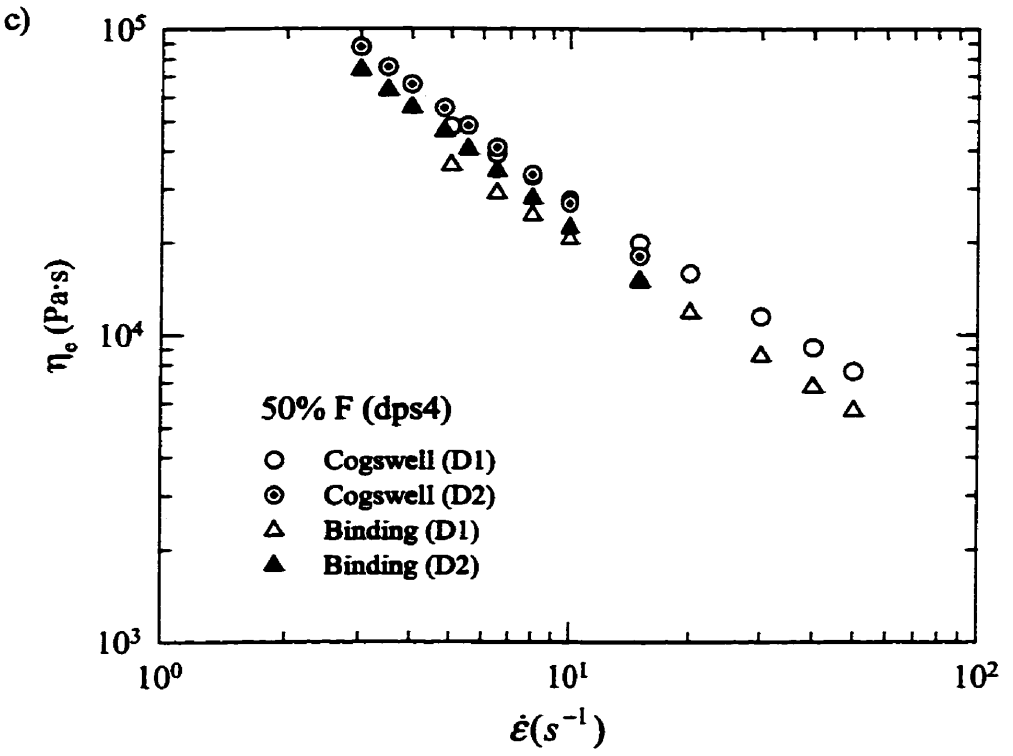

Figure 6.2 (continued)

The elongational viscosity calculated from the Binding method is lower than the one determined from the Cogswell analysis. Note that the viscosity data obtained from die D1 are not in perfect agreement with those from die D2. The extensional viscosities determined from experimental data do not overlap at a fixed elongational rate for pure PP as well as PP/CaCO3 compounds. The discrepancies are, however, acceptable considering the difficulties of carrying meaningful measurements and estimating accurately the shear contribution to the pressure drop, mainly at low flow rates.

The total pressure drops measured across the convergent die include the contribution from elongational and shear components, as can be seen in the analysis of Cogswell and Binding theories. It is of great interest to note that shear flow is not negligible and contributes significantly to the total entrance pressure drop. For the pure PP, about 40% is due to shear flow, while PP/$CaCO_3$ compounds possess as much as 50% of shear. The comparison of elongational viscosity of pure PP and two PP/$CaCO_3$ systems by the same techniques is given in Figure 6.3. The addition of mineral filler undoubtedly increases the elongational viscosity. The dispersion state has an influence on the elongational data as it does on the other rheological properties, which have been reported in chapter 5. The extensional viscosity of dps3 sample, which has the worst dispersion, is slightly higher than that of dps4 sample. However, the difference is insignificant compared to the differences found in the shear and dynamic viscosity data. It seems likely, therefore, the agglomerates of dps3 sample which has a higher value of dispersion index are much easier to be broken-down than that of the dps4 sample as they pass through the convergent dies under shear and elongational deformation.

The Trouton ratios in terms of the second invariant of the rate-of-deformation tensor, $\bar{\dot{\gamma}}$, for the three systems investigated, are presented in Figure 6.4. $\bar{\dot{\gamma}}$, which is defined as $\sqrt{\frac{1}{2}II_{\dot{\gamma}}}$, is equal to $\dot{\gamma}$ for simple shear flow, and to $\sqrt{3}\dot{\varepsilon}$ for uniaxial elongational flow. The shear data were obtained from slit die extrusion and the power-

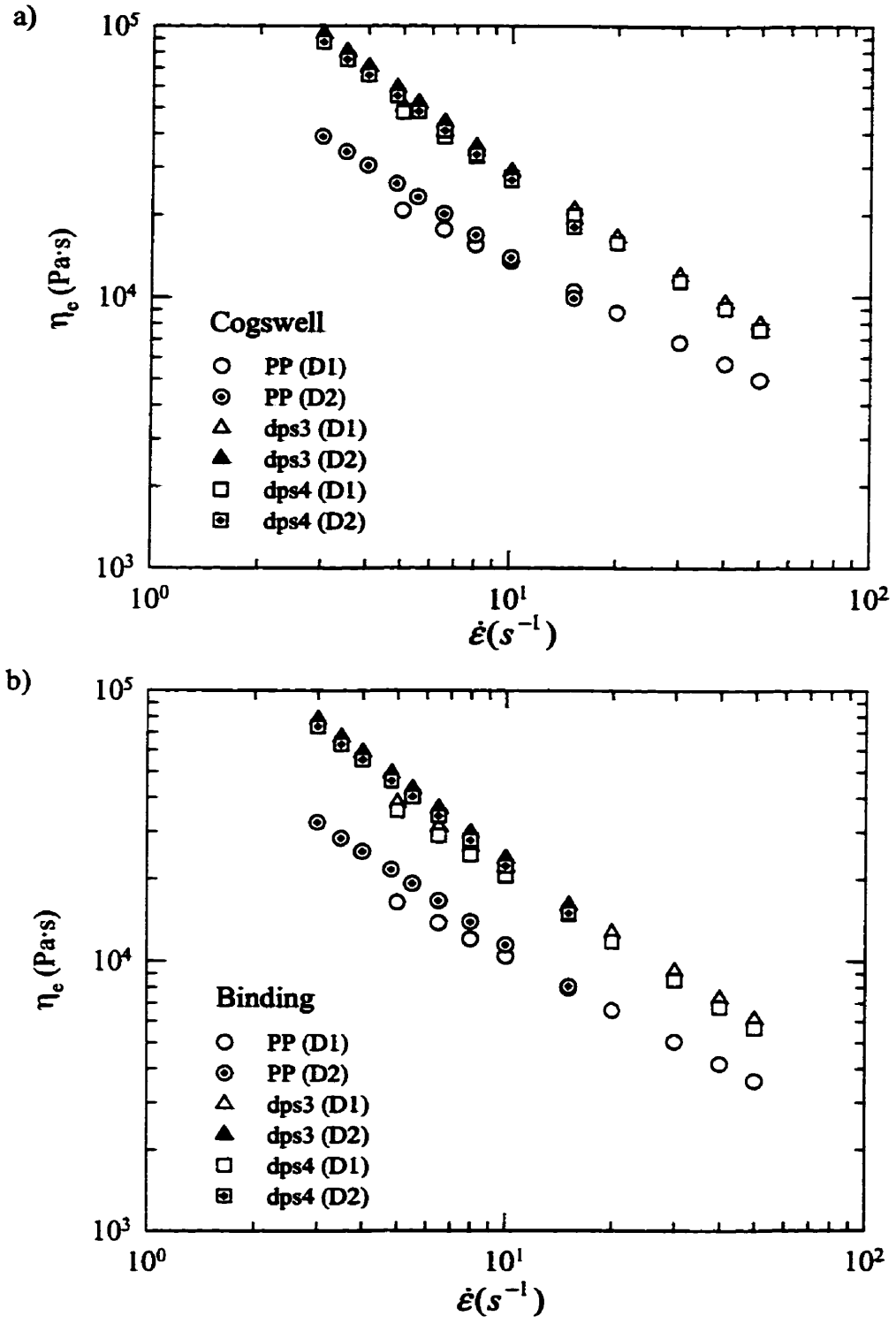

Figure 6.3: Comparison of elongational viscosity of: (a) Cogswell, (b) Binding at T=200°C

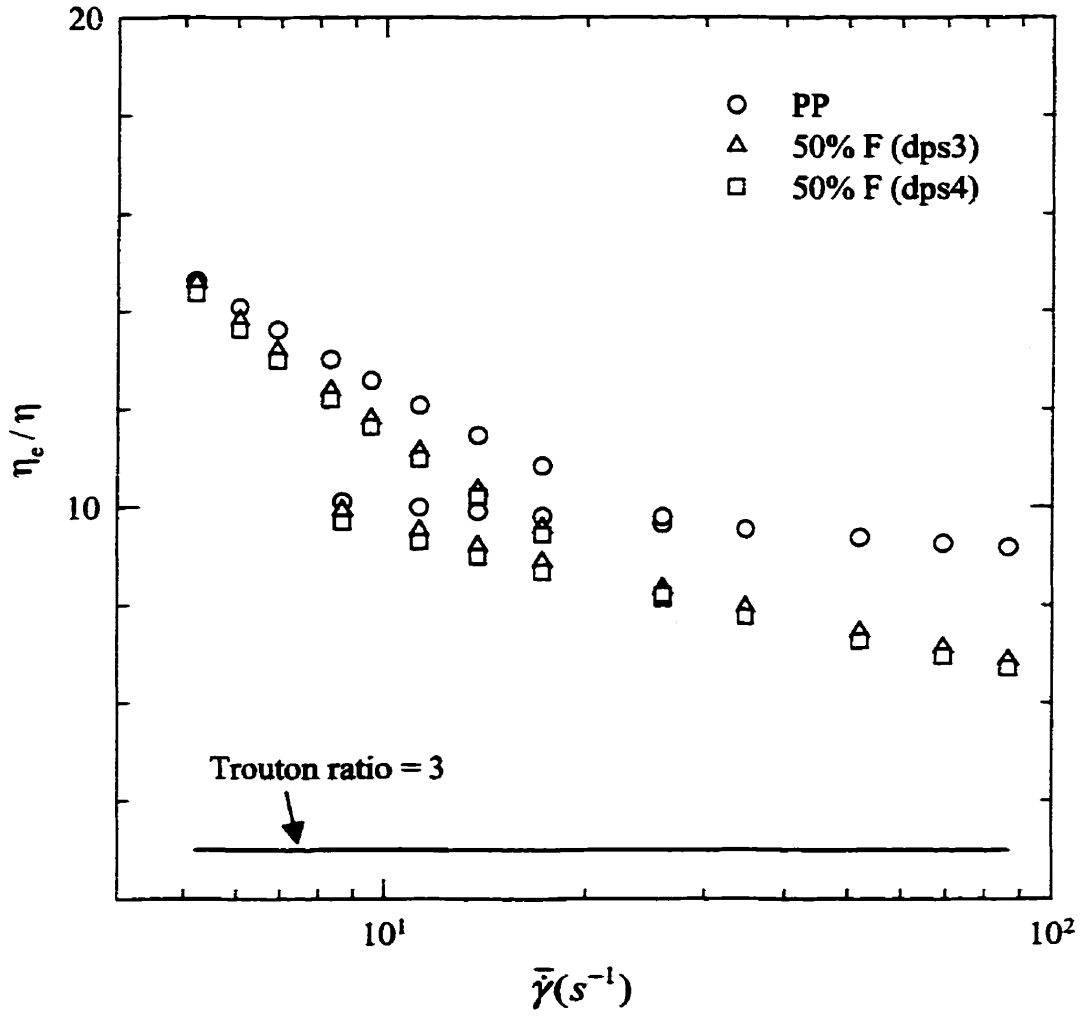

Figure 6.4: Trouton ratio for the PP, PP with 50% $CaCO_3$ (dps3), and PP with 50% $CaCO_3$ (dps4) at T=200°C

law parameters are given in Table 6.1. For all the systems studied, the Trouton ratios are always in excess of the value 3, which is the case for inelastic Newtonian fluids. The differences of viscosity data obtained from the two different dies, as shown in Figure 6.2, become marked in the plots of Trouton ratio. The $CaCO_3$ filled PP has a lower value of Trouton ratio than the pure PP. This can be interpreted as a decrease of η_e due to the agglomerate breakdown under shear and elongational deformation.

6.3 Effect of simple shear and elongational flow on filler dispersion

As mentioned in sections 6.1 and 6.2, dispersion of filler may probably be improved when shear or extensional flow is imposed on the materials. Experiments have been carried out to investigate how these two flows affect the agglomerates. In experimental section, we have mentioned that the setup of slit die as in Figure 3.3 and convergent die in Figure 3.6 allows us to extract samples before and after shear and/or converging section. Blown films were then prepared from the extracted samples and utilized to analyze the filler dispersion using microstructural and image analysis procedures. The results of dispersion index and volume average diameter are reported in Figure 6.5 and Table 6.3 respectively.

Table 6.3: Dispersion index and volume average diameter obtained after extrusion through slit and hyperbolic shaped dies (50% $CaCO_3$ Fine)

Sample extracted from	Dispersion index f		d_v (μm)	
	dps3	dps4	dps3	dps4
twin-screw	2.99	1.67	248	208
bypass	2.58	1.56	240	205
after slit	1.74	1.38	214	187
after convergent	1.53	1.32	203	179

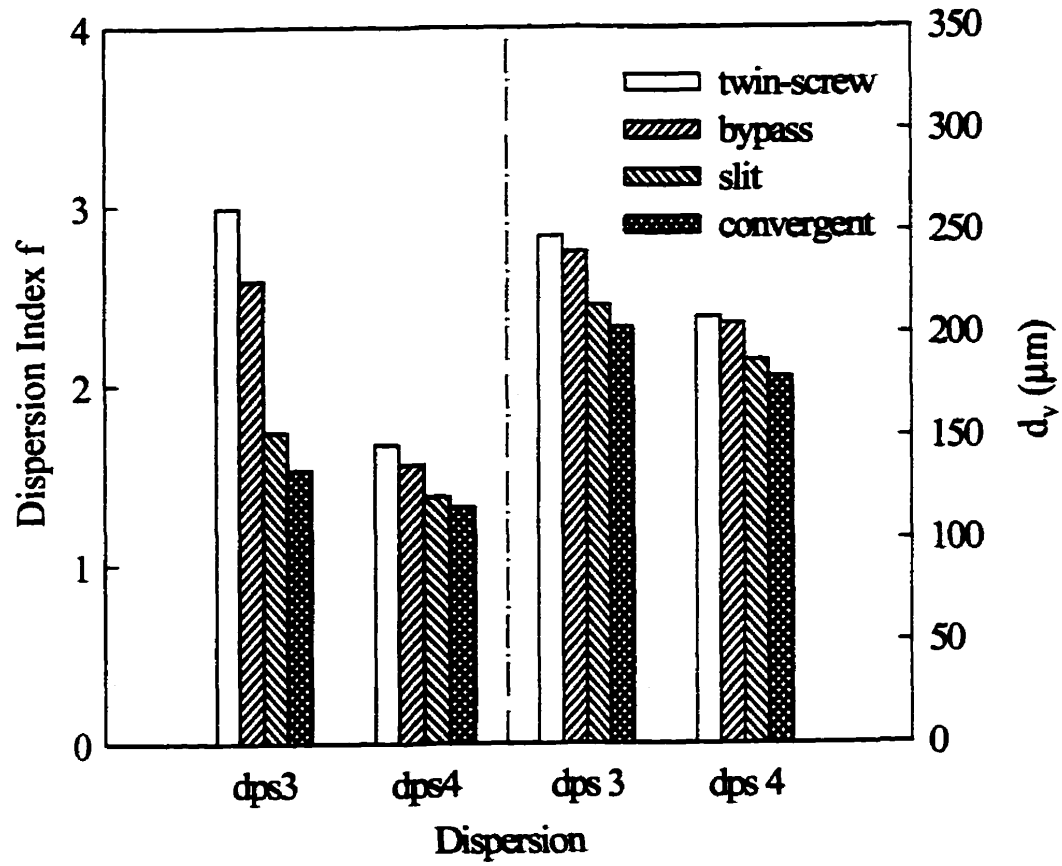

Figure 6.5: Effect of shear and extensional flow on dispersion index and volume diameter

The analysis of the samples from the bypass indicates that the dispersions are least affected by the shear generated in the single-screw extrusion. However, the influence of shear and extensional flow produced by the slit and the convergent die are significant, as can be seen from the volume average diameter data and dispersion index values in Figure 6.5. To characterize the flow field, the parameter λ was calculated using equation (3.26). The result of value λ is 0.5 for flow through the slit die and 0.58 for the converging die. Obviously, the elongational flow is more efficient than the simple shear flow in dispersive mixing. The results of flow field analysis is in agreement with that of dispersion index analysis, as we can see from Figure 6.5 that the value of dispersion index f for the compounds from the converging die is less than that from the slit die. The dispersion index f is an important parameter for characterizing the influence of processing variables on mixing efficiency.

CHAPTER 7 - CONCLUSIONS

The process of filler dispersion during twin-screw extrusion compounding has been studied using microstructural and images analysis procedures. The effect of selected processing parameters (screw speed, flow rate and screw configuration) have been investigated in terms of a dispersion index f. The quantity of kneading discs in either the melting or the mixing zones and the filler feeding position along with the screw affect the value of dispersion index. For adding the filler via hopper, a screw configuration with more melting elements gave good dispersion results due to the considerable energy input during passage of material through the kneading discs, which act as partial barriers to flow. Foe feeding the filler through downstream port, better results were obtained when the filler was introduced to solid or low-temperature molten polymer. Less kneading elements in the melting zone as configuration 2 cause a delay of the polymer melting and result in a better dispersion via downstream feeding. Lowering the flow rate or increasing the screw speed enhanced the dispersion state. Increasing filler concentration substantially alters the dispersion index over the range of value studied. The particle size of $CaCO_3$ was found to have an influence on dispersion only for the low concentration (25%) compounds, but less effect for high concentration (50%) ones.

The viscoelastic properties of molten polypropylene filled with ultra fine and fine $CaCO_3$ powders have been studied. Many difficulties arise in the measurement of rheological properties of such filled systems, mainly due to changes of rheological behavior with time. The interparticle reaction, particle network buildup, as well as particle-alignment at high filler concentration give rise to the property fluctuation with time under a given deformation. Temperature, deformation rate, and strain-amplitude are the key factors affecting the attractive forces acting between particles and modifying the network structure of the compounds. Steady shear deformation changes the degree of dispersion due to the agglomerate breakdown during the time the network is broken up. Imposing a small-amplitude pre-oscillatory shear is found to be the optimum method to

destroy the particle network and alter the filler dispersion state to the lowest limit. Strain sweep experiments show that the rheological response of filled polymer melts is sensitive to the level of strain. For 50% $CaCO_3$/PP compound, no linear viscoelastic domain is obtained. The minimum reliable strain of 1% for a given experimental device was applied to the viscoelasticity measurements for all the 50% $CaCO_3$/PP compounds under investigation.

The effects of filler concentration, degree of dispersion, particle/agglomerate size on the viscoelasticity have been determined. The complex viscosity increases with filler concentration, especially at low frequencies, as expected. An apparent yield stress is observed at a solid concentration of 50 wt%, due to the increase of the filler content and the agglomerate sizes which result in a solid-like structure. The particle-particle interactions are also responsible for the appearance of apparent yield stress. At a fixed concentration, the better dispersion results in the reduction of viscosity. For high concentrated polymer melts, the increase of agglomerate size, which gives rise to high dispersion index value, leads to more viscous, higher yield stress materials. The influences of particle size differences on the complex viscosity are observed for low concentrated systems. The Maron-Pierce and Mooney models cannot describe the rheological behavior of the systems used in our study, due to the significant yield stress and particle-particle interactions. The relative viscosity of untreated $CaCO_3$ filled PP system is much higher than that expected by the model equations. A correlation between complex viscosity and dispersion index is derived by superposition of viscosity curve at different dispersion index into a single curve, and can be described by:

$$\eta^*(\omega, f) = a_f \eta^*(a_f \omega, f_r)$$

The application of this equation is believed to subject to the system studied and should be proved case by case.

The extensional flow properties have been obtained using a convergent die with constant elongational rate, for which the flow is mostly extensional. The extensional viscosity has been calculated from entrance pressure drop, utilizing two techniques – the Cogswell and Binding analysis. The two methods lead to the elongational viscosity values in the same order of magnitude. The elongational viscosities of pure PP and $CaCO_3$/PP show tension-thinning behavior. The Trouton ratio values are well above 3 and the smallest value for the three systems is about 7. The dispersion states before and after elongational/shear flow have been analyzed using converging and slit die. Both flow fields change the degree of dispersion. The values of flow field characterization parameter λ confirm that the elongational flow is more efficient than simple shear flow in dispersive mixing.

In general, the results of the present study are very encouraging, but we are left with some unsolved questions, which would suggest some challenge in this area:

- Illustrate the role of particle interactions in the viscoelasticity of dispersed polymeric systems;
- Develop models to correlate the rheological properties of such a system to the microscopical parameters, both structural and physical, which are responsible for them;
- Develop an on-line experimental technique to determine the dispersion under applied flow and correlate it to the rheological response.

BIBLIOGRAPHY

ARAL, B.K., KALYON, D.M. (1997). Viscoelastic material functions of noncolloidal suspensions with spherical particles. Journal of Rheology, 41, (3), 599-620.

BAWISKAR, S., WHITE, J.L. (1995). Solids conveying and melting in a starve fed self-wiping co-rotating twin screw extruder. International Polymer Processing, 10, 105-109.

BIGG, D.M. (1983). Rheological behavior of highly filled polymer melts. Polymer Engineering and Science, 23, (4), 206-210.

BINDING, D.M. (1988). An approximate analysis for contraction and converging flows. Journal of Non-Newtonian Fluid Mechanics, 27, 173-188.

BINDING, D.M., JONES, D.M. (1989). On the interpretation of data from converging flow rheometers. Rheologica Acta, 28, 215-222.

BOAIRA, M.S., CHAFFEY, C.E. (1977). Effects of coupling agents on the mechanical and rheological properties of mica-reinforced polypropylene. Polymer Engineering and Science, 17, (10), 715-718.

BOMAL, Y., GODARD, P. (1996). Melt viscosity of calcium-carbonate-filled low density polyethylene: influence of matrix-filler and particle-particle interactions. Polymer Engineering and Science, 36, (2), 237-243.

BORIES, M. (1998). Influence des conditions opératoires d'extrusion sur la dispersion de carbonate de calcium dans une matrice de polypropylène. Thèse de Maîtrise, École Polytechnique de Montréal, Canada.

CARREAU, P.J., LAVOIE, P.-A., BAGASSI, M. (1996). Rheological properties of filled polymers. Eurofiller 95, FILPLAS and MOFFIS, Macromolecular Symposia, 108, 111-126.

CARREAU, P.J., DE KEE, D., CHHABRA, R.P. (1997). Rheology of Polymeric Systems: Principles and Application. New York, Hanser, 196-216.

CHENG, J.J., MANAS-ZLOCZOWER, I. (1990). Flow field characterization in Banbury mixer. International Polymer Processing, 3, 178-183.

COGSWELL, F.N. (1972). Converging flow of polymer melts in extrusion dies. Polymer Engineering and Science, 12, (1), 64-73.

COGSWELL, F.N. (1978). Converging flow and stretching flow: a compilation. Journal of Non-Newtonian Fluid Mechanics, 4, 23-38.

CZARNECKI, L., WHITE, J.L. (1980). Shear flow rheological properties, fiber damage, and mastication characteristics of aramid-, glass-, and cellulose-fiber-reinforced polystyrene melts. Journal of Applied Polymer Science, 25, 1217-1244.

EBELL, P.C., HEMSLEY, D.A. (1981). A novel optical method for estimating the dispersion of carbon black in rubbers. Rubber Chemistry and Technology, 54, 698-717.

ESS, J.W., HORNSBY, P.R. (1987). Twin-screw extrusion compounding of mineral filled thermoplastics: dispersive mixing effects. Plastics and Rubber Processing and Applications, 8, 147-156.

GADALA-MARIA, F., ACRIVOS, A. (1980). Shear-induced structure in a concentrated suspension of solid spheres. Journal of Rheology, 24, (6), 799-814.

GHOSH, T., LAVOIE, P.-A., CARREAU, P.J. (1997). Rheology of coating colours and their runnability on a cylindrical laboratory coater. Tappi Journal, 80, (11), 189-192.

HAN, C.D., KIM, Y.W. (1974). Studies on melt spinning. V. elongational viscosity and spinnability of two-phase systems. Journal of Applied Polymer Science, 18, 2589-2603.

HAN, C.D., VAN DEN WEGHE, T., SHETE, P., et al. (1981). Effects of coupling agents on the rheological properties, processability, and mechanical properties of filled polypropylene. Polymer Engineering and Science, 21, (4), 196-204.

HESS, W.M. (1991). Characterization of dispersions. Rubber Chemistry and Technology, 64, 386-449.

HUNEAULT, M.A., GENDRON, R., DAIGNEAULT, L.E. (1996). Residence time distributions in twin screw extruders: contribution of the different screw functions. ANTEC, Indianapolis, 329-332.

HUSBAND, D.M., AKSEL, N. (1993). The existence of static yield stresses in suspensions containing noncolloidal particles. Journal of Rheology, 37, (2), 215-235.

JAMES, D.F., CHANDLER, G.M. (1990). A converging channel rheometer for the measurement of extensional viscosity. Journal of Non-Newtonian Fluid Mechanics, 35, 421-443.

KAMAL, M.R., MUTEL, A. (1985). Rheological properties of suspensions in Newtonian and non-Newtonian fluids. Journal of Polymer Engineering, 5, 293-382.

KATAOKA, T., KITANO, T., OYANAGI, Y., et al. (1979). Viscous properties of calcium carbonate filled polymer melts. Rheologica Acta, 18, (5), 635-639.

KATAOKA, T., SASAHARA, M., NISHIJIMA, K. (1978). Viscosity of particle filled polymer melts. Rheologica Acta, 17, (2), 149-155.

KIM, H.C., PENDSE, A., COLLIER, J.R. (1994). Polymer melt lubricated elongational flow. Journal of Rheology, 38, (4), 831-845.

KITANO, T., KATAOKA, T. (1980). The effect of the mixing methods on viscous properties of polyethylene melts filled with fibers. Rheologica Acta, 19, (6), 753-763.

KITANO, T., NISHIMURA, T., KATAOKA, T., et al.(1980). Correlation of dynamic and steady flow viscosities of filled polymer systems. Rheologica Acta, 19, 671-673.

LACROIX, C., GRMELA, M., CARREAU, P.J. (1999). Morphological evolution of immiscible polymer blends in simple shear and elongational flows. Journal of Non-Newtonian Fluid Mechanics, (in press).

LAKDAWALA, K., SALOVEY, R. (1987a). Rheology of polymers containing carbon black. Polymer Engineering and Science, 27, (14), 1035-1042.

LAKDAWALA, K., SALOVEY, R. (1987b). Rheology of copolymers containing carbon black. Polymer Engineering and Science, 27, (14), 1043-1049.

LAVOIE, P.-A., GHOSH, T., CARREAU, P.J. (1996). The rheology of coating colours: a comprehensive approach. International Paper and Coating Chemistry Symposium, Ottawa, 253-257.

LAVOIE, P.-A., CARREAU, P.J., GHOSH, T. (1997). Rheology of suspensions: the flow behaviour of coating colours. Journal of Pulp and Paper Science, 23, (11), 543-547.

LAWAL, A., KALYON, D.M. (1995). Mechanisms of mixing in single and co-rotating twin screw extruders. Polymer Engineering and Science, 35, (17), 1325-1338.

LE, D.C., BHATTACHARYA, S.N. (1990). Influence of temperature on the viscous behavior of some concentrated dispersions. Journal of Rheology, 34, (5), 637-655.

LEIGHTON, D., ACRIVOS, A. (1987). Measurement of shear-induced self-diffusion in concentrated suspensions of spheres. Journal of Fluid Mechanics, 177, 109-131.

LEONOV, A.I. (1990). On the rheology of filled polymers. Journal of Rheology, 34, (7), 1039-1068.

LI, L., MASUDA, T. (1990). Effect of dispersion of particles on viscoelasticity of CaCO3-filled polypropylene melts. Polymer Engineering and Science, 30, (14), 841-847.

LOBE, V.M., WHITE, J.L. (1979). An experimental study of the influence of carbon black on the rheological properties of a polystyrene melt. Polymer Engineering and Science, 19, (9), 617-624.

MACK, M.H. (1990). Split-feed compounding of highly filled polymers. Plastics Engineering, 8, 31-36.

MACKAY, M.E., ASTARITA, G. (1997). Analysis of entry flow to determine elongation flow properties revisited. Journal of Non-Newtonian Fluid Mechanics, 70, 219-235.

MANAS-ZLOCZOWER, I. (1994). Dispersive mixing of solid additives. Mixing and Compounding of Polymers, Manas-Zloczower, I., Tadmor, Z. New York, Hanser, 56-83.

MANAS-ZLOCZOWER, I., FEKE, D.L. (1988). Analysis of agglomerate separation in linear flow fields. International Polymer Processing, 2, 185-190.

MANAS-ZLOCZOWER, I., NIR, A., TADMOR, Z. (1982). Dispersive mixing in internal mixers - A theoretical model based on agglomerate rupture. Rubber Chemistry and Technology, 55, 1250-1285.

MARON, S.H., PIERCE, P.E. (1956). Application of ree-eyring generalized flow theory to suspensions of spherical particles. Journal of Colloid Science, 11, 80- 95.

METZNER, A.B. (1985). Rheology of suspensions in polymeric liquids. Journal of Rheology, 29, 739-775.

MINAGAWA, N., WHITE, J.L. (1976). The influence of titanium dioxide on the rheological and extrusion properties of polymer melts. Journal of Applied Polymer Science, 20, 501-523.

MOONEY, M. (1951). The viscosity of a concentrated suspension of spherical particles. Journal of Colloid Science, 6, 162- 170.

OTTANI, S., VALENZA, A., LA MANTIA, F.P. (1988). Shear characterization of $CaCO_3$-filled linear low density polyethylene. Rheologica Acta, 27, (2), 172-178.

PHILLIPS, R.J., ARMSTRONG, R.C., BROWN, R.A., et al. (1992). A constitutive equation for concentrated suspensions that accounts for shear-induced particle migration. Physics of Fluids, 4, (1), 30-40.

POSLINSKI, A.J., RYAN, M.E., GUPTA, R.K., et al. (1988). Rheological behavior of filled polymeric systems I. yield stress and shear-thinning effects. Journal of Rheology, 32, (7), 703-735.

RONG, S., CHAFFEY, C.E. (1988). Composite viscoelasticity in glassy, transitional and molten states. II. Dynamic mechanical behavior. Rheologica Acta, 27, 186-196.

RWEI, S.P., MANAS-ZLOCZOWER, I. (1990). Observation of carbon black agglomerate dispersion in simple shear flows. Polymer Engineering and Science, 30, (12), 701-706.

RWEI, S.P., MANAS-ZLOCZOWER, I., FEKE, D.L. (1991). Characterization of agglomerate dispersion by erosion in simple shear flows. Polymer Engineering and Science, 31, (8), 558-562.

SASTROHARTONO, T., JALURIA, Y. (1995). Numerical simulation of fluid flow and heat transfer in twin-screw extruders for non-newtonian materials. Polymer Engineering and Science, 35, (15), 1213-1221.

SCOTT, C., ISHIDA, H., MAURER, F.H.J. (1988). Interfacial effects on the melt state behavior of polyethylene-EPDM-calcium carbonate composites. Rheologica Acta, 27, 273-278.

SUETSUGU, Y. (1990). State of dispersion - Mechanical properties correlation in small particle filled polymer composites. International Polymer Processing, 5, (3), 184-190.

SUETSUGU, Y., WHITE, J.L. (1983). The influence of particle size and surface coating of calcium carbonate on the rheological properties of its suspensions in molten polystyrene. Journal of Applied Polymer Science, 28, 1481-1501.

SZYDLOWSKI, W., BRZOSKOWSKI, R., WHITE, J.L. (1987). Modelling flow in an intermeshing co-rotating twin screw extruder: flow in kneading discs. International Polymer Processing, 1, 207-214.

SZYDLOWSKI, W., WHITE, J.L. (1988). Improved model of flow in the kneading disc region of an intermeshing co-rotating twin screw extruder. International Polymer Processing, 2, 142-150.

TADMOR, Z., BOGOS, C.G. (1979). Characterization of mixtures and mixing. Principles of Polymer Processing, New York, John Wiley & Sons, 196-216.

TANAKA, H., WHITE, J.L. (1980). Experimental investigations of shear and elongational flow properties of polystyrene melts reinforced with calcium carbonate, titanium dioxide, and carbon black. Polymer Engineering and Science, 20, (14), 949-956.

WANG, Y., WANG, J.J. (1999). Shear yield behavior of calcium carbonate-filled polypropylene. Polymer Engineering and Science, 39, (1), 190-198.

APPENDIX A -
FIGURES OF RHEOLOGICAL PROPERTIES

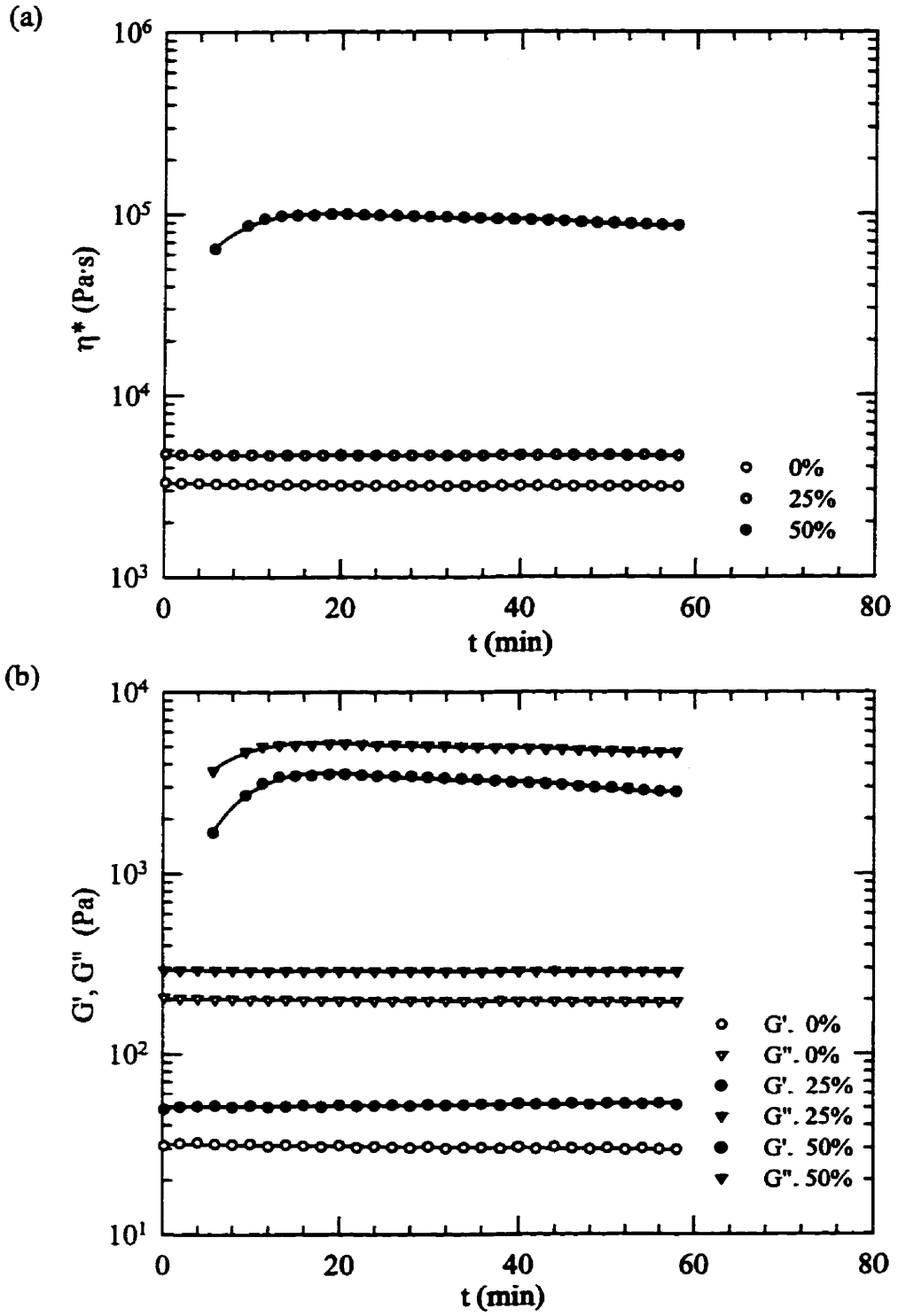

Figure A.1: Variations of rheological properties with time measured at T=200°C and 0.01 Hz for PP with $CaCO_3$ (F) (dps1): (a) η*, (b) G' & G"

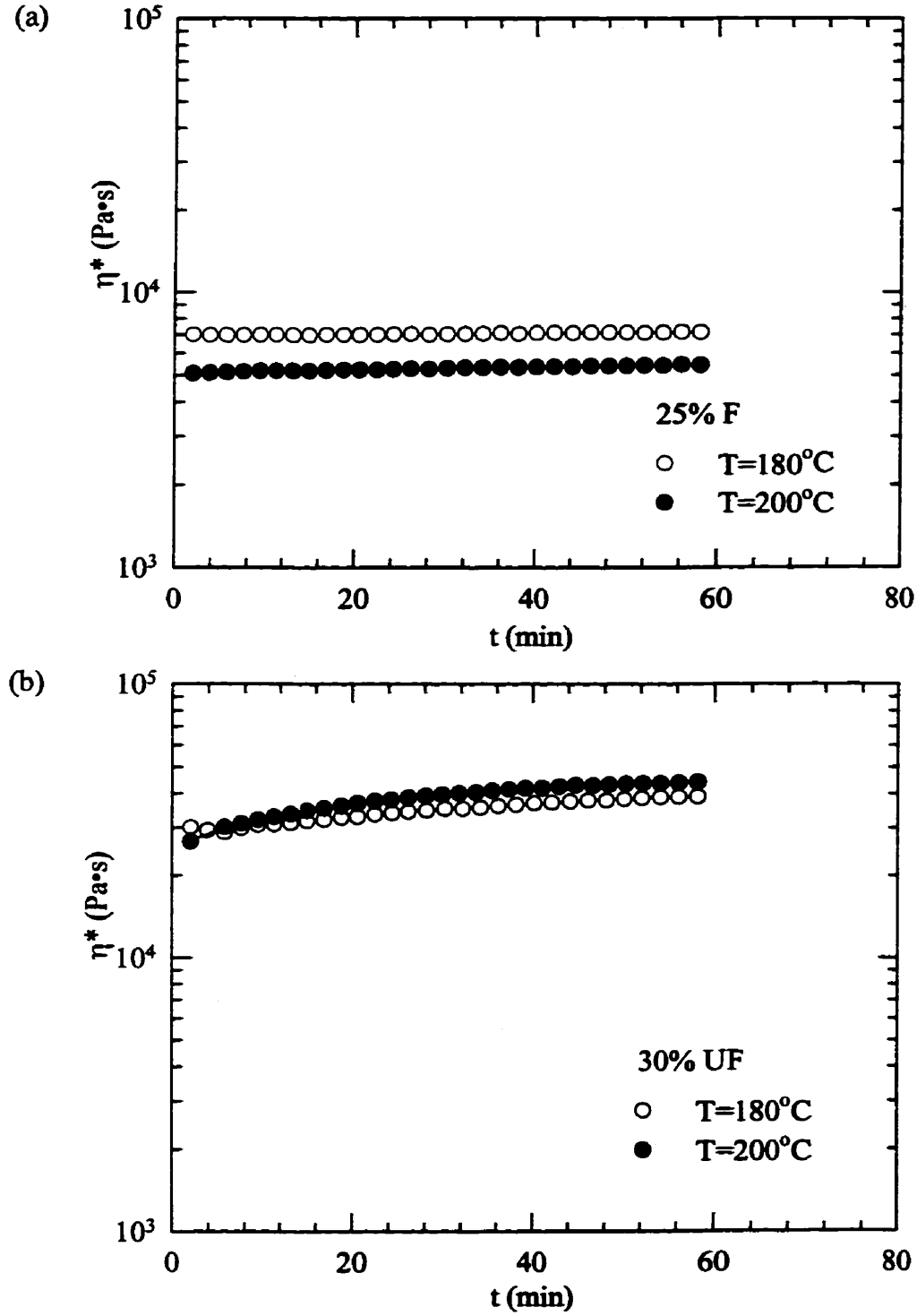

Figure A.2: Effect of temperature on complex viscosity measured at 0.01 Hz for PP with $CaCO_3$ (dps2): (a) 25% F, (b) 30% UF, (c) 50% F & UF

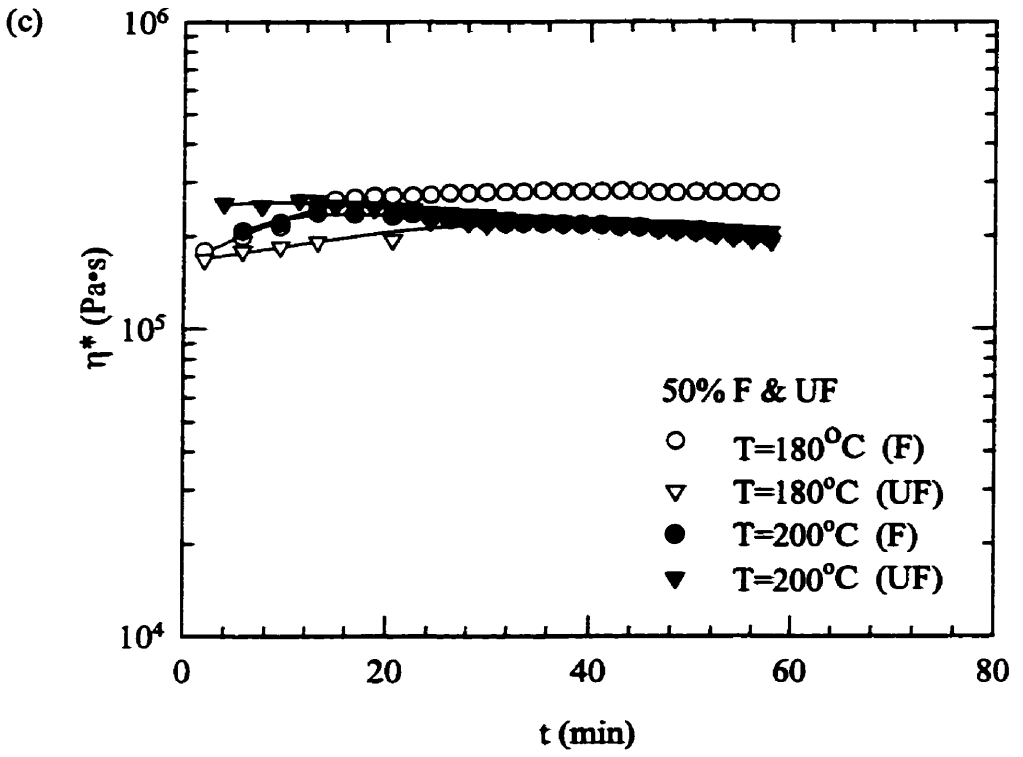

Figure A.2 (continued)

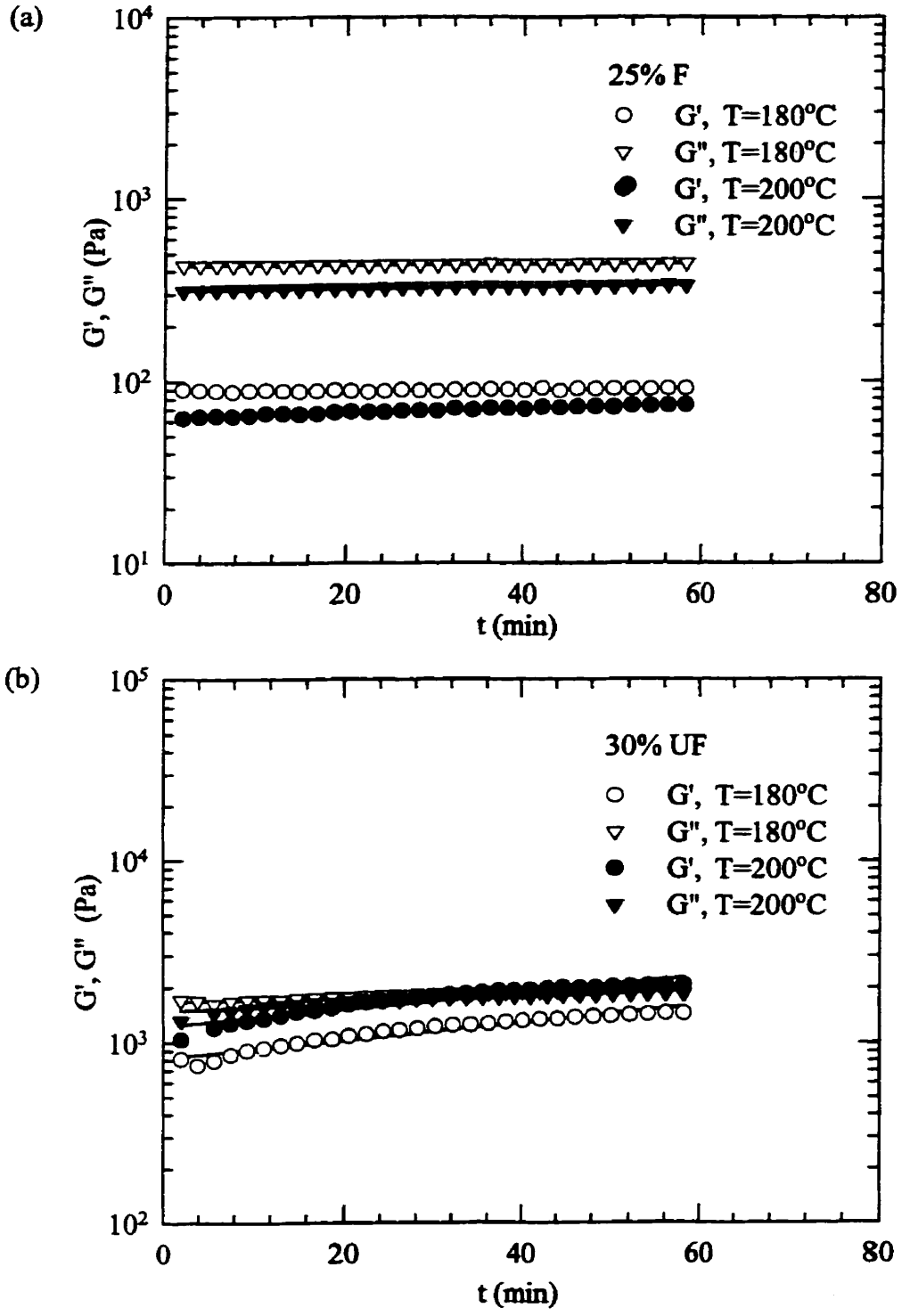

Figure A.3: Effect of temperature on dynamic storage and loss moduli measured at 0.01 Hz for PP with $CaCO_3$ (dps2): (a) 25% F, (b) 30% UF, (c) 50% F, (d) 50% UF

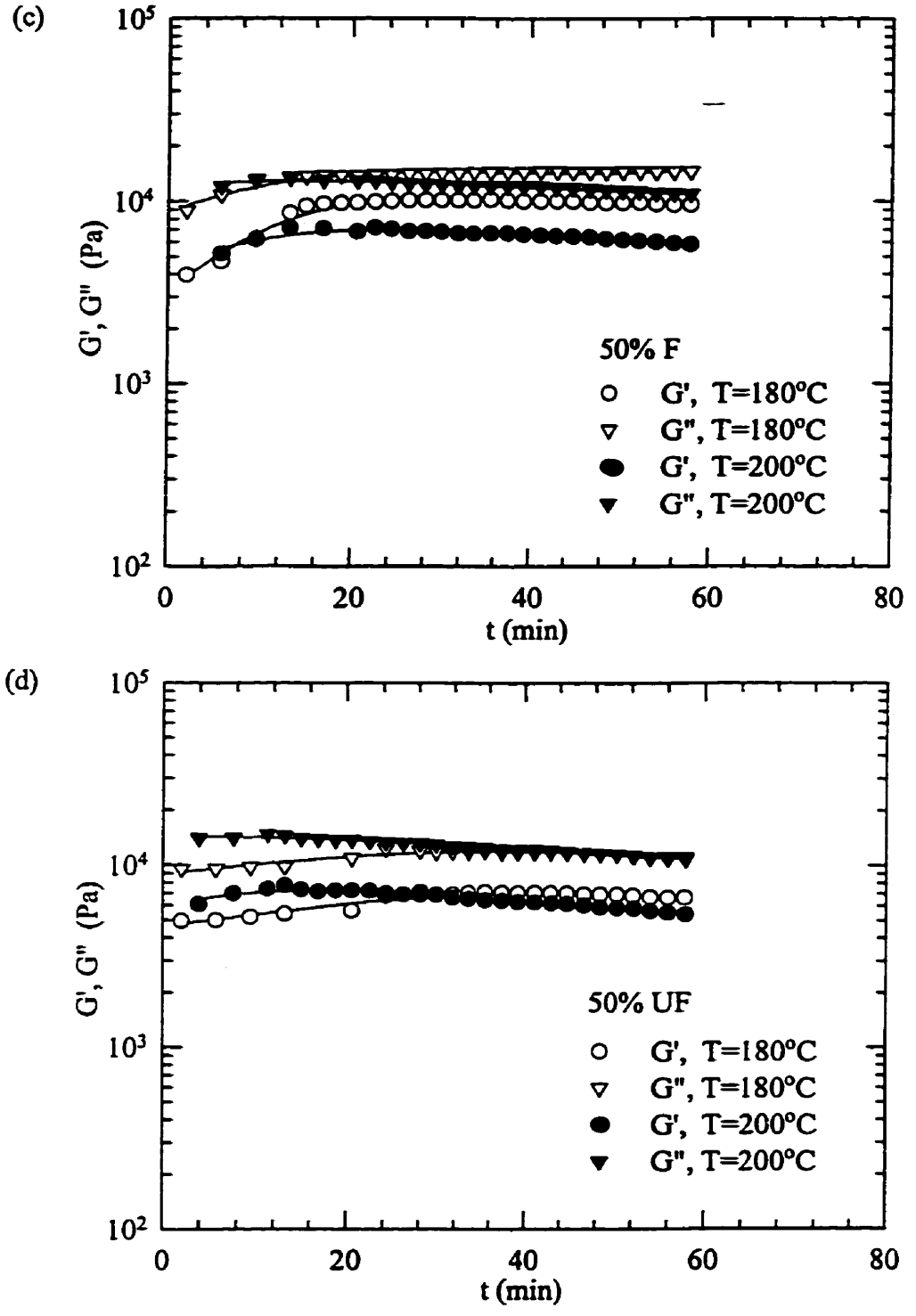

Figure A.3 (continued)

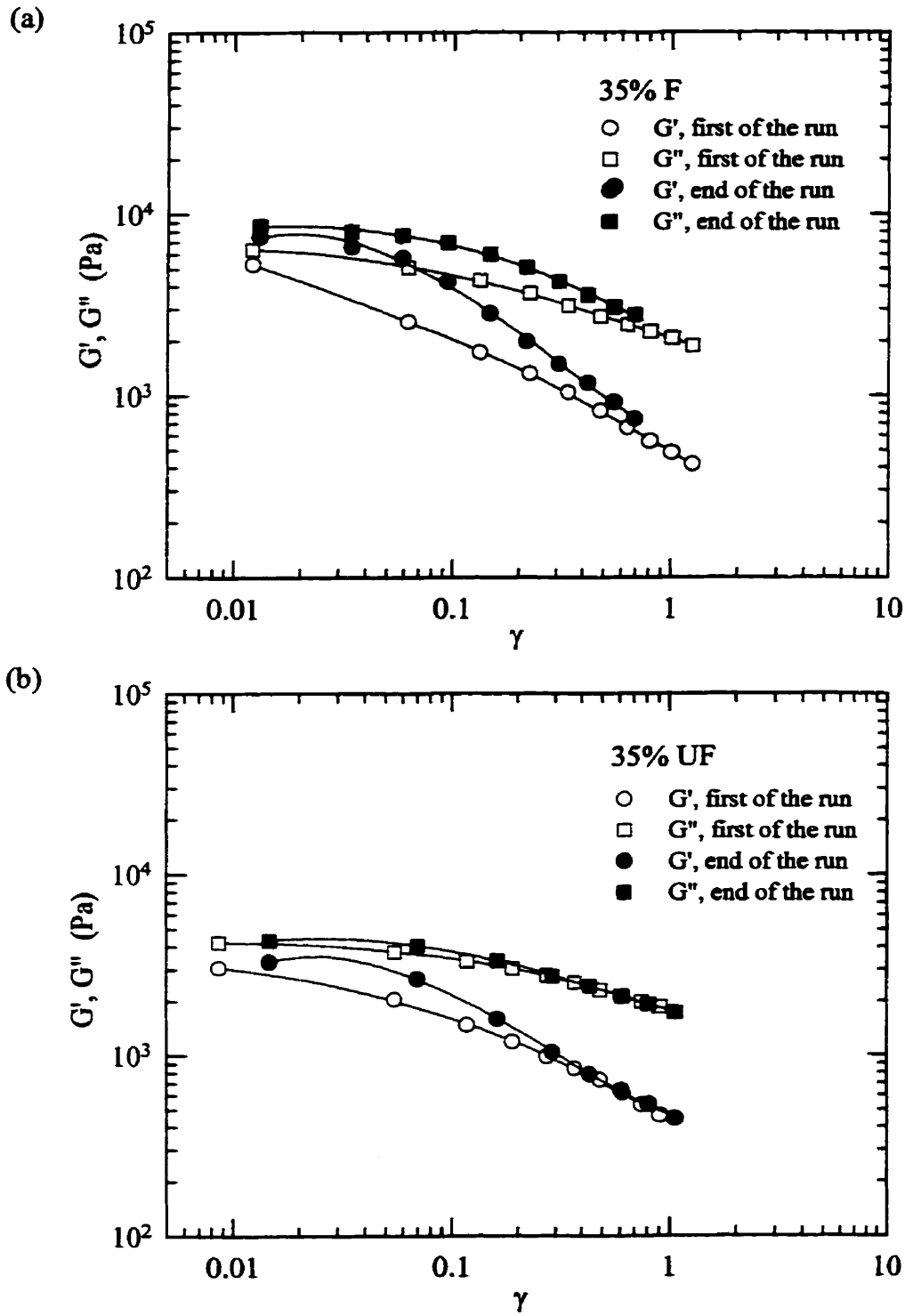

Figure A.4: Dynamic moduli as functions of strain amplitude at T=200°C and 0.1 Hz for PP with $CaCO_3$ (dps1): (a) 35% F, (b) 35% UF, (c) 50% F, (d) 50% UF

(c)

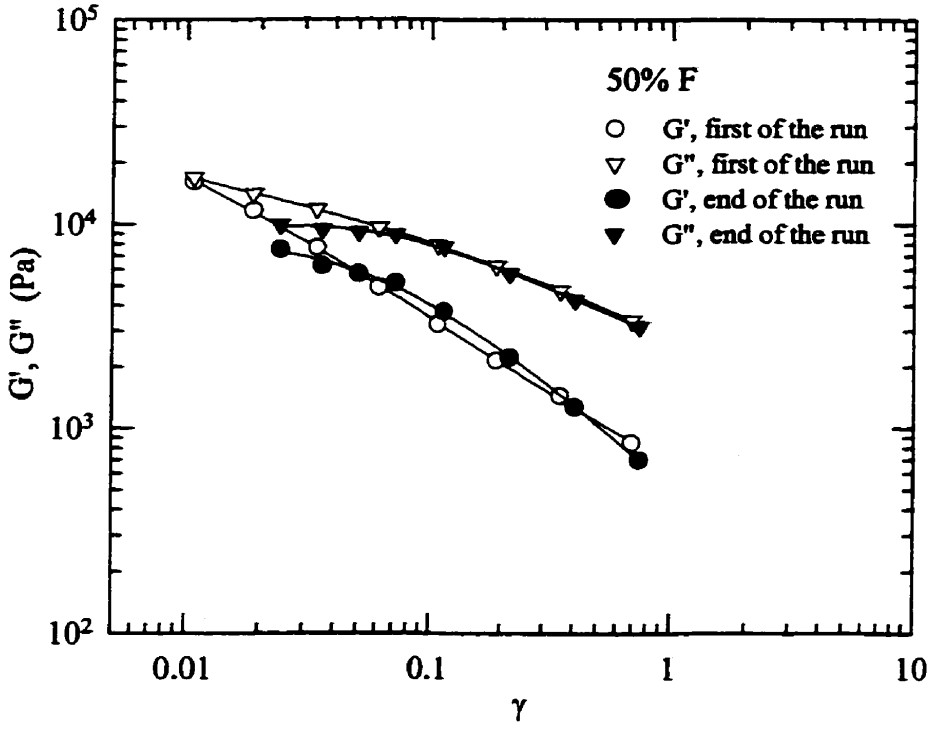

(d)

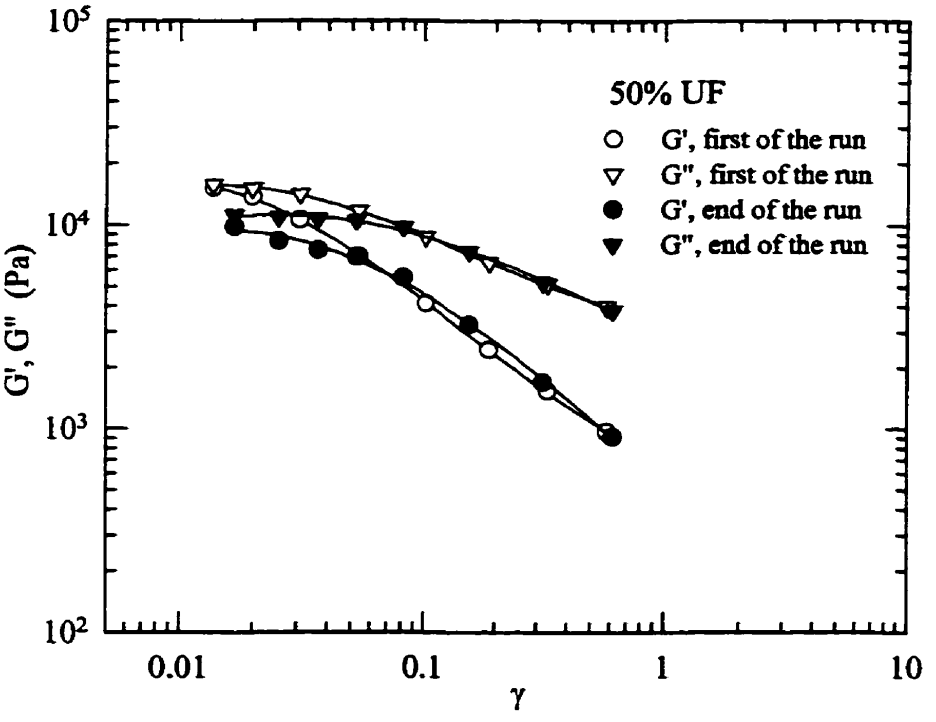

Figure A.4 (continued)

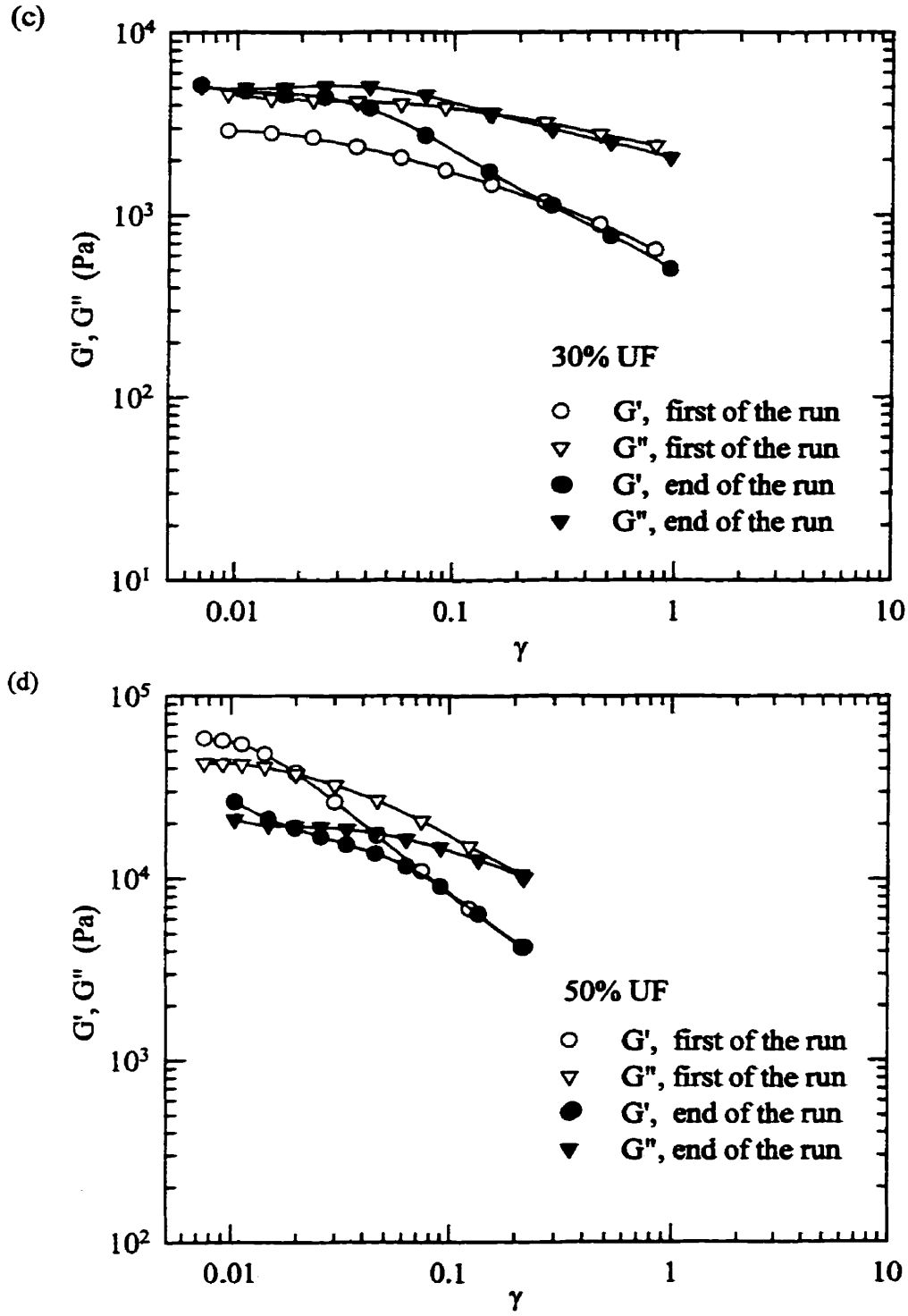

Figure A.5: Dynamic moduli as functions of strain amplitude at 200°C and 0.1 Hz for PP with $CaCO_3$ (dps2): (a) 30% UF, (b) 50% UF

APPENDIX B -
MICROGRAPHS OF COMPOUNDS

(a)

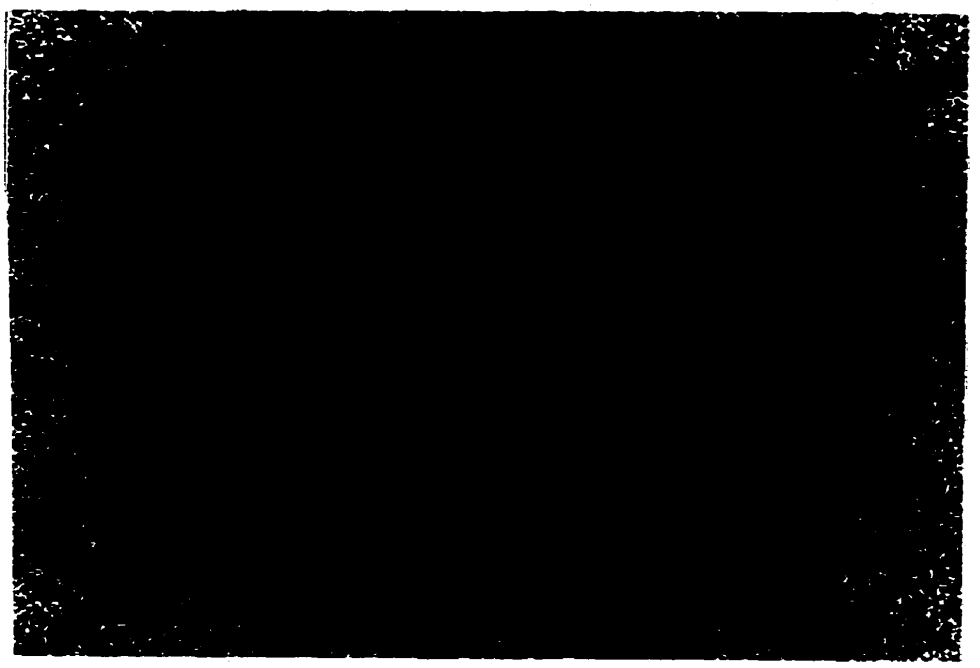

100 μm

(b)

Figure B.1: Micrographs of PP/$CaCO_3$ (50% UF, dps2): (a) without pre-shear (f = 3.25), (b) pre-shear 1 hour